

T10-5788

CONTROL AND DYNAMICS  
PERFORMANCE OF A SODIUM  
COOLED REACTOR POWER SYSTEM

by  
P. D. Hansen  
J. H. Eaton

Approved by  
J. P. Barger

Submitted to

ALCO Products, Inc.  
Research and Development  
Schenectady, New York

December 28, 1959

MICROTECH RESEARCH COMPANY  
639 Massachusetts Avenue  
Cambridge 39, Massachusetts

Report No. 171

AT(11-1)-666

## TABLE OF CONTENTS

	<u>Page</u>
LIST OF FIGURES	i
ABSTRACT	v
1. INTRODUCTION	1
1.1. Objectives and Method of Approach	1
1.2. Conclusions	4
1.2.1. Uncontrolled Behavior	4
1.2.2. Controlled Behavior	4
2. NORMAL OPERATION AND CONTROL PHILOSOPHY	6
2.1. Definition of Normal Operation	6
2.2. The Role of Linear Theory	7
2.3. The Cascaded Control	8
2.4. Local Loops	10
2.4.1. Sodium Flow Control	10
2.4.2. Reactor Rod Control	14
2.4.3. Feedwater Control	15
2.4.4. Steam Turbine Governor	15
2.5. Pressure Control	17
2.5.1. Computer Model	17
2.5.2. Closed Loop Pressure Response	19
2.6. Temperature	24
2.7. Boiler Liquid Level Control	29
2.7.1. The Dynamic Model	29
2.7.2. Computer Results	30
3. CASUALTY OPERATION AND CONTROL	32
3.1. Possible Casualty Operation	32
3.1.1. No-Control	32

## TABLE OF CONTENTS (cont)

	<u>Page</u>
3.1.2. System Under Control	32
3.2. Signal Propagation	33
3.3. Control Scheme	33
3.4. Failures	37
3.4.1. Loss of Feedwater	37
3.4.2. Reactor Scram	42
3.4.3. Loss of Load	43
3.4.4. Loss of Secondary Pump, Flow or Flow Sense	44
3.4.5. Loss of Primary Pump, Flow or Flow Sense	45
3.4.6. Controller Failure	45
3.4.7. Loss of Steam Pressure and Flow Sense	46
3.5. Transient Response Under Casualty Control	46
4. MODELING OF HEAT EXCHANGER DYNAMICS	49
4.1. Superposition and Reticulation	49
4.1.1. Heat Transfer	51
4.1.2. Energy Transport	56
4.2. Heat Exchanger Models	58
4.2.1. Solutions of Partial Differential Equations	58
4.2.2. Non-Linear Computer Models	63
4.2.3. Linear Computer Models and Results	69
4.3. Assumptions	74
4.3.1. Single-Phase Heat Exchanger Representation	74
4.3.2. Two-Phase System Behavior	75
4.3.3. Other Components	75
REFERENCES	76

## TABLE OF CONTENTS (cont)

	<u>Page</u>
A.1. DYNAMICS OF TWO-PHASE FLUIDS	A.1.1
A.1.1. Energy Storage	A.1.1
A.1.2. Two-Phase Mass Storage	A.1.3
A.1.3. Stability of Forced and Natural Circulation Loops in Steam Generators	A.1.8
A.2. COUNTERFLOW HEAT EXCHANGER COMPUTER MODEL	A.2.1
A.2.1. Uncoupled Responses	A.2.1
A.2.2. Coupled Responses	A.2.3
A.3. BOILER COMPUTER MODEL	A.3.1
A.3.1. Uncoupled Responses	A.3.1
A.3.2. Coupled Responses	A.3.3
A.4. PIPE-PUMP DYNAMICS	A.4.1
A.4.1. Sodium Pipe-Pump Loops	A.4.1
A.4.1.1. Pipe Model	A.4.1
A.4.1.2. Pump Model	A.4.3
A.4.2. Feedwater-Pipe-Pump and Valve Model	A.4.9
A.4.3. Steam Pipe Model	A.4.10
A.4.4. Steam Valve Model	A.4.14
A.4.5. Summary of Computer Models	A.4.14
A.5. BOILER LEVEL CONTROL	A.5.1
A.5.1. Feedwater Tray	A.5.1
A.5.1.1. Feedwater Continuity and Weir Equation	A.5.3
A.5.1.2. Tray Condensation	A.5.4
A.5.2. Header	A.5.6
A.5.2.1. Feedwater Tray Pressure Drop	A.5.7
A.5.2.2. Separator Level	A.5.8



## TABLE OF CONTENTS (concl)

	<u>Page</u>
A. 5. 3. Boiler Circulation	A. 5. 11
A. 5. 4. Computer Models	A. 5. 13
A. 6. REACTOR DYNAMICS	A. 6. 1
A. 7. MONOTONE ANALOGY	A. 7. 1
A. 8. METHOD OF PERTURBATION AND NORMALIZATION	A. 8. 1
A. 8. 1. Perturbation	A. 8. 1
A. 8. 2. Normalization	A. 8. 2
A. 8. 3. Combined Linearization and Non-Dimensionalization	A. 8. 2
NOMENCLATURE	

## LIST OF FIGURES

	<u>Page</u>
* - Computer Results	
1.1. System Schematic Diagram	2
2.1. Synthesis of an Arbitrary Function from Step Responses	7
2.2. Cascaded Controllers	9
2.3. Sodium Stream Local Control Loop	11
*2.4. Sodium Cascade Flow Control Loop Response to Step In Set Points	13
2.5. Feedwater Flow Control	15
2.6. Synchronous Generator Power-Speed Curves	16
2.7. Open Loop System Block Diagram	18
*2.8. System Responses	21
*2.9. Closed Loop Pressure Response to Step Disturbance in Turbine Valve	22
2.10. Forgetter Step Response	25
*2.11. Closed Loop Liquid Level Disturbance	28a
2.12. Pressure Control Diagram; Berkeley 1100 Ease Computer	27
3.1. System Modulation Concept and Control Modes	35
3.2. Controller Systems	36
*3.3. Casualty Level Control - Loss of Feedwater	39
3.4. Turbine-Generator-Load Block Diagram	40
3.5. Turbine Momentum Equation	41
*3.6. Casualty Steam Pressure Responses at 100% Load Level	48

## LIST OF FIGURES (cont)

	<u>Page</u>
4.1. Statics of Counterflow and Parallel Flow	55
*4.2. Boiler Uncoupled Transient Responses	60
*4.3. Intermediate Heat Exchanger Temperature	65
4.4. Energy Flow Diagram for a Counterflow Heat Exchanger	67
4.5. Transport Operator, Analog Representation	67
4.6. Heat Transfer Node, Analog Representation	68
*4.7. Superheater Temperature Responses to Large Flow Variations	70
*4.8. Intermediate Heat Exchanger Temperature Responses to Temperature Inputs	71
*4.9. Superheater Temperature Responses to Temperature Inputs	72
*4.10. Linearized Exchanger Terminal Flow Responses	73
A.1.1. Two-Phase Energy Storage Derivation	A.1.17
A.1.2. A, B, and C Non-Dimensional Thermodynamic Parameter Pressure Dependence	A.1.21
A.1.3. Pressure Dependence of Normalized Thermodynamic Parameters	A.1.22
A.1.4. Pressure Dependence of Normalized Thermodynamic Parameters	A.1.23
A.1.5. Pressure Dependence of Normalized Thermodynamic Parameters	A.1.24
A.1.6. Riser Out-Flow Response to a Step In Downcomer Flow Rate	A.1.9
A.1.7. Vector Diagram for Sinusoidal Variations in $W_D$	A.1.11

## LIST OF FIGURES (cont)

	<u>Page</u>
A. 1. 8. Vector Diagram Showing Stability	A. 1. 12
A. 2. 1. IHX - Superheater Uncoupled Model	A. 2. 9
A. 2. 2. Superheater Control Study Computer Model	A. 2. 10
A. 2. 3. Intermediate Heat Exchanger Control Study Computer Model	A. 2. 11
*A. 2. 4. Open Loop Superheater Coupled Responses to Step Increase in Steam Valve Area	A. 2. 12
*A. 2. 5. Open Loop Intermediate Heat Exchanger Coupled Responses to Step Increase in Steam Valve Area	A. 2. 13
A. 3. 1. Steam Boiler Control Study Computer Model	A. 3. 7
A. 3. 2. Steam Boiler Uncoupled Computer Model	A. 3. 8
A. 4. 1. Generalized One-Dimensional Pipe-Pump Model	A. 4. 1
A. 4. 2. Secondary Sodium Loop Schematic	A. 4. 2
A. 4. 3. A Proposed Gas Blanket Isolation	A. 4. 4
A. 4. 4. Pump Characteristic Curve	A. 4. 7
A. 4. 5. Induction Motor Torque-Speed Curves	A. 4. 8
A. 4. 6. Water-Steam Steady-State Pressure Drop Loop	A. 4. 9
A. 4. 7. Steam Pipe Pressure Pulse Dynamics	A. 4. 12
A. 4. 8. Load Curve for 200 HP Wound Rotor Induction Motor	A. 4. 16
A. 4. 9. Sodium Control Loop Computer Models	A. 4. 17

## LIST OF FIGURES (concl)

	<u>Page</u>
A. 5. 1. Schematic Representation of the Boiler Drum Separator	A. 5. 2
A. 5. 2. Condensation Rate Step Responses	A. 5. 5
A. 5. 3. Drum Separator Capacity Simplification	A. 5. 8
A. 5. 4. Graph of Boiler Tube Load Vs Position	A. 5. 16
A. 5. 5. Boiler Cross-Plot	A. 5. 17
A. 5. 6. Boiler Circulation Block Diagram	A. 5. 18
A. 5. 7. Drum Separator Computer Model	A. 5. 19
A. 6. 1. Reactor Computer Model	A. 6. 7
A. 6. 2. Reactor Rod Control Model	A. 6. 8
A. 7. 1. Step Responses	A. 7. 1
A. 7. 2. Impulse Responses	A. 7. 2
A. 8. 1. Isometric Expansion of Computer Solution to the Reticulated Heat Exchanger	A. 8. 5

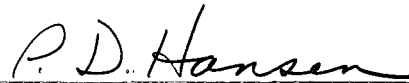
## ABSTRACT

At the request of ALCO Products, Inc., under the sponsorship of the Atomic Energy Commission (Contract No. AT(11-1)-666), Microtech Research has performed an analytical and analog computer study of a high performance sodium cooled reactor system.

As a final stage of the overall design program conducted by ALCO Products on the intermediate heat exchanger (IHX), boiler, and superheater (References 1.1 and 1.2), Microtech Research has investigated transient performance, controllability, and casualty behavior. Methods developed in an earlier study of the SM-2 System (Reference 1.3) are refined, leading to a general criterion for stability of natural circulation boilers. Also, a control scheme is devised which enables fixed parameter commercial controllers to maintain extremely tight control over the steam and sodium states despite rapid and large disturbances occurring at any load level between 15% and 100% of maximum load.

A control signal propagation philosophy employing controller over-rides is developed, enabling orderly system operation following a process or control component failure, thus insuring fail-safe behavior.

Results of analog computer studies of the controlled system behavior are included. The philosophies of control and analog modeling are discussed.



P. D. Hansen  
Project Manager

Approved by



J. P. Barger  
General Manager

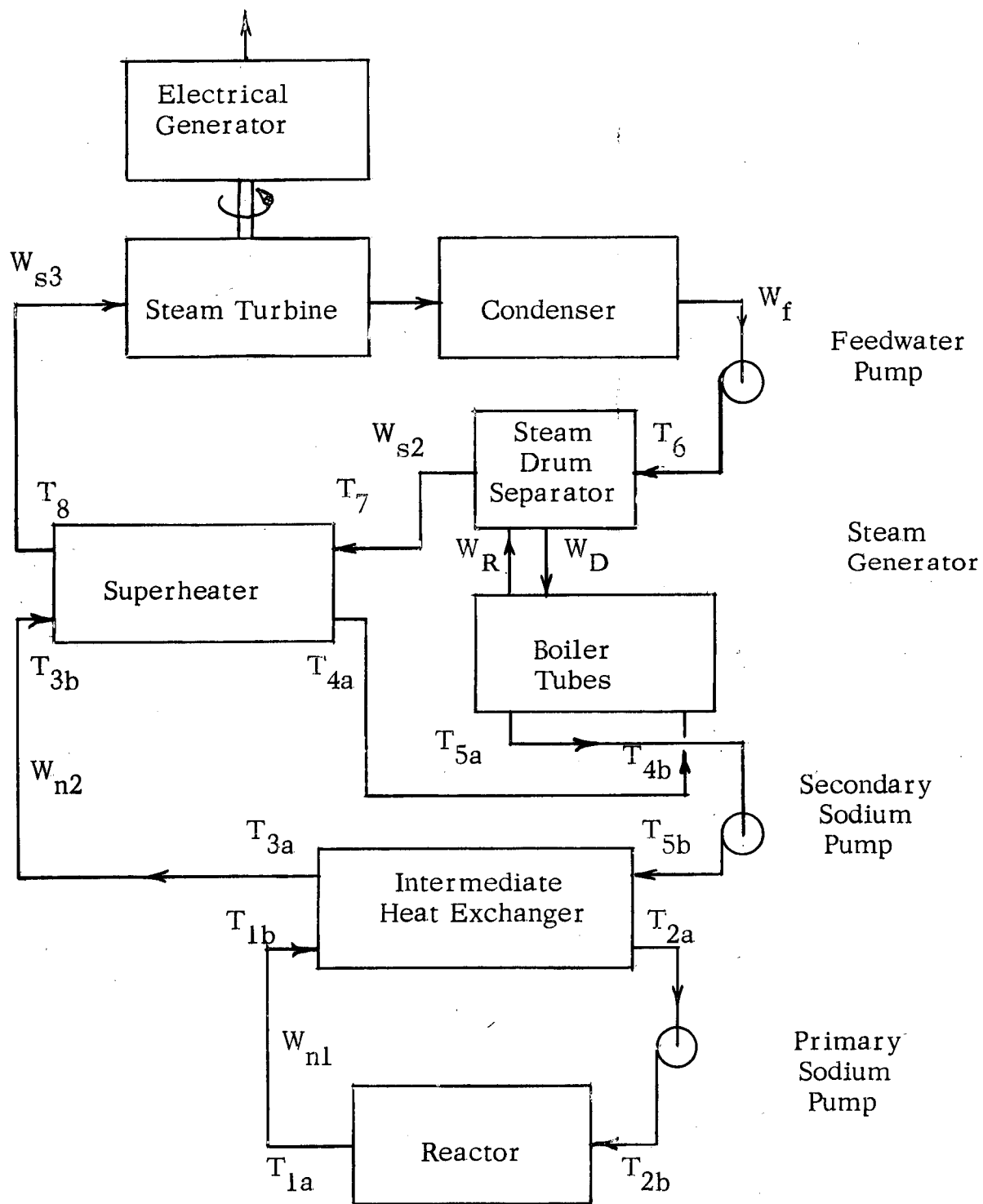
## 1. INTRODUCTION

### 1.1. Objectives and Method of Approach

High plant efficiencies can be realized without excessively high core temperatures and high coolant pressures through the use of a liquid metal coolant; problems associated with the handling of liquid metals, however, have limited widespread application. In an attempt to prove the feasibility of liquid sodium as a reactor coolant, ALCO Products, Inc., under the sponsorship of the Atomic Energy Commission, is undertaking a design study of three vital system components: the intermediate exchanger, the boiler, and the superheater. (References 1 and 2). Since, in the submarine reactor program, the nuclear reactor had been the major focus of attention, the development of the sodium cooled reactor and sodium pumps for this application are thought to need less attention than the heat exchanger equipment. Consequently, parallel design studies of the reactor, pumps, and other system components have not yet been initiated.

The system schematic is shown in Figure 1.1. The static and dynamic behavior of the heat exchange equipment depend to some extent on the behavior of the other system components. Therefore, static and dynamic models of these other components must be formulated in order to account for their interactions. However, since the behavior of these as yet unspecified components is not of central interest in this study, crude models have been formulated without commitment to any specific hardware design. More articulate models for the heat exchangers and those elements limiting controllability have been formulated.

Static and transient thermal stresses as well as a high steam pressure make difficult the structural design of the sodium heated boiler and superheater. The greatest structural problem appears to be associated with the superheater



System Schematic Diagram

Figure 1.1

129 012



tube sheets, thick slabs of metal supporting the superheater tubes and separating the steam from the sodium. Rapid and large changes in fluid temperature coupled with the slow thermal diffusion time through the metal could cause significant transient thermal stress in addition to the already large static pressure, bending, and thermal stresses. Many other parts of the system could also be significantly stressed if large temperature transients occur. Hence, it is desirable to control thermodynamic states to prevent fluid temperature surges at any point in the sodium or steam loops during normal and casualty operation.

The steady-state heat exchanger design, for the most part, facilitates this kind of control. Because each of the exchangers has a high effectiveness and because the steam and sodium flows are maintained proportional to the load power, the steady-state sodium and steam temperatures do not vary appreciably with load over the entire useful load range. This investigation shows that, during transient changes in load, the steam and sodium systems' temperature changes will not significantly exceed the small steady-state temperature changes, provided that the control system maintains the design steady-state ratio between the flow rates and power level during the transient. In order to achieve this, the controlled response of both sodium flow rates to a change in power level must be made significantly faster than the longer characteristic (transport) times of the heat exchangers.

Generally, power level changes are initiated at the load end. Hence, normal control is geared for this type of disturbance. Power level changes may be initiated at other points in the thermodynamic system, however. Reactor scram, sodium pump failure, or feed water pump failure would require a shut-down. Temperatures can be maintained after such a casualty disturbance provided all flow rates and the output power are maintained proportional to the transient disturbance power level. This is achieved through a bi-directional control signal propagation scheme. When an abnormal signal occurs,

it propagates in both directions toward the power source (the reactor) and the power sink (the electrical load) - overriding the normal control signal (derived from the electrical load variations).

An analog computer study of the controlled system behavior for normal control is discussed in Chapter 2 and for casualty control in Chapter 3. Details of the analog computer models for the heat exchangers are discussed in Chapter 4. Details of the modeling of other system components are presented in the appendices. A detailed treatment of two-phase energy and mass storage appears in Appendix 1. Also in this appendix is a criterion for natural circulation loop stability which resulted from a refinement of an earlier analog study of the SM-2 pressurized water reactor power system (Reference 6).

## 1.2. Conclusions

### 1.2.1. Uncontrolled Behavior

1. An accurate analog model for the complete system, valid for large disturbances, is not feasible with the size of available computers.
2. Large temperature and pressure swings can occur. The maximum amplitude of variation will not be significantly different from the new steady-state value following a step disturbance.
3. The natural circulation loop is stable and non-oscillatory according to both the analytical prediction, using the criterion of Appendix 1, and the analog computer study.

### 1.2.2. Controlled Behavior

1. Extremely good normal control can be achieved with fixed parameter commercially available electronic controllers.

Fast flow measuring instruments are required. Also reactor-control-rod motion during transients is necessary. Good control of boiler level results with measurement of level only, in spite of a large tray lag, provided a fast differential pressure (level) sensor is used.

2. It is desirable to baffle tightly one of the argon gas blankets in either the boiler or superheater, in order that the flow through these exchangers may follow a transient change in secondary sodium pump flow.
3. The optimum controller adjustments and system performance are relatively insensitive to parameter variations. The transient performance depends primarily on the boiler two-phase energy storage time constant, which is derived in Appendix 1. It is desirable that this time constant be large compared to the secondary sodium loop inertia-resistance time constant. It is also desirable that one transport time (the shell side) in each exchanger be large relative to the inertia-resistance time constant of the sodium loops. In the reactor, a small sodium transport time appears to be desirable (this has not been modeled in the analog study).
4. Casualty bi-directional control signal propagation with override capability appears to cause successfully a power coast-down following a component failure without subjecting any part of the thermodynamic system to significant transient temperature or pressure variations. Flow rates and power level track down to the 15% power level, corresponding to the minimum controlled sodium flow rate, before allowing system temperatures to vary. With this small flow, subsequent temperature coast-down is more than six times slower than when 100% load sodium flow rates are employed. A finite minimum flow through the reactor is required to remove the decay heat.

## CHAPTER 2 - NORMAL OPERATION AND CONTROL PHILOSOPHY

Normal operation has been defined by the steady-state design. Control shall maintain the steady-state characteristics and provide best path between steady-state thermodynamic state points. Three control or regulation problems exist in this design - pressure regulation, sodium-steam temperature regulation, and boiler liquid level regulation.

### 2.1. Definition of Normal Operation

The steady-state steam and sodium temperatures have been determined by ALCO Products during the design of the IHX, boiler, and superheater (References 1 and 2).

The design provides nearly constant terminal temperatures for each exchanger over the entire useful load range. The Atomic Energy Commission has placed requirements on the flow and load transients that each exchanger must structurally withstand. (Reference 4).

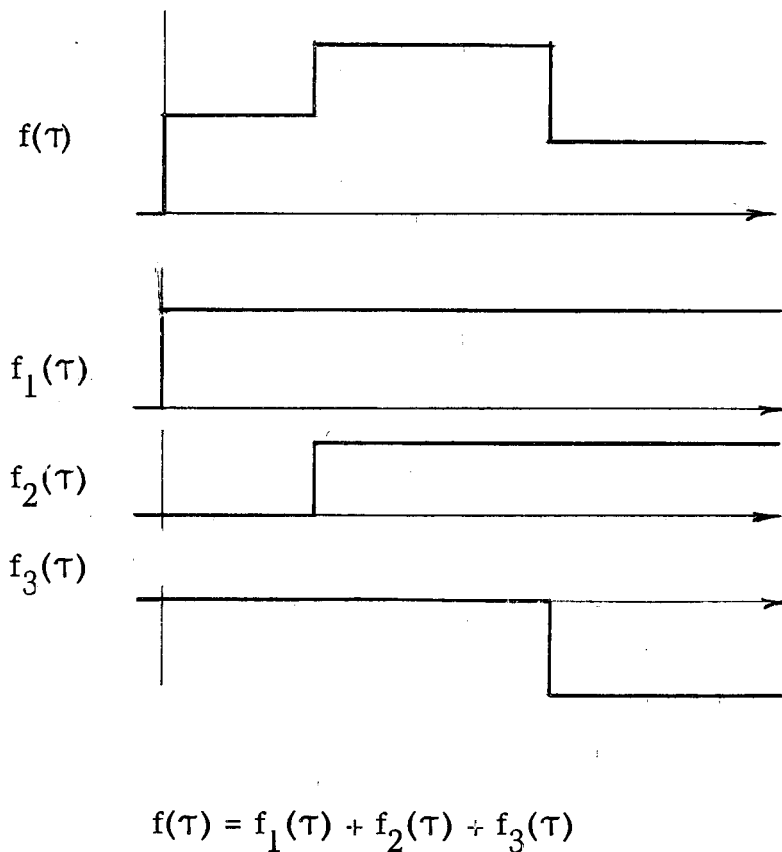
During normal operation, the system must withstand the following load changes:

- a. Full range ramp:  $\pm 5\%$  (of full load value) per minute from 20% - 100%.
- b. Short-time ramp:  $\pm 20\%$  (of full load value) in 1 minute.
- c. Step change:  $\pm 10\%$  (of full load value)

Normal operation and control divide into three areas which are discussed separately - pressure regulation, temperature regulation, and boiler liquid level regulation.

## 2.2. The Role of Linear Theory

The fields of linear algebra and linear differential equations have reached a relatively high degree of development and have proved useful tools in many fields of physical analysis. In particular, most of the theories, tools, and practices in feedback control rely upon linear equations or representations. The most important characteristic associated with linearity is superposition; that is, any system or signal may be constructed by the linear summation or superposition of other known systems or signals. As an example, the trace in Figure 2.1 may be synthesized from the basic step functions illustrated.



Synthesis of an Arbitrary Function from Step Responses

Figure 2.1

Fortunately, many physical systems are linear or may be considered linear within some range of operation or variation. For these cases, all of the associations, techniques, and experience of linear analysis may be drafted for the problem study. If the linear model is analyzed at various load levels, comparison of the results at the various load levels indicates the degree of non-linearity involved. The effect of linearized non-linearities in closed loop studies appear as variations in time constants or loop gains. Since some non-linearities are essential, a linearizing technique may give erroneous conclusions. These non-linearities generally have discontinuous first derivatives. Linearization generally describes or formulates a function in terms of its local slope. Chordal approximations are also commonly used. For essential non-linearities, no well-defined slope exists at the discontinuity. Furthermore, the slope of the chordal approximation varies significantly with input amplitude.

In the following two sections, the modeling and analysis of the various control modes is based upon linear concepts and models. The actual non-linear effects and/or considerations are discussed in the respective sections.

### 2.3. The Cascaded Control

Feedback control is a means of achieving desired performance with an imperfect power modulator and with load disturbances. Within the scope of normal operation, pressure and boiler liquid level regulation provide the desired performance. The manipulated variables, primary and secondary sodium flow rate, feedwater flow rate, and reactor rod position, were selected during the steady-state design. The communication path between the regulator output and the feedback input, however, involves a number of significant time lags. These lags and the power available limit the maximum level of controllability. Thus, a reduction in the significant lags will increase the maximum achievable controlled system performance.



The fast speed of response is achieved by high gains. The small loop permits high gains with non-oscillatory responses. A high controller gain, however, may not be achievable because of saturation. The initial hard hit of the manipulated variable following a step input may require a disproportionately high power level with regard to steady-state requirements. This requirement should be considered in any closed loop design.

Small local loops not only provide dynamics isolation but also an insensitivity to loop parameter variations. Linearization of a non-linear relationship develops load variable coefficients; that is, the coefficients vary between operating points. System time constant variations do not affect proportional loop stability or overshoot. Furthermore, the controller gain may be high enough to mask any variations of the system gain. Hence, local loops reduce the sensitivity to variations of loop parameters. This consideration is important in the application of fixed parameter controllers.

#### 2.4. Local Loops

The advantages of local loops to minimize the effects of dynamics or parameter variations have four likely applications in this system.

##### 2.4.1. Sodium Flow Control

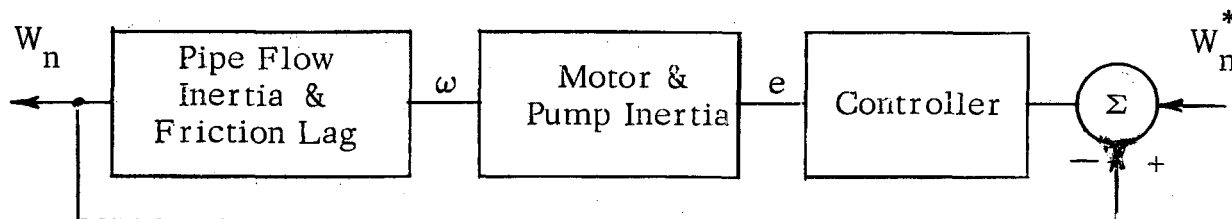
Two of the manipulated variables in this system are the primary and secondary flow rates. A detailed design of these two transport loops has not been completed. This study assumes that each sodium loop employs a variable speed centrifugal pump driven by a wound rotor induction motor.

Appendix A.4 presents the specific details of the selected pump and motor. Variable flow magnetic pumps might also be used. The dynamic behavior of the magnetic pumps may be more favorable for control, depending on the size of the magnetic flux lag and power saturation level. In any case, the analog



dynamic representations are similar.

Each sodium flow control manipulates armature resistance in response to the difference between the pump output flow rate and the demand flow rate. The demand flow rate is the set point of the controller. Figure 2.3 illustrates this control action.



Sodium Stream Local Control Loop

Figure 2.3

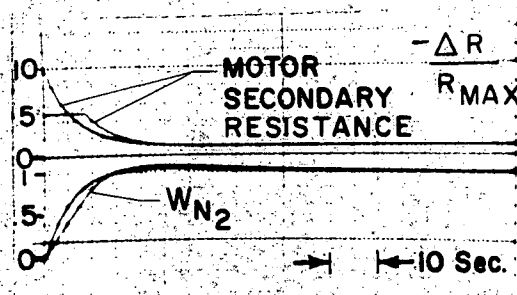
In this scheme, the controller closes a loop around two lags. The intermediate variable, speed, is measurable. Therefore, another loop around just the pump and motor inertia may improve the response. The results of the computer study, however, indicate the present arrangement is satisfactory. In the secondary loop, two mass storage regions, the gas blankets in the boiler and superheater, can severely limit the performance of the secondary loop and therefore the overall control. All the following analysis assumes that, by tightly baffling one of the gas blankets so that transient flow through the baffle is small, only one gas blanket is effectively coupled to the sodium flow. Appendix A.4 discusses this assumption in detail. Figure 2.4 presents the analog computer responses of the flow control loops to step changes in the set point. Figures 2.4A and 2.4C apply to the secondary loop at 100% and 20% load, respectively; 2.4B and 2.4D apply to the primary sodium loop. An equivalent loop length of 150 feet and 300 feet are used for the primary and secondary sodium loops respectively. A more detailed discussion of these assumptions as well as of the detailed computer model appears in Appendix A.4.

In steady-state the energy provided by the pump equals the energy dissipated in pipe friction. During a transient however, the time integral of the difference between power in and power out to the sodium loop equals the change in the stored kinetic energy of the rotor-pump-fluid. System load decreases demand less power to the loop. The minimum however is zero power-in corresponding to infinite secondary resistance. Large load decreases such as during casualty control may demand a larger difference between power in and power out than possible through the pump manipulation to achieve the desired speed of response. Such instances require an additional means of energy dissipation or removal. Some form of dynamic braking must be provided in the system and coupled with the controller output. Several methods are available. An eddy current brake with the centrifugal pump drive is one possibility. The magnetic pump provides a simple solution in that a reversal of polarity of the pump control voltage changes the pump to a motor or energy in to an energy out device. The dynamic model used in the computer studies assume an energy removal capacity over and above the normal pipe friction.

Four traces appear in Figure 2.4.A. The top two traces are the manipulation variables with and without manipulated variable saturation and the bottom two traces are the flow rate responses. It is highly probable that saturation will occur when a high gain controller is employed. The second trace accounts for this possibility. According to Reference 3, the wound rotor motor can provide 150% maximum nominal torque, the bounding value used in the second trace. The slower response results from the torque limited model. This 50% over-load saturation corresponds to a 10% change in set point. For the 20% load case, however, saturation is not likely, but the same relationship is arbitrarily used. A bound at 50% over the local torque value is used. On physical grounds, this is a ridiculous choice but illustrates well the quality of this loop. Even with this impossibly low bound, the control loop provides good performance. The saturated response deviates but a small amount from the non-saturated response. The same discussion applies to the primary loop.

FIGURE 2.4

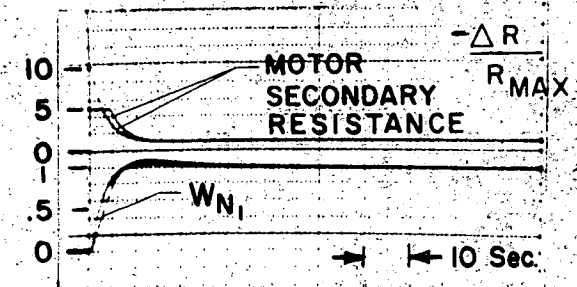
# SODIUM CASCADE FLOW CONTROL LOOP RESPONSE TO STEP IN SET POINTS.



20 % LOAD

A

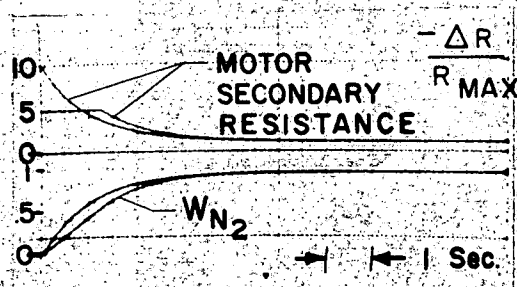
$$W_{N2} = \frac{\Delta W_{N2}}{1,665,000 \text{ lbs/hr}}$$



20 % LOAD

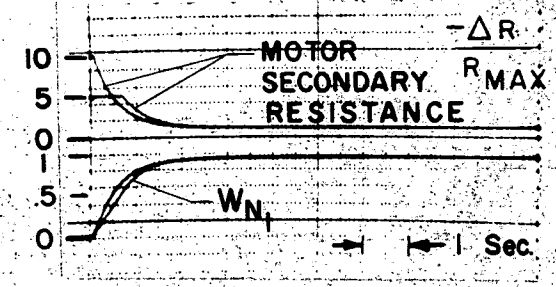
B

$$W_{N1} = \frac{\Delta W_{N1}}{1,665,000 \text{ lbs/hr}}$$



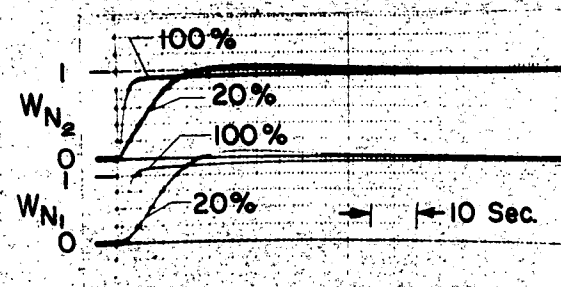
100 % LOAD

C



100 % LOAD

D



E

Controller parameter variations on the analog computer indicate that higher controller gains are possible from the viewpoint of response oscillation. However, the gains of 10 in each controller represent the usual upper limits in process control. Responses in Figure 2.4.E are to a step in secondary controller set point with the primary controller set point sensing secondary flow rate. The top traces represent secondary flow rate at 100% and 20% load, respectively, and the bottom traces represent 100% and 20% primary flow rate.

This scheme relies upon the quality of the flow instrumentation. Should difficulty arise in measuring the sodium flow rate, all alternative sensing of the sodium temperature may provide satisfactory results. Temperature measurement tends to be slow in responding to disturbances. This sluggishness, however, might be eliminated by a lead compensation network and by an anticipatory signal through measurement of steam flow rate. This scheme has not been studied on the computer. However, it is anticipated that the steam flow rate signal will require a gain proportional to the load level, since temperature variations are proportional to the percentage change (or logarithmic change) in flow rate as discussed in Chapter 4. It may prove helpful to measure pump speed and cause this to be proportional to steam flow rate (or proportional to a lead compensated steam flow rate measurement), thus again employing the cascade concept.

#### 2.4.2. Reactor Rod Control

Thermal reactors generally have rods of a moderator which may be manipulated to affect the neutron population. The rod actuator is a positioning device. The inertia of the rod and actuator mechanism provides a lag between the demand and response. However, this may be controlled as first order lag and should be quite simple to speed-up within the limitations of power supply saturation (see Appendix A.6).

### 2.4.3. Feedwater Control

The feedwater flow control, like the sodium flow control, has not been designed as yet. A conventional form of feedwater control is anticipated. According to Reference 13 most high pressure boiler systems use a staged constant speed centrifugal pump with a flow control valve. This analog computer study incorporates such a feedwater scheme. A more detailed discussion appears in Appendix A.4. Negligible dynamics are involved in this system, a good justification for such a scheme. However, should a variable speed feedwater pump appear more desirable, the local loop concept can reduce the effect of motor-pump-flow inertia. The local loop concept may prove valuable even in the fast valve control system in order to minimize the effects of valve stroke vs flow non-linearity and stroke rate saturation. See Figure 2.5.

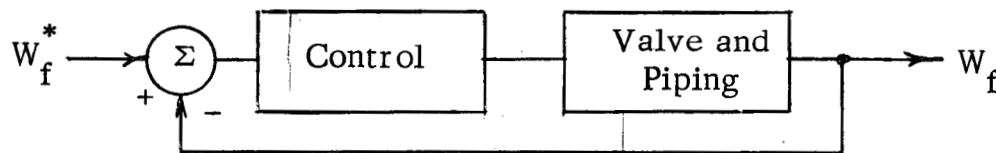


Figure 2.5 - Feedwater Flow Control

### 2.4.4. Steam Turbine Governor

Another local loop common to electric power generating stations is the turbine speed governor. The dynamics enclosed by this cascade controller are the turbine steam storage capacity and the turbine-generator rotor inertia. This cascade loop has little bearing on the normal thermodynamic control problem, for the loop is far faster than the steam-sodium system. However, a distinct characteristic of the system is used in the casualty control problem.

Consider the speed power characteristics of this generator with respect to the rest of the network sources. Figure 2.6 is the speed-drive curve for this generator to the left and the other system generators to the right.

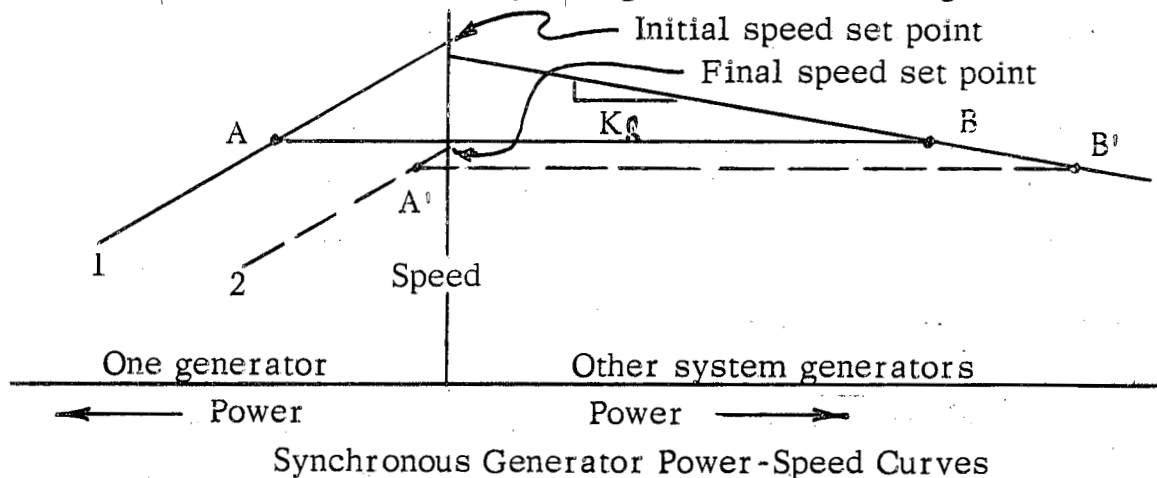


Figure 2.6

The solid lines reflect the speed power droops of the two for a given speed governor set point. Should the governor set point on the turbine be changed, such as to the operating curve number 2, the new steady-state operation is located at A' and B', this maintaining a constant total system load. For a large change in load on one generator, the system operating frequency changes very little. Minimum frequency shift results from a shallow speed-power curve for the other generators feeding the electrical network.

Just as the network frequency is controlled largely by the external system, so also is the network voltage. Hence, as the real function of the speed control is to control active power, the real function of the voltage control is to control power factor or reactive load supplied by the particular generator.

During normal operation, the governor manipulates power-in to match power-out. The casualty control philosophy uses the governor to adjust the power-out to match power-in; the turbine governor set point senses steam pressure rather than turbine speed.

## 2.5. Pressure Control

Two separate conditions require pressure regulation. The steam turbine design generally provides a peak operating efficiency at a specific supply pressure, the efficiency dropping with any deviation from this design supply pressure.

Also maintenance of constant temperatures within the boiler and superheater requires constant steam pressure. The mode of control and the computer results are discussed in the following sections.

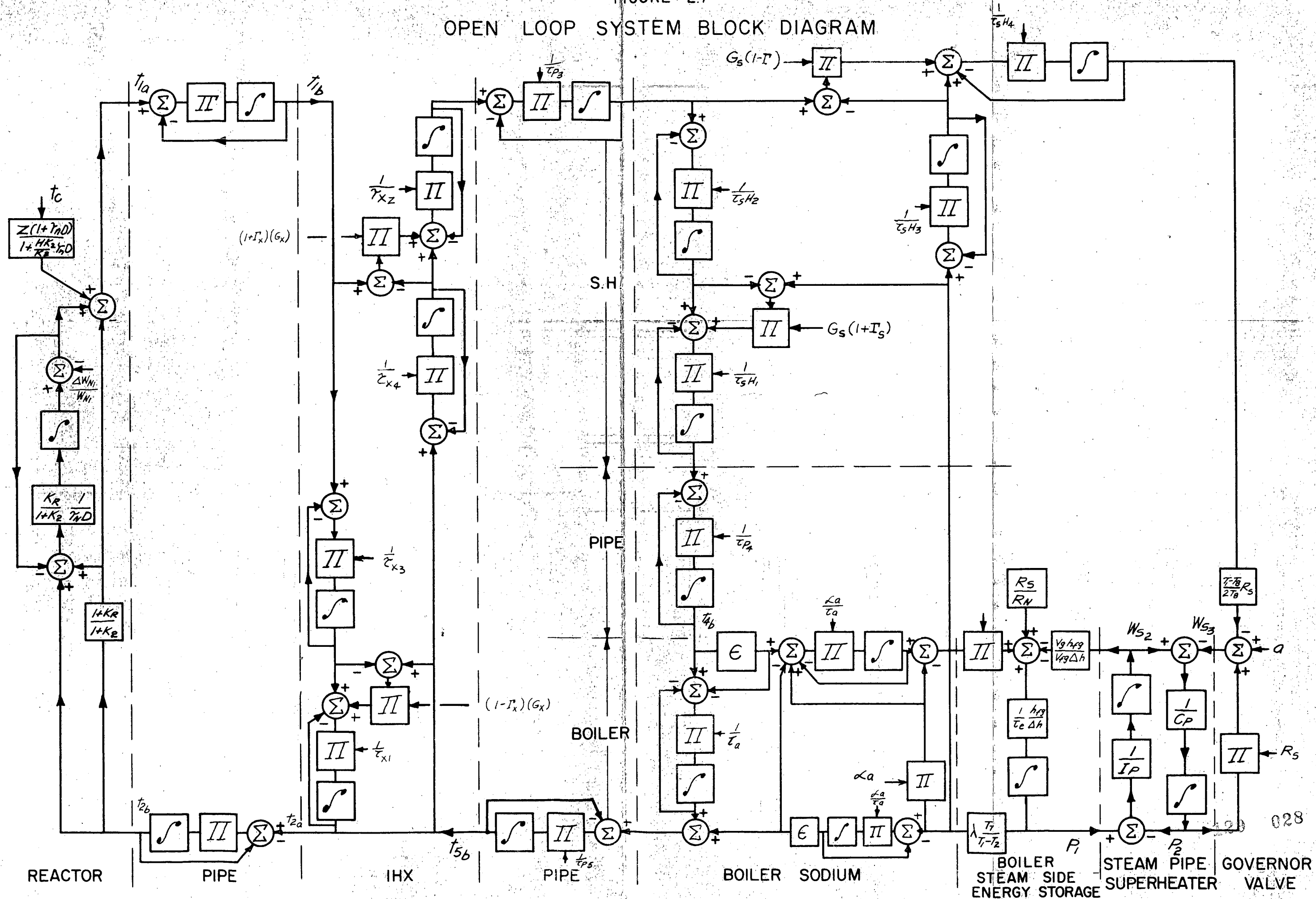
### 2.5.1. Computer Model

To handle the pressure control problem, one must consider the system from the turbine throttle valve back to the reactor. A manipulation of the steam valve may be considered a disturbance to the pressure control system. Turbine back-pressure does not affect the steam flow since the turbine and valve appear as a choked restriction. Also, since the controlled speed and voltage responses are much faster than the boiler response, a load change is almost immediately reflected in a valve manipulation.

Figure 2.7 is a block diagram of the open loop system. An analysis of each element appears in the respective appendices. Sub-system block diagrams also appear in the appendices. These diagrams provide a clear representation of the intercouplings within the system. However, the effect of the couplings may not be entirely clear without a computer study.

The block diagram of Figure A.3.1 is the boiler two-phase energy equation. A step change in valve area is a step in steam flow rate. The integral of this provides the change in boiler pressure. However, the pressure flow dependence at the steam valve provides a negative feedback path. This path provides an open loop (no pressure regulator) stabilization of the boiler pressure droop. The paths of communication to the left of the pressure reflect the change in

# OPEN LOOP SYSTEM BLOCK DIAGRAM





steam generation (no sodium flow rate change) from the increase in boiler sodium to steam temperature difference. This is also a negative feedback which tends to stabilize the pressure droop. However, the combined effects of increased steam flow rate and decrease in saturation temperature as viewed by the superheater provides a superheater outlet sodium temperature droop since more energy is extracted from the sodium. This is a destabilizing effect since less energy is available to the boiler for steam generation. The final steady-state pressure droop depends upon the combined gains in these feedback paths. Figure 2.8 presents the open loop steam response and pressure droop to a step increase in steam valve area at the 100% load level. The large droop indicates the system is nearly a flow source at steady-state. Other system components affect the steam system behavior after appreciable transport time. In particular, the reactor tends to return the steam states toward their initial conditions causing some overshoot in the transient response.

#### 2.5.2. Closed Loop Pressure Response

The methods of Sections 2.3 and 2.4 for controlling sodium flow rates provide a fast or a minimum dynamic distortion path for pressure control. The question of what to measure in order to command the secondary flow controller setpoint must be answered. This mode of control must provide good pressure regulation and isolate the loop temperatures from system disturbances. The steady-state thermodynamic state points of the system maintain nearly constant terminal temperatures over the useful load range, provided the steam flow and sodium flow rates are nearly in a fixed proportion. Maintenance of these state conditions throughout a transient response would provide the best possible control.

Two separate philosophies of control provide this idealized control. The essence of regulation is to isolate the regulated variable from its disturbances.

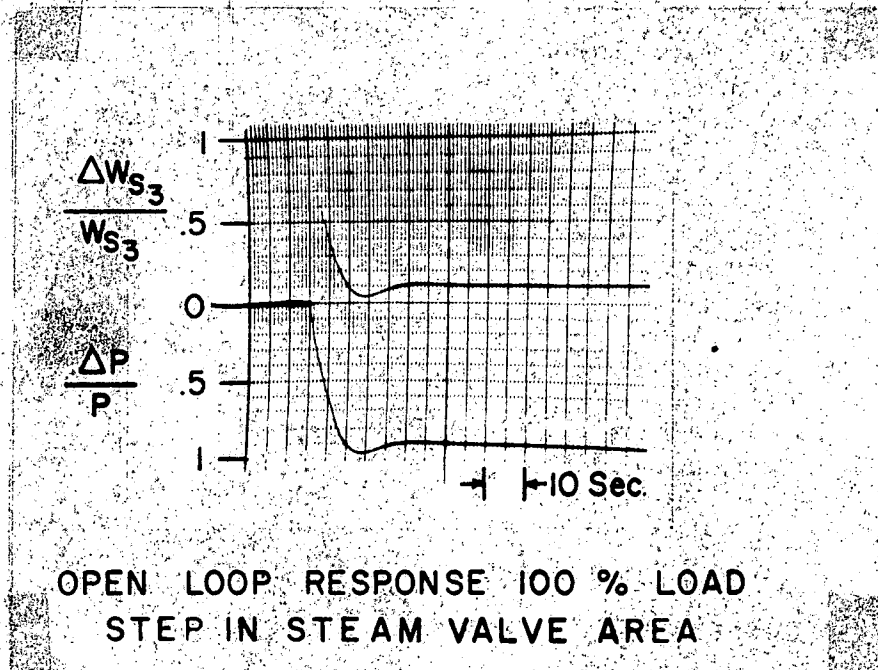
The control action should weaken the coupling between regulated variable and the disturbance. Feed forward control can theoretically provide a complete uncoupling.

Feed forward control is a means of parallel path communication in which a corrective action along one path just "bucks out" the effects of a disturbance feeding along a natural path in the system. The bucking signal is directly initiated by the disturbance. This method of control however does not provide an actual comparison between input and output. Should some piece of equipment stray from its initial design characteristics, the system has no means of self correction.

Feedback control philosophy has inherent differences from feed forward control. The disturbance does not directly initiate a correction action. An error in the regulated variable must ensue before a corrective action can take place. This is not true if a derivative mode is provided in the controller; however, in practice this is a poor mode of control because the derivative action is sensitive to high frequency signals. Any "noise" in the sensed variable is amplified by the derivative mode. The advantage of feedback control is its self corrective capacity. Should some system parameter drift or a non-measured disturbance occur, a path of communication is available to feed back this information to the manipulated variable.

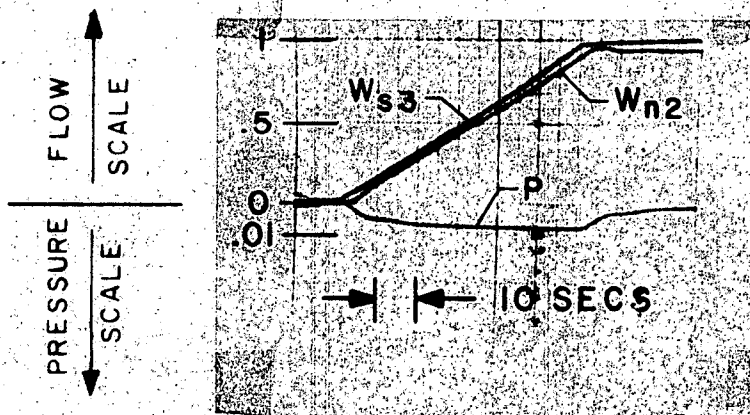
The scheme of control in this systems study uses the low distortion path of secondary flow manipulation for pressure regulation. The setpoint to the flow controller is in both a feed forward and feedback path. The pressure regulator output and the steam flow rate establish the flow controller setpoint. The steam flow sense provides a feed forward path which anticipates the disturbance to the pressure. If no distortion (lagging) occurred in the sodium control loop perfect cancellation would ensue; however, some distortion does occur which

# SYSTEM RESPONSES



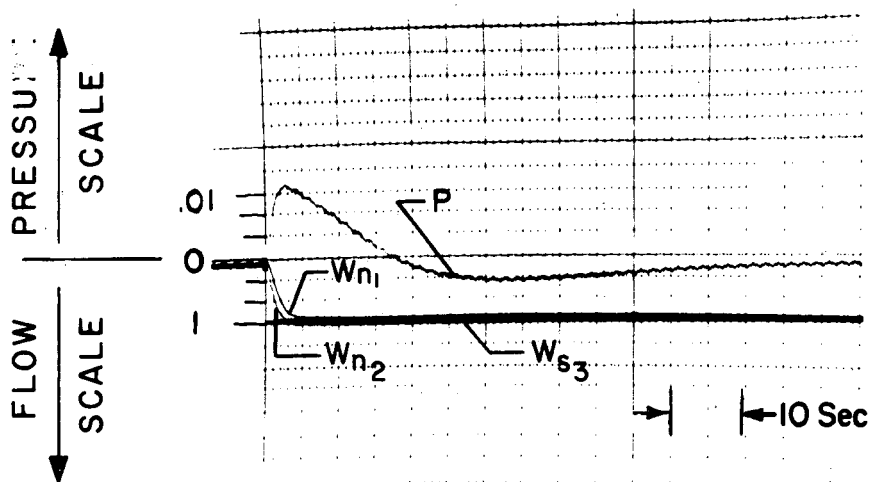
$$P = \frac{\Delta P}{2200 \text{ psi}} \quad W_{s3} = \frac{\Delta W_{s3}}{270,000 \text{ lbs/hr}}$$

$$W_{n2} = \frac{\Delta W_{n2}}{1,665,000 \text{ lbs/hr}}$$



CLOSED LOOP SYSTEM RESPONSE TO A 60 SEC RAMP  
CHANGE IN STEAM VALVE AREA AT 100% LOAD LEVEL

# CLOSED LOOP PRESSURE RESPONSE TO STEP DISTURBANCE IN TURBINE VALVE



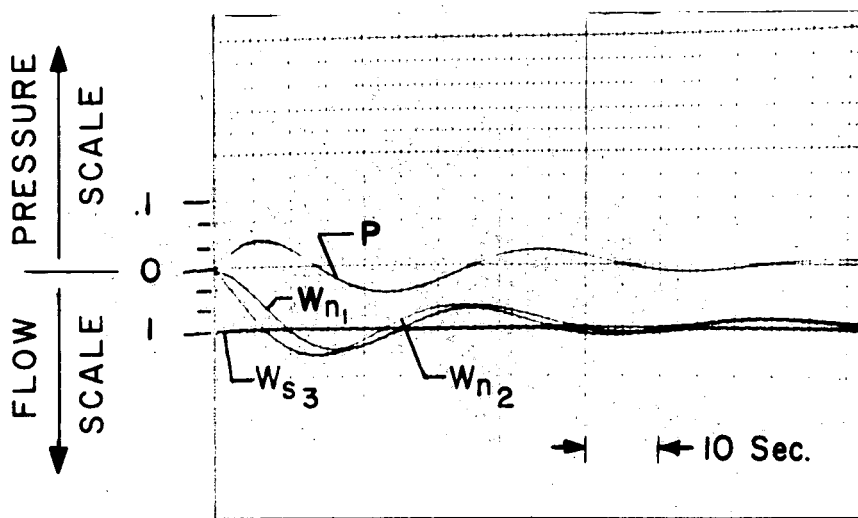
100% LOAD LEVEL

$$P = \frac{\Delta P}{2200 \text{ psi}}$$

$$W_{s3} = \frac{\Delta W_{s3}}{270,000 \text{ lbs/hr}}$$

$$W_{n1} = \frac{\Delta W_{n1}}{1,665,000 \text{ lbs/hr}}$$

$$W_{n2} = \frac{\Delta W_{n2}}{1,665,000 \text{ lbs/hr}}$$



20% LOAD LEVEL

129 032

provides a pressure droop. In steady-state the ratio of steam flow to sodium flow is nearly constant. Therefore, the primary task of the pressure regulator is to "trim" the sodium flow rate to eliminate the slight pressure offset and insure proper steady-state correspondence between steam and sodium flow rates. This is the feedback path.

The results of the normal pressure control problem are presented in Figures 2.9, A and B. They are for the 100% and 20% cases respectively. The same controller settings are used for both cases. The initial peak is determined by the relative times of the sodium loop and the boiler time constant. The pressure regulator mainly achieves steady-state correspondence. At 20% load, the deviation from the 100% response rests mainly upon the increased sluggishness of the sodium control loop and the larger relative change in load.

The fact that the controller gains may be maintained constant with large load variations indicates that conventional constant parameter controllers may be employed throughout. However, if steam flow rate is not sensed, the optimum loop gain should vary inversely with the load level. The feed forward path does not change the variable optimum pressure gain requirement, but it facilitates good performance with less than optimum control adjustment.

The local loop scheme for isolating the sodium dynamics and anticipatory action of the steam feed forward control action provide the heart of the solution to the pressure regulation problem. The anticipation provided by the steam sense is in the main equivalent to the derivative mode of feedback control but without the noise sensitivity.

Parameter Values for Figure 2.12

Pot. No.	Parameter	100% Load Pt.	20% Load Pt.
1	$K_P$		
2	$\frac{1}{\tau_2}$		
3	$\frac{K_P}{\tau_2}$		
4	$\frac{1}{\tau_2}$		
5	$\frac{1}{\tau_{x2}}$	.1538	.0699
6	$\frac{1}{2R_N}$	.500	2.500
7	$\frac{1}{2}(1-\Gamma^2)\frac{1}{R_S}$	.4482	2.118
8	$\frac{1}{2}(1-\Gamma^2)\frac{1}{R_N}$	.4482	2.224
9	$\frac{1}{\tau_{x1}}$	.1538	.0699
10	$\frac{1}{\tau_P}$		
11	$\frac{(T_1 - T_8)R_S}{2T_8}$	.0493	.0455
12	$R_S$	1.000	.2120
13	$\frac{1}{\tau_1}$		
14	$\frac{1}{\tau_e}$	.1612	.1612
15	$\frac{1}{2R_N}$	.5000	2.500
16	$\frac{\alpha_a}{\tau_a}$	.3950	.1880
17	$\epsilon \frac{\alpha_a}{\tau_a}$	.3720	.1878
18	$\frac{\alpha_a}{\tau_a}$	.3950	.1880

Pot. No.	Parameter	100% Load Pt.	20% Load Pt.
19	$\frac{R_q}{B}$	1.776	.3560
20	$\frac{\lambda T_7}{T_1 - T_2}$	.3000	.2800
21	$\alpha_a \frac{R_q}{B}$	5.150	2.460
22	$\frac{\alpha_a}{\tau_a}$	.3950	.1880
23	$\epsilon \frac{\alpha_a}{\tau_a}$	.3720	.1878
24	$\frac{1}{(1 + K_R) R_N}$	.3750	1.875
25	$\frac{K_R - 1}{1 + K_R}$	.2500	.2500
26	$\epsilon$	.9430	.9990
27	$1 - \epsilon$	.0570	.0010
28	$\frac{1}{\tau_{P5}}$	.7800	.1560
29	$\frac{1}{\tau_{P5}}$	.7800	.1560
30	$\frac{1 - G_x}{\tau_{x1}}$	.0174	.0030
31	$\frac{G_x}{\tau_{x1}}$	.1364	.0669
32	$\frac{G_{FN}}{\tau_{SH1}}$	.2281	.0529
33	$\frac{1 - G_{SH}(1 \mp \Gamma)}{\tau_{SH1}}$	.1797	.0305
34	$\frac{G_{SH}(1 \mp \Gamma)}{\tau_{SH1}}$	.1289	.0257
35	$\frac{1}{\tau_{SH1}}$	.3086	.0562
36	$\frac{1}{\tau_{P4}}$	1.008	.202

Parameter Values for Figure 2.12

POT. NO.	PARAMETER	100% LOAD PT.	20% LOAD PT.
37	$\frac{1}{\tau_{P4}}$	1.008	.202
38	$\frac{1}{\tau_{S2}}$	.9250	.1850
39	$\frac{K}{\tau_{S2}}$		
41	$\frac{1}{\tau_{a2}}$	420.0	49.7
44	$\frac{1}{\tau_{a2}}$	420.0	497.0
45	$\frac{1}{\tau_{a1}}$	420.0	497.0
46	$\frac{K}{\tau_{a1}}$		
47	$\frac{1}{\tau_{S1}}$	1.800	.3700
48	$\frac{1}{\tau_{S1}}$	1.800	.3700
49	$\frac{1}{\tau_N}$	.8130	.8130
50	$\frac{1}{\tau_N}$	.8130	.8130
51	$\frac{2 K_R}{(1+K_R) \tau_N}$	1.016	1.016
52	$\frac{K_R}{(1+K_R) \tau_N R_N}$	.5080	2.540
53	$\frac{K}{\tau_{R1}}$		
54	$\frac{1}{\tau_{R1}}$		
55	$\frac{2 K_R}{(1+K_R) \tau_N}$	1.016	1.016
56	$\frac{K_R}{(1+K_R) \tau_N}$	.5080	.5080
57	$\frac{1}{2 K_R R_N}$	.300	1.667
58	$\frac{1}{\tau_R}$		

POT. NO.	PARAMETER	100% LOAD PT.	20% LOAD PT.
59	$\frac{1}{2 K_R R_N}$	.300	1.667
60	$\frac{2 K_R}{1+K_R}$	1.250	1.250
61	$\frac{1}{1+K_R}$	.3750	.3750
62	$\frac{1}{\tau_{P1}}$	1.560	.312
63	$\frac{1}{\tau_{P1}}$	1.560	.312
64	$\frac{1 - G_X}{\tau_{X1}}$	.0174	.0030
65	$\frac{1}{\tau_{X1}}$	.1538	.0699
66	$\frac{1}{\tau_{P2}}$	1.560	.312
67	$\frac{1}{\tau_{P2}}$	1.560	.312
68	$\frac{G_X}{\tau_{X2}}$	.1364	.0669
69	$\frac{1}{\tau_{X2}}$	.1538	.0699
70	$\frac{1}{\tau_{P3}}$	.7800	.1560
71	$\frac{1}{\tau_{P3}}$	.7800	.1560
72	$\frac{G_{SH}(1 - \Gamma_S)}{\tau_{SH2}}$	.3450	.0617
73	$\frac{1}{\tau_{SH2}}$	.4237	.0677
74	$\frac{1 - G_{SH}(1 - \Gamma_S)}{\tau_{SH2}}$	.0787	.0060
75	$\frac{G_{FS}}{\tau_{SH2}}$	.1822	.0258
76	$\frac{R_g}{R_N}$	1.000	1.059
78	$\frac{(a_a)^2}{\tau_a}$	1.144	1.297

## 2.6. Temperature Regulation

In order to minimize transient thermal stresses, it is desirable to maintain system temperatures as nearly constant as possible. Three things have been provided in the control program to achieve this. Good pressure regulation has virtually eliminated any temperature deviations at the boiler and super-heater terminals. However, the intermediate exchanger terminal temperatures may drift from a constant condition if the reactor outlet temperature changes or if an unbalance between primary and secondary flow rates occur. To eliminate the second condition, secondary flow rate provides the set point to the primary flow controller. This essentially isolates the intermediate exchanger from temperature variations.

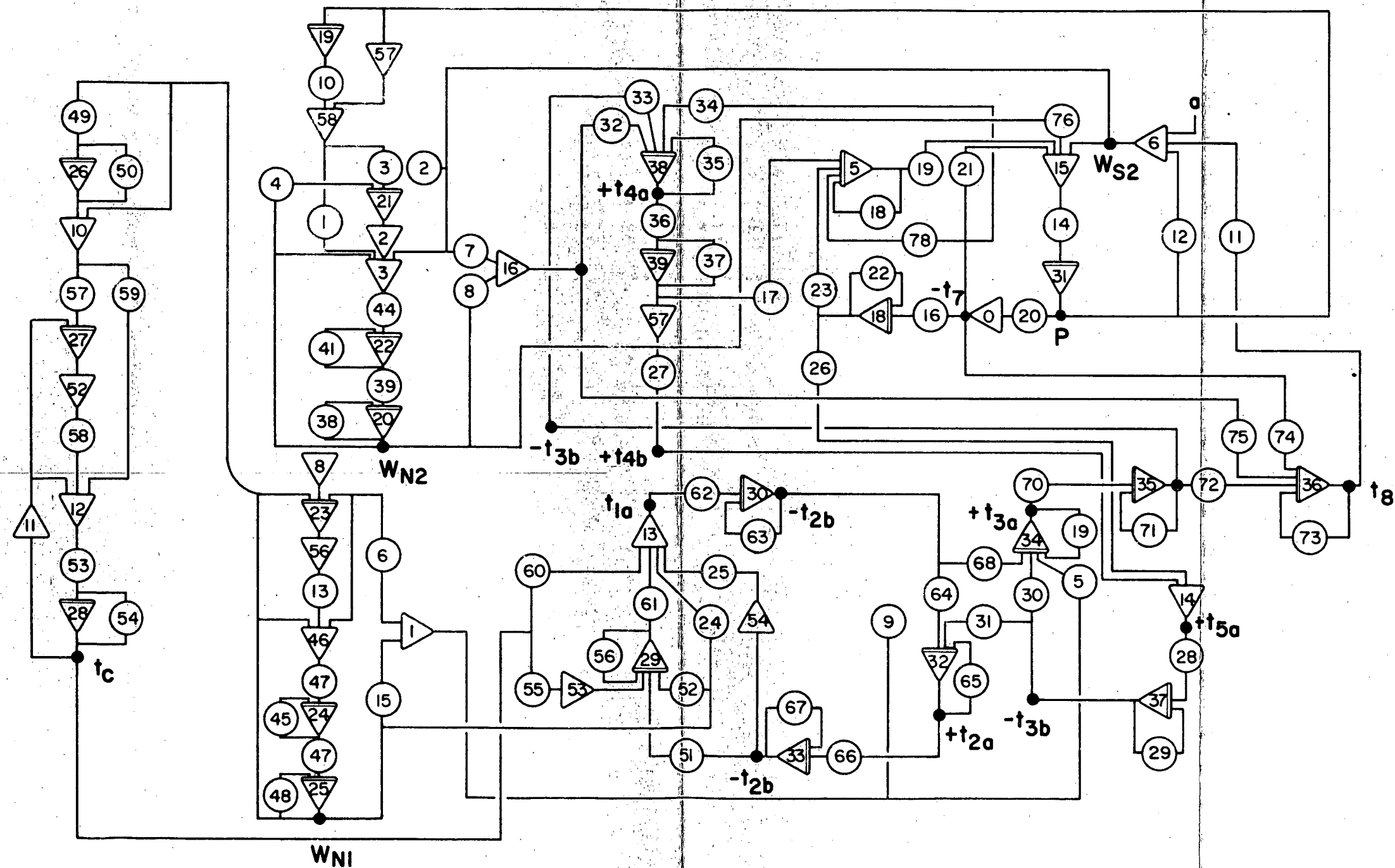
Even though the steady-state reactor temperatures do not vary as load changes with fixed rod position, transient temperature variations may occur in response to a coolant flow rate variation. The analysis in Appendix A.6 provides a scheme of compensation by which a disturbance (flow change) response (outlet temperature) may be eliminated. This compensation also reduces temperature variations within the reactor. Here again the disturbance isolation bases upon a local loop for minimum distortion and a feed forward path to "buck out" the effect of the disturbance. The transfer relationship between flow rate and reactivity is a "forgetter" function such as Equation 2.1.

$$\frac{\tau_1 D}{\tau_2 D + 1} \quad (2.1)$$

This operator has a zero steady-state value and a finite value at infinite frequencies. Figure 2.10 is the step response of the "forgetter" transference. The rod position in the reactor is a manipulatable variable. If the transference from rod position to outlet temperature is exactly equal and opposite to the flow transference, then a means of exact cancellation is possible. In practice however, the actuator dynamics and thermal lags provide a limitation



# PRESSURE CONTROL DIAGRAM BERKELEY 1100 EASE COMPUTER



COMPUTER TIME = 10 REALTIME

FIGURE 2.12

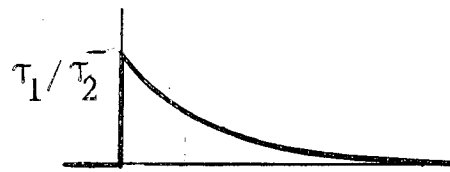
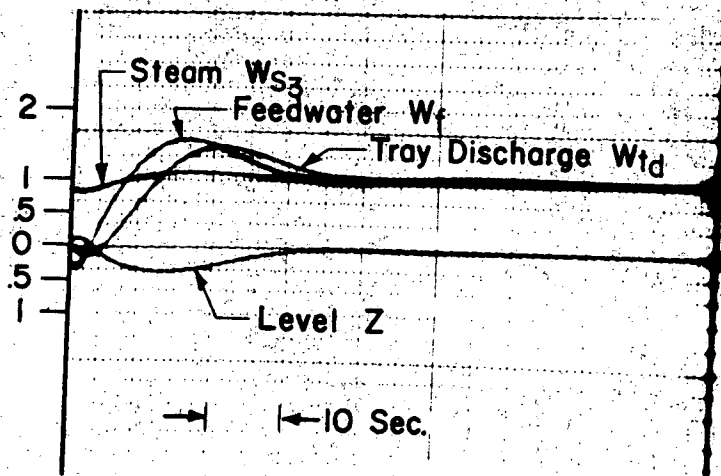


Figure 2.10  
Forgetter Step Response

to this correction. The local loop around the rod actuator minimizes the actuator distortion. Since the transient change in reactivity is proportional to the percentage change in flow, a variable compensation gain inversely proportional to the local flow is required. This is the only variable gain required in this control scheme. It should also take into account non-linearity in the rod stroke vs. the coolant steady-state average temperature. The non-constant gain can be realized with a diode function generator or a non-linearly wound resistor.

# CLOSED LOOP LIQUID LEVEL DISTURBANCE RESPONSES



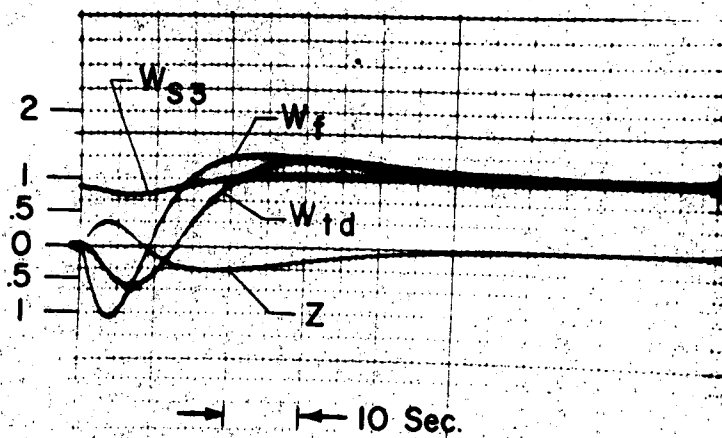
LEVEL CONTROL RESPONSE  
STEP DISTURBANCE IN  
STEAM VALVE; 100%  
LOAD LEVEL

$$Z = \frac{\Delta Z}{12''}$$

$$W_{s3} = \frac{\Delta W_{s3}}{270,000 \text{ lbs/hr}}$$

$$W_f = \frac{\Delta W_f}{270,000 \text{ lbs/hr}}$$

$$W_{td} = \frac{\Delta W_{td}}{320,000 \text{ lbs/hr}}$$



LEVEL CONTROL RESPONSE  
STEP DISTURBANCE IN  
STEAM VALVE; 20%  
LOAD LEVEL

FIGURE 2.11

## 2.7. Boiler Liquid Level Control

The prime objective of liquid level regulation is insurance against liquid carry-over to the superheater or liquid starvation to the boiler tubes. A feedback loop from liquid level measurement to feedwater manipulation provides a mode of self regulation.

### 2.7.1. The Dynamic Model

The illustration in Figure A.5.1 provides a functional interpretation of the boiler drum separator. Liquid feed to the boiler tubes is by natural circulation. This liquid is supplied by the drum separator. The riser discharges to the drum separator. Feedwater supplied to the boiler enters onto the perforated deck plate and flows radially to the center. The flow on the deck plate discharges to the central downcomer which feeds into the liquid hold-up region in the separator. The perforated deck plate is a means of increasing the feedwater enthalpy up to the saturation temperature. Steam passes through the perforations, some of which condenses in the feed flow. The response of the deck plate weir liquid out-flow to liquid in-flow provides a significant lag to the feedwater system.

Another dynamic effect is in the boiler circulation. The disturbance to the liquid level problem is a change in steam generation. Since pressure regulation is good, pressure variations have negligible effect on circulation or boiler level. With an increase in steam flow, the riser out-flow increases. This increase however leads the downcomer response. This phase shift accounts for the initial surge in boiler level.

Also the phase shift provides an additional disturbance to the liquid level regulation. A block diagram is provided in Figure A.5.6. The drum separator is a mass capacitance with four streams feeding in or out. Feed flow is manipulated to provide a balance between in-flow and out-flow as well as to correct

any drifting of the liquid level and to account for blowdown.

### 2.7.2. Computer Results

The mode of control provided in the analog computer study utilizes a proportional plus integral controller which senses only liquid level. This is a one term controller as opposed to the typical three term controller being provided with contemporary boiler systems. The responses in Figures 2.11, A and B to a step in steam valve are for 100% and 20% load levels respectively. The maximum deviation to a 10% step for the load range is approximately half an inch. Since the one term controller provides good regulation, the three term controller would provide little improvement. However, if the valve characteristics are non-linear, it may be desirable to employ a local feedback loop to control feed flow, the set point being varied according to errors in liquid level. The only advantage to be gained from measurement of steam flow would appear to be a feed forward anticipation with constant (unity) gain which would make less than optimum level gain adjustment possible, thus increasing stability without sacrificing speed of response. This is similar to the pressure control scheme. The level upward surge following a load increase is much smaller at 2200 psi than at low pressure. Hence, the complicated delays employed by some three element controller manufacturers are unnecessary.

The good control is inherent in the static design of the drum separator. The cross-sectional area of the boiler is large enough to provide low one-dimensional effective throughput velocities. Therefore, deviations are slow to occur. The controller provides correction before the error can reach any sizeable magnitude. The effect of the deck lag is evident in the phase shift between the in and out-flows. This apparently is not sufficiently detrimental but a means of isolation may be provided by a "forgetter" transference to the level controller set point. This transference could sense the pressure drop

across the deck plate. The sensitivity would be to rates of change of steam flow. Valve rate or area saturation generally limits achievable performance however.

The well known paradox in boiler liquid level control is in evidence in these traces. The initial level surge has caused the feed flow to be reduced which is contrary to what is actually needed. Boiler surge or swell is caused by a step increase in riser out-flow upon a step change in load. The downcomer inertia is sufficient to prevent instantaneous downcomer flow change. The step increase in riser out-flow is attributable to an increase in steam generation caused by flashing due to a finite rate of pressure decay and increased heat transfer due to increased sodium flow and temperature difference. Of the three, the sodium flow change is by far the most important in this system.

## CHAPTER 3 - CASUALTY OPERATION AND CONTROL

The results of Chapter 2 concern normal operation. In normal operation, the system operates at the static design state points which have been predetermined as safe operating conditions. The results of the normal control analog computer study indicates that none of the transient variations deviate far from the desired steady-state values. This chapter concerns abnormal or casualty control and the possible transient and steady-state deviations from the normal state points.

### 3.1. Possible Casualty Operation

Two separate points of view may be applied to the casualty problem. One involves control and the other no control.

#### 3.1.1. No Control

In the no-control philosophy, the system must ride-out the transient condition. This is a brute force approach and requires a "hefty" (strength-wise but not transient thermal stress-wise) design of the system equipment. With no-control, there likely would be large amplitude variations in the system states. Such variations would represent large deviations from the desired normal operating state points.

Complete modeling requires large amplitude accuracy. This may require a general non-linear system model. This model however does not require a "high" degree of frequency matching with the system for this is an open loop mode of action and the final steady-state values are of major importance.

#### 3.1.2. System Under Control

The other approach to casualty problems is some mode of control action which tends to isolate the casualty. Should such a control be possible then the normal

operation state points are maintained. This reduces or eliminates the possible destructive action that could occur with the open loop approach.

Computer modeling is the same as for normal operation control studies. A higher frequency matching is necessary in a closed loop study. If the control action provides a minimum deviation from the state points, then the linearized small amplitude model is satisfactory.

### 3.2. Signal Propagation

A simple but instructive visualization of the casualty problem is the pebble in the pond analogy. Consider a still pond as analogous to a system functioning under normal operation. Drop a pebble into the pond. This is a casualty disturbance to the system. If the system is permitted to function open loop with respect to this disturbance, then the casualty would propagate throughout the system much like a wave front propagates away from the pebble. However if some mode of action could be initiated at the point of casualty, equal and opposite in effect, then the effect of the casualty would be "bucked out" before it had an opportunity to propagate to other regions of the system. In the pebble and pond analogy, this "bucking out" would be a wave originating at the same place and time as the pebble wave and equal but opposite in amplitude. This wave propagates with the same speed as the disturbance so that a net zero amplitude disturbance is insured at all times and places.

### 3.3. Control Scheme

In Chapter 2 various paths of control communication are developed. In each case, a local control loop is used if performance warrants. In so doing, the dynamic performance has been greatly improved. These are very fast paths of communication. In normal control, the set point dependencies of the local loop controllers are determined. For casualty control however, different set points are necessary. The scheme of control is one of selection. For



each casualty considered a desired set point is determined for each controller. The role of the selector is two-fold. It determines the existence of a casualty and then establishes the desired controller set point correspondence. Figure 3.1 presents a view of the overall system and the individual controllers.

The selectors are binary intelligence units. Several schemes of selector design are possible. This design used here is a lower selection scheme. Various signals may enter the selector but the lowest signal determines the mode of control. Necessarily then a casualty must be sensed as a low signal and during normal operation the normal modes of control must be the low valued signal to the selector.

For the casualty problem several additional communication paths have been added. These additions are discussed in connection with the specific casualty problem. The final control scheme provides fast communication between problem and response. The overall result is "bucking out" or isolation of a disturbance at its origin; thereby leaving the rest of the system at a normal operating state.

Many of the normal states however are selected at the low load level. For pressure regulation, the power to and from the boiler must be matched. Many of the casualty controls presented reverse the causality of normal control. In the casualty control the turbine speed regulator set point tracks pressure. This provides for a reduction of load to the boiler to match the boiler incoming power. The implications of this mode with regard to frequency regulation are discussed in Section 2.4.4.

The equipment requirements of the casualty control modes discussed are well within the capabilities of conventional off-the-shelf electronic control components.

# SYSTEM MODULATION CONCEPT AND CONTROL MODES

## CONTROL COMMUNICATION FOR POWER FLOW MODULATION

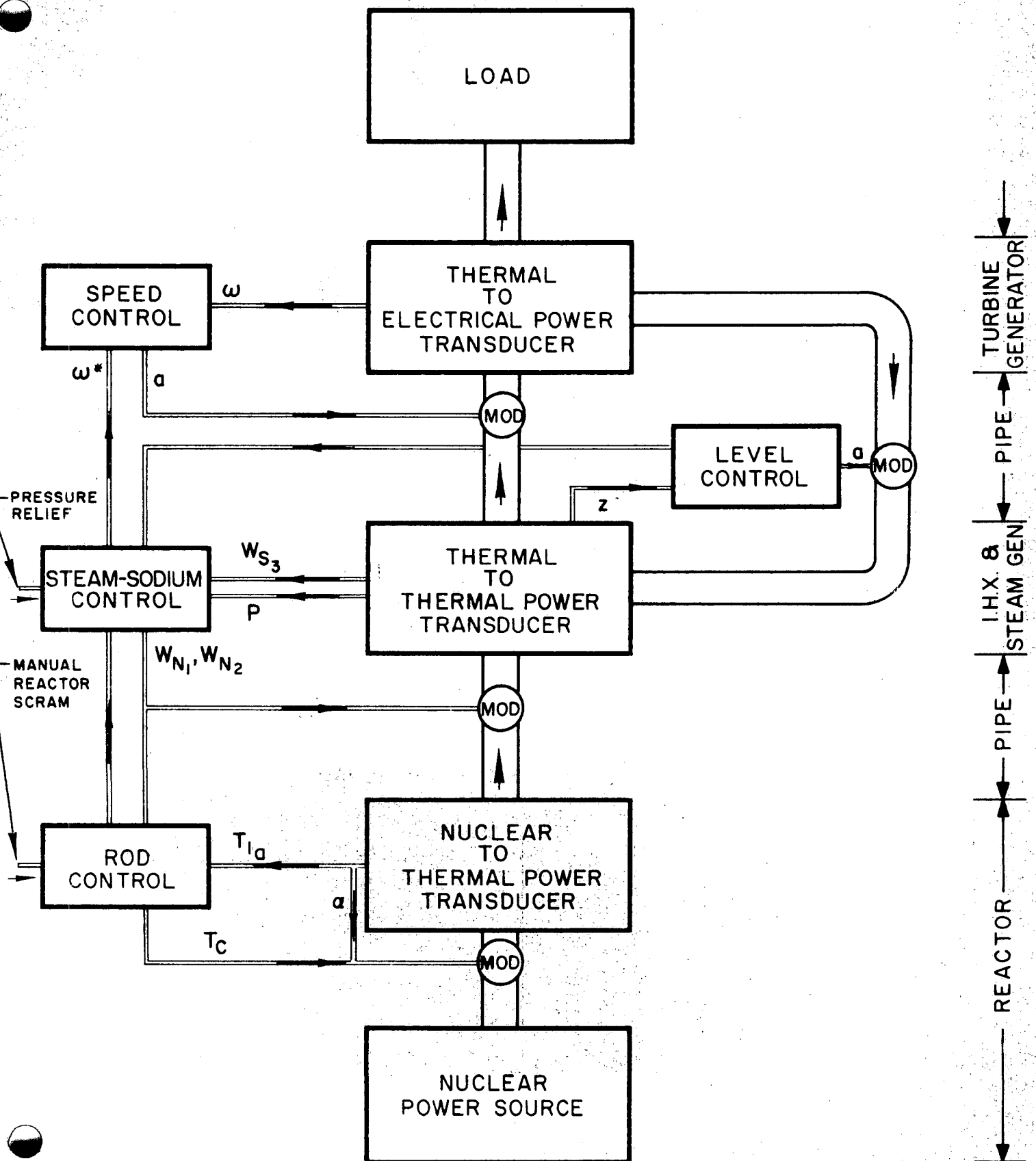
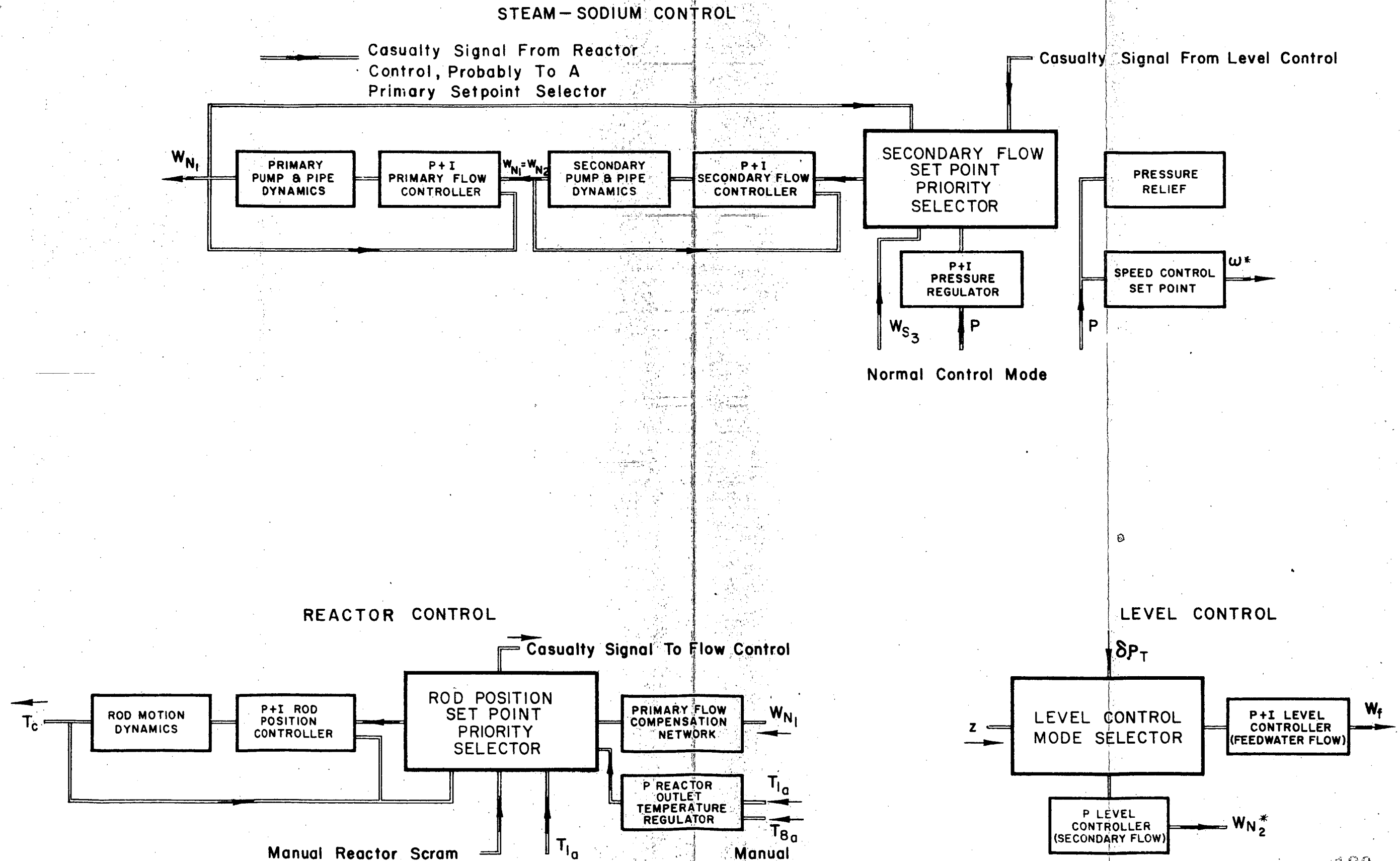


FIGURE 3.1

FIGURE 3.2



### 3.4. Failures

The failures and the modes of correction are discussed under their specific headings. The first three casualty conditions are problems which occur from without the sodium-steam exchange network. The latter occur within this network.

#### 3.4.1. Loss of Feedwater

Should control over the feedwater be lost, then a control mode should preserve a balance between out-flow and in-flow. During normal operation, the feed flow must track the steam generation; however, in the casualty mode, the steam generation tracks the feed flow. A liquid level override signal from a lower limit provides a signal to the secondary flow controller selector which requests the sodium flow to control liquid level. Again the pressure regulation is maintained through a pressure override on the turbine governor. All other control actions function normally.

Figure 3.3 presents the computer results to a loss of feedwater control. Figure 3.3.A is at 100% load level; Figure 3.3.B is at 20% load level. The upper trace is boiler pressure and the lower trace is boiler liquid level. Each is controlled by a proportional controller with no reset or integral action. The gain of the pressure regulator is 50 and the gain of the level regulator is 2. The level response is sensitive to the gain setting particularly at low loads. However, the maximum level error is within safe limits.

This override pressure controller gain setting and the pressure response of Figure 3.3 are representative of all modes of casualty control in which the pressure override on the turbine speed governor provides pressure regulation. The regulation loop is the same for each casualty condition which selects this mode. Differences in the responses occur only in the disturbances to this loop.

In the event the feed flow control is lost at a high value, then an over level sense should actuate some means of correction such as a motor operated gate valve. This could be to full closure or some intermediate point. For partial closure then the previous level casualty control will automatically take over. The advantage here is the thermodynamic states are maintained so that a slow manual shutdown, if desired, is possible.

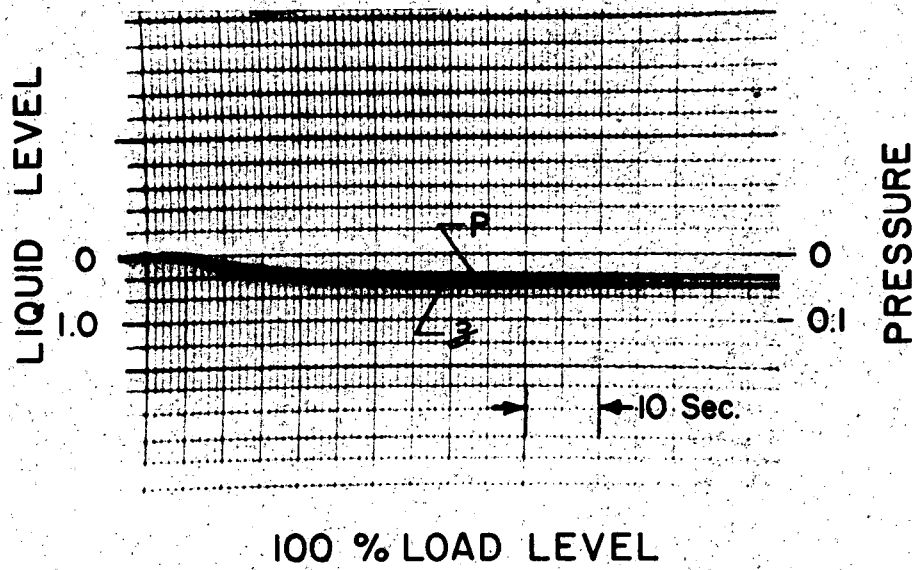
Figure 3.4 presents the turbine-generator-electrical load model used in this study. The turbine and generator models are taken from Reference 6. However, this model accounts for the interaction of the generator with the other generators in the network. Equation(3.1) is an energy balance for the generator

$$\text{Power}_{\text{in}} - \text{Power}_{\text{out}} = I D \omega \quad (3.1)$$

where  $I$  is the turbine-generator moment of inertia.  $\text{Power}_{\text{out}}$  is the total network electrical load less the power supplied by the other system generators. From Figure 2.6, the power supplied by the rest of the system is  $K_l \omega$ . Figure 3.5 presents a block diagram representation of equation (3.1). The values of the parameters used in this model are present in Table 3.1.

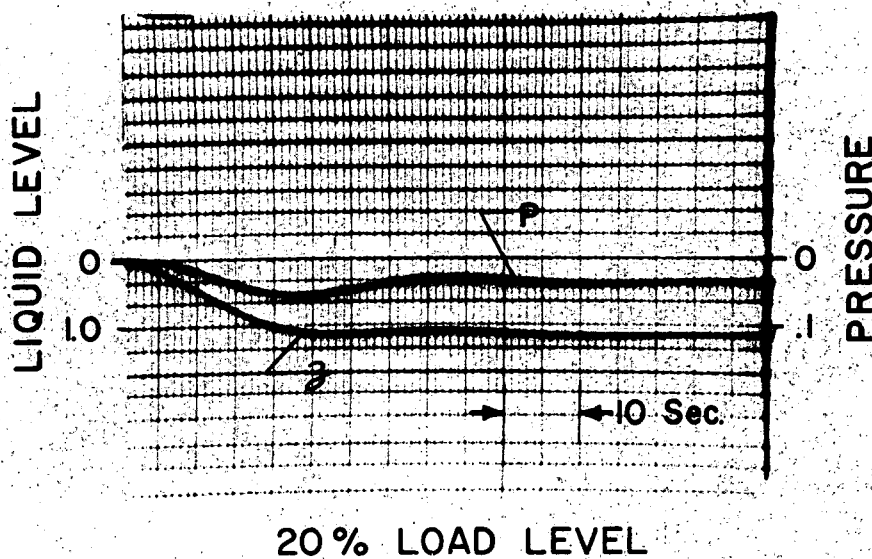
TABLE 3.1

$$\begin{aligned} \tau_t &= .4 \text{ sec} \\ K_l &= 100 \\ T_t &= 20 \text{ sec} \\ \tau_m &= .1 \text{ sec} \end{aligned}$$



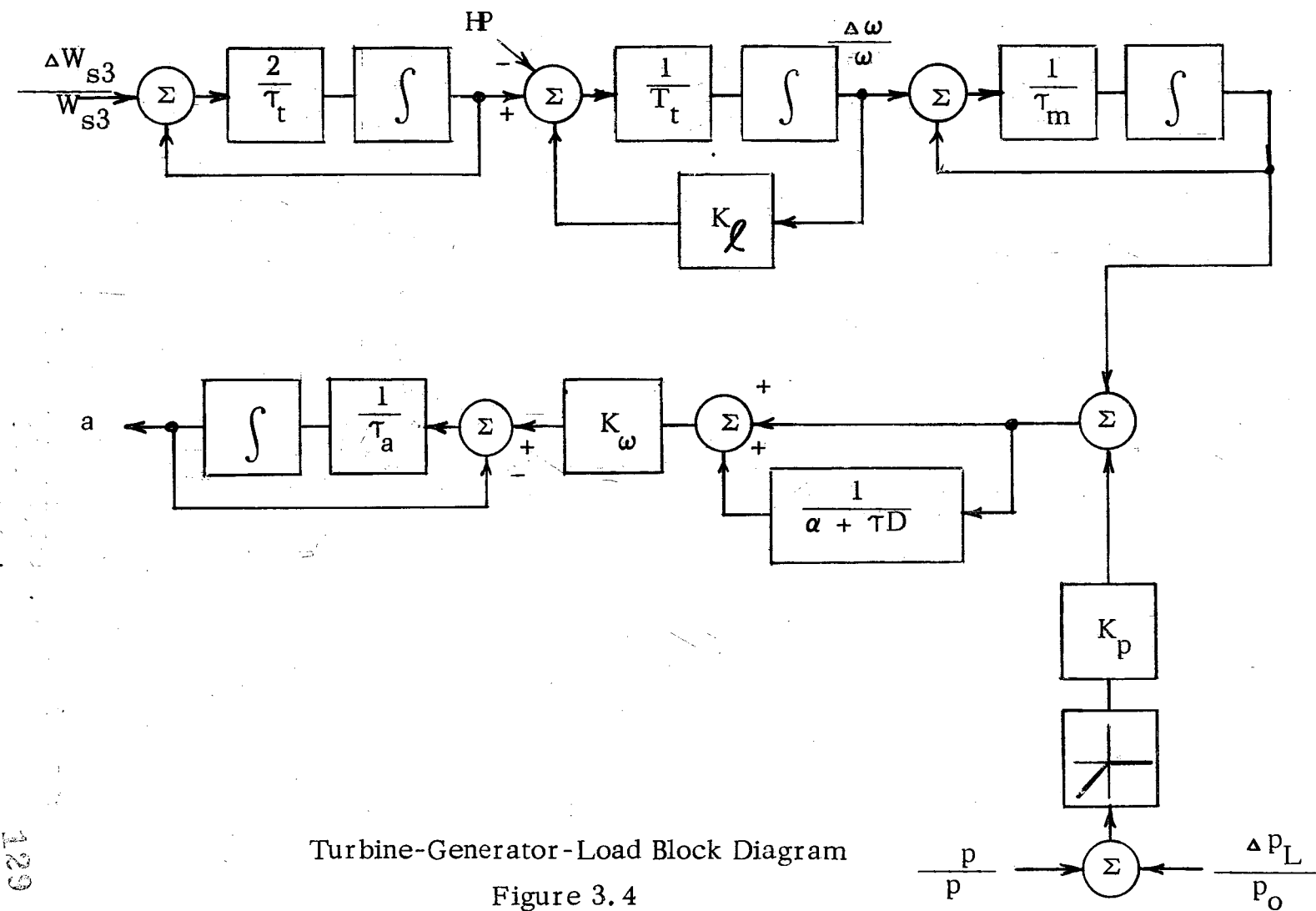
$$P = \frac{\Delta P}{2200 \text{ psi}}$$

$$Z = \frac{\Delta Z}{12''}$$



CASUALTY LEVEL CONTROL-LOSS OF FEEDWATER

129 051



Turbine-Generator-Load Block Diagram

Figure 3.4

Table 3.1 (Cont)

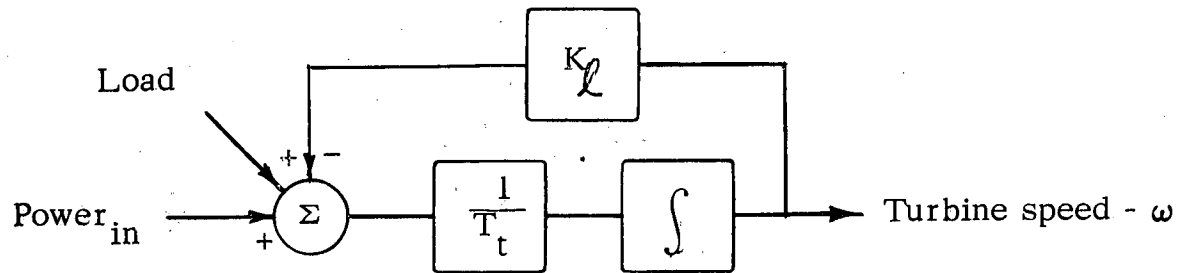
$$\tau = \infty$$

$$\alpha = 0$$

$$K_{\omega} = 50$$

$$\tau_a = .1 \text{ sec}$$

$$K_p = 50$$



Turbine Momentum Equation

Figure 3.5



The symbols used for the turbine model do not correspond to the definitions in the nomenclature. Figure 3.4 and Reference 6 define these symbols.

### 3.4.2. Reactor Scram

Reactor scram calls for a complete and immediate shutdown of the energy source. This mode may be excited through a manual request or some one of the automatic safety provisions on the reactor may request this mode. The control rods are dropped immediately. If no other manipulation occurred such as a flow change, the reactor outlet temperature would drop. A low temperature selector on the reactor outlet temperature selects this temperature as the sodium loop set point. In this case, however, it is advisable to have primary sodium flow control the reactor outlet temperature directly. A signal provision discussed under loss of sodium pumps and measurement provides a possible mode in which secondary sodium flow tracks primary flow rate. Primary flow control of reactor outlet temperature insures a minimum of temperature variation to the intermediate heat exchanger. Maintenance of balanced primary and secondary flows minimizes temperature variations from the intermediate exchanger.

This, however, is a proposed scheme which requires detailed information about the reactor. The sodium loop becomes slower with diminishing flow rates. The effective control loop gain increases with decreasing flow, therefore, a fixed parameter controller necessarily must be adjusted for the worst system condition. This necessarily sacrifices the initial speed of response. This control mode may not prove feasible if the temperature response to rod motion is fast relative to the control loop dynamics.

To eliminate this lagging, the sodium loops could also scram. This is an open loop mode of action with respect to reactor outlet temperature and therefore nothing can be said about its variation. If the sodium flows drop

faster than the rod, then an over-temperature might be possible. In any event, analysis requires a more detailed knowledge of the reactor.

The boiler liquid level control is maintained through the normal modes prescribed in Chapter 2. The rate of change of steam flow however may be too fast for the feed flow to track; the feedwater control valve may rate saturate for the large amplitude change associated with casualty operation. For all other flow rates fixed, an incremental statement of continuity on the drum separator is

$$\Delta W_f = \rho_f A_H \frac{\Delta y}{\Delta t}$$

Consider a drop to the 10% load level. Then for a 20 second valve actuation time (for rate saturation this is a 20 second ramp response) the incremental change in liquid level is

$$\left( \frac{243,300}{3,600} \right) \frac{(20/2) (12)}{(50.3) (37.3)} = 4.3''$$

This saturation problem is possible in many of the casualty possibilities but apparently is not a severe problem.

### 3.4.3. Loss of Load

Should some casualty occur at the electrical end of the system, circuit breakers could be opened. This reflects as a near instantaneous dropping of load. The turbine governor would react immediately and shutdown the steam valve. In order to minimize the thermal energy stored in the system, it is necessary to scram the reactor immediately. Signals propagate from both ends of the system through the normal and casualty control paths and meet somewhere in the middle. To reach final steady-state, the after-heat from the reactor must be removed and the sodium and steam allowed to reach isothermal equilibrium. Minimum bounds on the sodium flow rates enable energy to be

transported from the reactor to the boiler. A pressure relief valve may be set to maintain some maximum steam pressure. Ultimate safety to personnel is provided by a high flow relief valve set at a higher pressure. This mode is non-regulatory once the high-flow relief valve is opened, it remains open until manually reset. Necessarily the steam system drops rapidly to ambient conditions introducing a severe thermal transient to the system. Hence the latter is to be avoided if possible.

The low-flow pressure relief might be a turbine by-pass from the steam generator to condenser. A cascade of restrictions could provide the necessary pressure drop resistance and reduce the local erosion problem at each restriction. If the throttled steam temperature to the condenser is too high from a thermal shock viewpoint, a liquid spray injected into this stream can eliminate this problem. A detailed study of this system requires knowledge of the reactor after-heat.

After-heat is a problem common to all thermal reactors. Experimental reactors typically have several coolant streams available. During the failure or shut-down of one, another may be put into service to insure the continuous removal of energy.

#### 3.4.4. Loss of Secondary Pump, Flow or Flow Sense

Should some casualty occur whereby the secondary sodium flow rate drops, the normal control action of the primary loop still occurs; i.e. primary and secondary flow still track. The loss of secondary flow develops an error signal at the secondary controller which would drive the secondary pump motor field current to its maximum value. However, if the secondary set point selector sense primary flow rate then the secondary controller will track primary flow for it will be the low signal to the selector. A small gain should be in this sense path otherwise the selector would be actuated under a normal load change. Maximum normal load change is a 10% variation; therefore, a

1.15 gain in the primary sense path should be satisfactory. Through the speed governor set point override the steam valve controls system pressure.

Should flow sense be lost then the signal or lack of signal from the sensor should be down at the bottom end of the calibration range when a lower selection operation is used. Then the primary flow rate will drop to its low value which in turn actuates the secondary selector and drops the secondary flow rate.

Flow is lost in a pipe fracture. The very same mode of action ensues as a loss of sense or pump.

#### 3.4.5. Loss of Primary Pump, Flow or Flow Sense

The primary flow rate drops for a loss of primary pump. This signal actuates the secondary set point selector. The secondary pump flow then tracks 1.15 times the primary flow. The reduced signal feedback to the primary controller provides a large error signal which would drive the pump motor field current to its upper limit. However, the reduced set point, secondary flow, prevents this. Also in this mode, the turbine governor override provides pressure control to the system. The very same step-by-step argument for loss of primary sense or pipe fracture follows and the very same mode of action goes into operation.

#### 3.4.6. Controller Failure

Controller failure differs from the failures considered in that no means are available to operate the manipulated variable. This is open loop operation. The system has no controlled means of regulation or isolation from disturbances. The safest condition may be a controlled shutdown.

Sodium flow controllers should fail to a low value. This takes the system down to its shut-off flow rate.

Level controller failure is not quite so critical for a supplementary control exists when the sodium flow controllers track boiler liquid level.

The pressure controller should fail to a low signal. This means no pressure feedback. The system regulation now follows through the feed forward control of steam sense to sodium controller set point.

#### 3.4.7. Loss of Steam Pressure and Flow Sense

The pressure regulation scheme relies upon a pressure and flow rate measurement of the steam system. If pressure sense fails, the regulator will drive the sodium flows to their upper limit. This could lead to a severe over-pressurization of the boiler. The pressure relief valve provides the ultimate safety. Two remedies may be possible. The pressure signal could be biased to the regulator set point valve so that upon failure no signal or the biased signal ensues. This failure would then be identical to a pressure regulator failure. Under this scheme regulation persists through the feed forward steam flow action. (See Figure 3.6).

If the steam sense goes out, then the system persists under the action of the pressure regulator. This mode provides sufficient regulation but lacks the speed of response associated with the feed forward action. (See Figure 3.6).

#### 3.5. Transient Response Under Casualty Control

Analog studies have shown that control adjustment of flows can be achieved in much less time than the characteristic temperature response times of the heat exchangers. Therefore, with respect to the heat exchanger temperature response time, the casualty and normal control systems assure virtually instantaneous tracking of the two sodium flows and the steam and feedwater flows down to 15% of the rated values. For this reason, the maximum transient variation in temperature at any point in the sodium or steam path is not

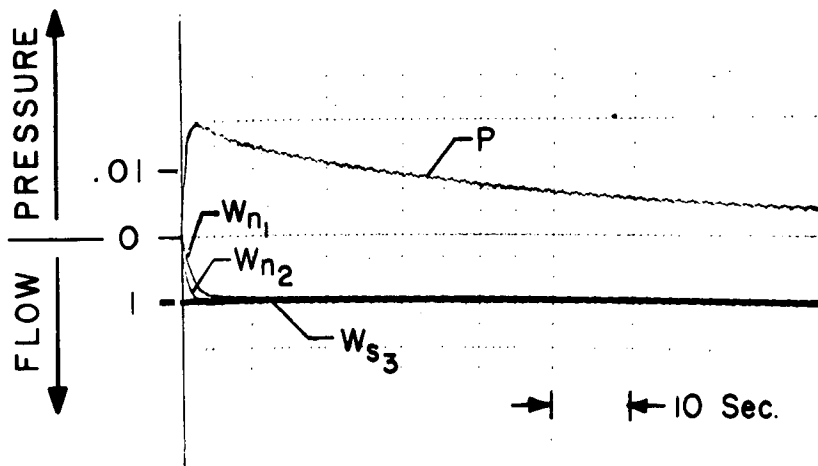
significantly different from the value predicted by steady-state analysis (Reference 2).

These temperature changes are so small, that an accurate computer determination of the actual transients requires very detailed modeling of the system behavior. It was felt that the information which could be gained from such a computer study would not justify the added sophistication required for reasonable accuracy, particularly since the film coefficient dependencies are not accurately known.

The input disturbance under casualty control corresponds to a variation in the parameter  $G$  which is introduced in the next chapter. An order of magnitude estimate of the characteristic (mean delay) time of response to a flow change for each exchanger is half the exchanger's largest transport time. This time is inversely proportional to the flow rates and is therefore very large at low loads.

The minimum controlled sodium flow rates are 15% of the rated values. Therefore, should a casualty occur such that one flow drops below this value, the casualty control will not cause the flows to track. Therefore, large variations in system temperatures might occur, but the characteristic time for these variations would be six or more times slower than at rated load. Hence transient thermal stresses are made smaller because the time available for thermal diffusion through the tube sheets is much greater than if no casualty control existed in the 100 to 15% of rated load range.

At very low flow rates, the prediction of transients is difficult because of the importance of reactor decay heat, axial conductivity in the tubes and liquid sodium, and unusual flow distributions. No attempt is made to treat the low flow problem in this study.



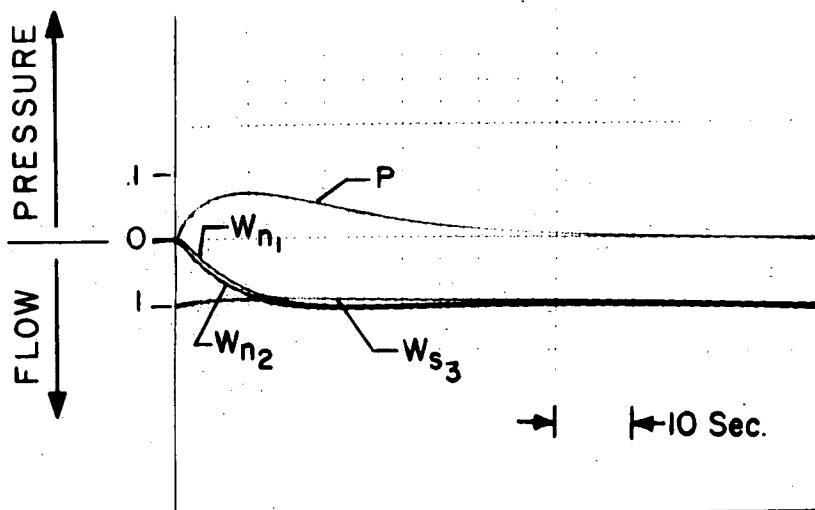
### LOSS OF PRESSURE CONTROLLER

$$P = \frac{\Delta P}{2200 \text{ psi}}$$

$$W_{s3} = \frac{\Delta W_{s3}}{270,000 \text{ lbs/hr}}$$

$$W_{n1} = \frac{\Delta W_{n1}}{1,665,000 \text{ lbs/hr}}$$

$$W_{n2} = \frac{\Delta W_{n2}}{1,665,000 \text{ lbs/hr}}$$



### LOSS OF STEAM SENSE

### CASUALTY STEAM PRESSURE RESPONSES

AT 100% LOAD LEVEL

129 059

STEP IN STEAM VALVE AREA

FIGURE 3.6

## 4. MODELING OF HEAT EXCHANGER DYNAMICS

### 4.1. Superposition and Reticulation

It is difficult to model the dynamic behavior of heat exchangers because non-linear heat transfer, energy transport, energy storage, and mass storage operations are tightly coupled and distributed spatially. The non-linear operations may be classified as "non-essential", however; i. e. for small inputs the system behaves linearly. Analysis of linear systems is far simpler than analysis of non-linear systems principally because of superposition. The behavior of linear systems with respect to any arbitrary input can be constructed from known impulse or step responses using the convolution integral.

$$\begin{aligned} y(t) &= \int_{\tau=0}^{\tau=\infty} x(t-\tau) dF(\tau) = \int x(t-\tau) f(\tau) d\tau \\ &= \int_0^{\infty} x(\tau) f(t-\tau) d\tau \end{aligned} \quad (4.1)$$

where:

$x(t)$  = arbitrary input

$y(t)$  = output response

$F(t)$  = system step response

$f(t) = \frac{dF(t)}{dt}$  system impulse response

$t$  = time

$\tau$  = dummy variable of integration



Thus, in principle, one need determine only the step or impulse response in order to completely specify linear system behavior. The same is not true for non-linear systems.

Each different input poses a new problem for a non-linear system. In general, knowledge of previous responses to other input forms is not sufficient to enable prediction of the new output response. Furthermore, in the case of the heat exchanger, boundary conditions are not specified functions of time, but depend on interactions or couplings of the heat exchanger with its interconnected equipment which may also behave non-linearly.

The conventional tools for the analytical study of non-linear systems are not powerful enough to effectively predict heat exchanger dynamics because of the spatially distributed nature of the non-linearities. Using either analog or digital computational techniques, the heat exchanger must be sub-divided (lumped) into a finite number of discrete primitive heat exchanger elements. Further, simplicity in calculations results when these elements in turn are constructed from basic operations such as heat transfer, energy transport, energy storage, and mass storage. These operations are discussed in detail in Reference 10.. There it is shown that when the wall charging time:

$$\tau_w = \frac{C_w}{H_a A_a + H_b A_b}$$

where:

$C_w$  = wall capacity

$H_a A_a$  = "a" side conductance

$H_b A_b$  = "b" side conductance

is small compared to a fluid transport time, the wall charging time may be neglected with little error and great reduction in complexity. This is the case in the IHX, superheater and boiler. With this assumption, the representations for the basic operations of heat transfer and transport are presented in the following paragraphs. Two phase energy and mass storage and their effect on natural circulation loop stability are discussed in Appendix A. 1.

#### 4.1.1. Heat Transfer

Local heat transfer between two fluid streams may be characterized by:

$$q = U (T_b - T_a) \quad (4.2)$$

where:

$q$  = local rate of heat transfer per unit area (  $\frac{\text{BTU}}{\text{sec ft}^2}$  )

$U$  = overall heat transfer coefficient (  $\frac{\text{BTU}}{\text{ft}^2 \text{ } ^\circ\text{F sec}}$  )

$T$  = local fluid temperature.

Wall capacity effects can be easily taken into account in the transport operators and are therefore neglected in the transfer representation. This also is discussed fully in Reference 10.

Equation 4.2 is an inconvenient form for analog or digital calculation. Integrating this equation over a finite (but possibly very small) region  $A_{ij}$  there results:

$$Q_{ij} = \int_{A_{ij}} dq = \int_{A_{ij}} U (T_b - T_a) dA \quad (4.3)$$

Let:

$T_{bj}$  = "b" side temperature entering the region

$T_{ai}$  = "a" side temperature entering the region

Then  $U_{ij}$  may be defined such that:

$$U'_{ij} \equiv \frac{1}{A_{ij} (T_{bj} - T_{ai})} \int_{A_{ij}} U (T_b - T_a) dA \quad (4.4)$$

and hence:

$$Q_{ij} = U'_{ij} A_{ij} (T_{bj} - T_{ai}) \quad (4.5)$$

For a single phase fluid:

$$\frac{Q_{ij}}{W_a C_{pa}} = T_{a(i+1)} - T_{ai} \quad (4.6)$$

where:

$W_a$  = "a" side mass flow rate

$C_{pa}$  = "a" side specific heat

$T_{a(i+1)}$  = exit temperature from ij region.

then substituting to eliminate  $Q_{ij}$ :

$$T_{a(i+1)} - T_{ai} = \frac{U'_{ij} A_{ij}}{W_a C_{pa}} (T_{bj} - T_{ai}) \quad (4.7)$$

If  $W_a C_{pa} < W_b C_{pb}$ ,  $\frac{U_{ij} A_{ij}}{W_a C_{pa}}$  is the effectiveness defined by Kays and London,

Reference 11. When both fluids are single-phase as in the intermediate exchanger and superheater, the parameters defined by Kays and London are inconvenient for dynamic modeling. Instead the parameters defined in Reference 10 are used here.

$$\frac{U'_{ij} A_{ij}}{W_a C_{pa}} = \frac{\alpha_{aij}}{\beta_{ij}} G_{ij} = (1 + \Gamma) G_{ij}$$

similarly

$$\frac{U'_{ij} A_{ij}}{W_b C_{pb}} = \frac{\alpha_{bij}}{\beta_{ij}} G_{ij} = (1 - \Gamma) G_{ij}$$

where:

$$\alpha_a = \frac{1}{W_a C_{pa}} \int_{A_{ij}} U_{ij} dA_{ij}$$

$$\alpha_b = \frac{1}{W_b C_{pb}} \int_{A_{ij}} U_{ij} dA_{ij}$$

$$\Gamma = \frac{W_b C_{pb} - W_a C_{pa}}{W_b C_{pb} + W_a C_{pa}} = \frac{\epsilon}{\beta}$$

$$\beta_{ij} = \left( \frac{\alpha_a + \alpha_b}{2} \right)_{ij}$$

$$\epsilon_{ij} = \left( \frac{\alpha_a - \alpha_b}{2} \right)_{ij}$$

$$G_{ij} = G_{ij} \left\{ \beta_{ij}, \Gamma, \text{configuration} \right\}$$

For counter-flow:

$$G = \frac{\tanh \beta \Gamma}{\Gamma + \tanh \beta \Gamma} \quad (4.8)$$

and when  $\Gamma = 0$  as for the steady-state behavior of the IHX.

$$G = \frac{\beta}{1 + \beta} \quad (4.9)$$

For parallel flow and any

$$G = \frac{1 - \Gamma^{-2\beta}}{2} \quad (4.10)$$

Hence both counter flow and parallel flow give the same  $G$  for the boiler ( $\Gamma=1$ ). See Figure 4.1.

For small  $\beta$ ,  $G$  is independent of  $\Gamma$  and configuration while for large  $\beta$ ,  $G$  is independent of  $\beta$ . This has great significance in the modeling of heat exchanger behavior with respect to flow rate changes. In the intermediate exchanger superheater, and boiler, the overall values of  $\beta$  are sufficiently high that changes in  $\beta$  resulting from changes in flow rates do not appreciably effect the overall values of  $G$ . Hence for load changes with constant  $\Gamma$ , the temperature distributions throughout the sodium and steam loops remain essentially constant as is shown in Reference 2. The local distribution of temperature within each exchanger may vary as load changes, however. Primary interest in this analysis has been on terminal temperatures for tube sheet thermal stresses and for establishing system couplings. Thus, for the sake of simplicity, in computation, internal temperatures have been sacrificed in most of this study and  $G$  has been assumed to be a function of  $\Gamma$  for each exchanger.

Furthermore, if good control is maintained,  $\Gamma$  for each exchanger is nearly constant even during transients. Hence, the relationship between  $G$  and  $\Gamma$  may be linearized for the study of controlled performance provided good dynamic tracking of the sodium and steam flows may be achieved. Even during casualties, the proposed control scheme assures close enough tracking of

## STATICS OF COUNTER-FLOW AND PARALLEL FLOW

$$T_{o2} = (1+\Gamma)G T_{o1} + (1-(1+\Gamma)G)T_o$$

$$B = \frac{UA}{2} \left( \frac{1}{W_o C_{po}} + \frac{1}{W_b C_{pb}} \right)$$

$$\Gamma = \frac{W_b C_{pb} - W_o C_{po}}{W_b C_{pb} + W_o C_{po}}$$

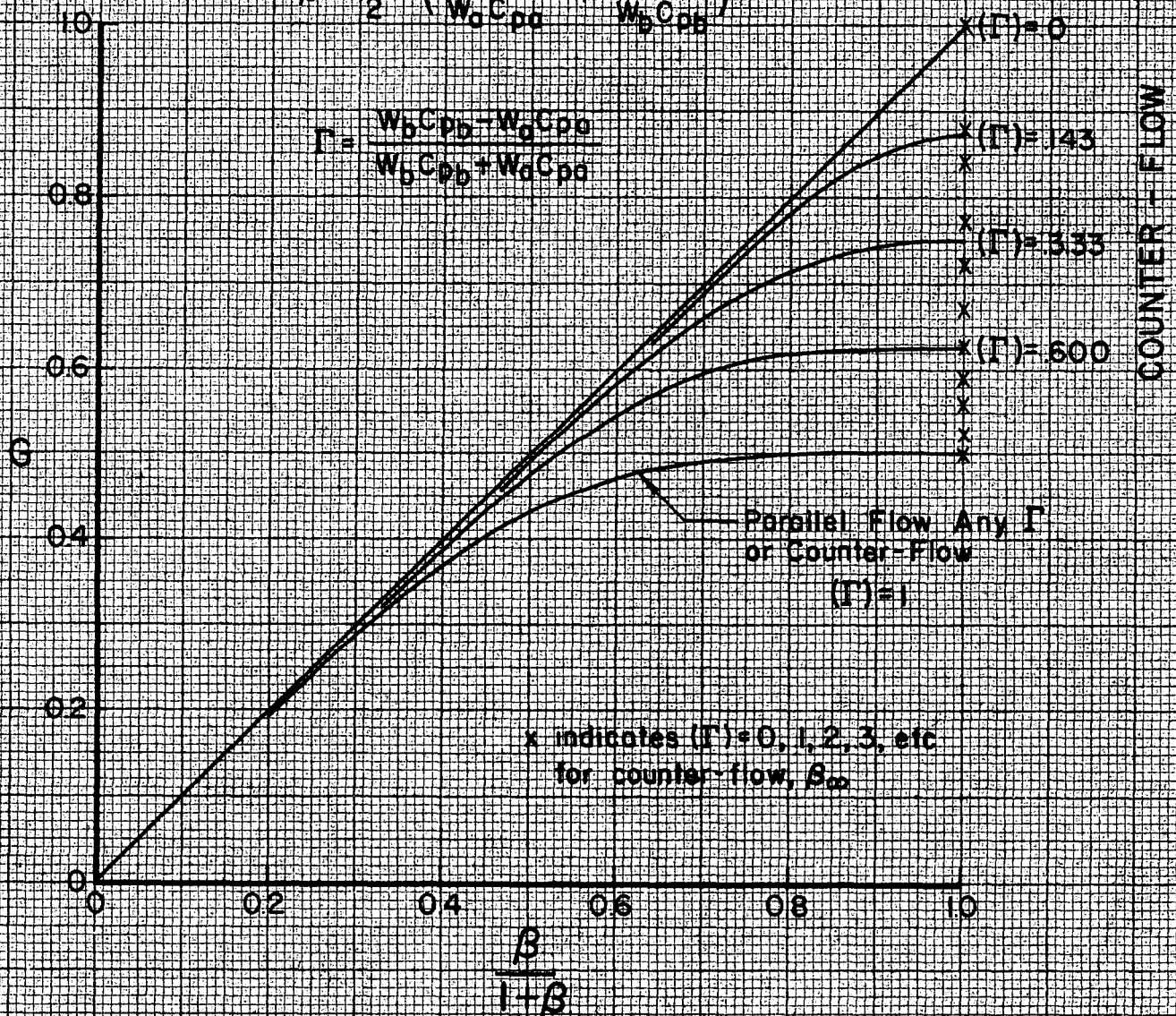


FIGURE 4.1

these flows to enable linearization of the  $G(\Gamma)$  relationship. Thus, the temperature dependence on flow rates is reflected only through changes in  $\Gamma$  which are small, hence assuring small variations in temperature and a linear dependence of temperature on  $\Gamma$ .

In turn, the small variations in  $\Gamma$  can be shown to be linear functions of the percentage change of the present value of flow rate.

$$\Delta\Gamma = \frac{1 - \Gamma_o^2}{2} \left( \frac{\Delta W_b}{W_b} - \frac{\Delta W_a}{W_a} \right) \quad (4.11)$$

or

$$\Delta\Gamma = \frac{1 - \Gamma_o^2}{2} \left[ \Delta(\ln W_b) - \Delta(\ln W_a) \right] \quad (4.12)$$

#### 4.1.2. Energy Transport

For pure transport of a single phase fluid with a one dimensional velocity profile in a pipe and with no heat transfer, the temperature at Station 2 is related to the input temperature at Station 1 by the pure delay operator.

$$T_{a2} = e^{-\tau_a D} T_{a1}$$

where:

$$\tau_a = \frac{M_a}{W_a} = \frac{L_a}{V_a}$$

$V_a$  = fluid velocity

$M_a$  = mass of fluid in pipe

With gases and vapors the stored mass is generally small making other dynamic parameters more significant.

The wall capacity correction, when the wall charging time is negligible, causes the effective transport time to be: (see Reference 10).

$$\tau_a = \frac{M_a C_{pa} + r_b C_w}{W_a C_{pa}}$$

where:

$$r_b = \frac{UA}{H_b A_b} = \frac{H_a A_a}{H_b A_b + H_a A_a}$$

The effects of mixing, non-uniform velocity profile and axial conduction are discussed in Reference 10. It is shown that the dispersion (deviation from idealized pure delay) is small for pure pipe flow. However, for shell side flow there may be significant dispersion. Mixing regions established by baffle spacings might better be characterized by simple lag operators than by pure delays. Further, short circuiting of flow through baffle openings, tends to create relatively stagnant regions with consequent increased dispersion and reduced effective transport time. These effects tend to make "exact" solutions of partial differential equations in error.

With analog equipment, it is not possible to model each transport operator as a pure delay. Instead a cascade of lags is selected. The number of lags may be determined by matching the dispersive effects caused by mixing and non-one-dimensional flow, thus enabling a truer representation of fluid transport than the pure delay itself. For tube side flow the number of lags is likely to exceed 30 (Reference 10), whereas a smaller number results for the shell side flow because of fairly well defined mixing regions.

Because the tube side transport times are small compared to the shell side times it is not important to match the tube side dispersion (very high frequency characteristics), hence a small number of lags may be used. Furthermore, the shell side outlet temperature response to a shell side temperature input is



of relatively minor importance, it not being involved directly in any control loop. Hence, a small number of lags may be used to achieve approximate responses, accurate enough for stress calculations, since the heat exchanger cross response (shell side output, tube side input or tube side output, shell side input) and responses to flow inputs are relatively insensitive to the number of lags.

## 4.2. Heat Exchanger Models

### 4.2.1. Solutions of Partial Differential Equations

Idealized linear partial differential equations applying to the counter flow exchangers and to the boiler have been solved in Reference 10. The basic equations are of the form:

$$L \frac{\partial T_a}{\partial x} (\alpha_a + \tau_a D) T_a = \alpha_b T_b \quad (4.13a)$$

$$-L \frac{\partial T_b}{\partial x} + (\alpha_b + \tau_b D) T_b = \alpha_a T_a \quad (4.13b)$$

where:

$$\alpha_a = \frac{UA}{W_a C_{pa}}, \quad \alpha_b = \frac{UA}{W_b C_{pb}}$$

$$\tau_a = \frac{M_a C_{pa} + C_w r_b}{W_a C_{pa}}, \quad \tau_b = \frac{M_b C_{pb} + C_w r_a}{W_b C_{pb}}$$

$$D = \frac{\partial}{\partial t}$$

It is assumed that  $\alpha_a$ ,  $\alpha_b$ ,  $\tau_a$  and  $\tau_b$  are constants.

The solutions for the outlet temperatures become:

$$T_{a \text{ out}} = \frac{1}{1 + (\beta + \tau D) \frac{\tanh b}{b}} \frac{e^{-\epsilon - \delta D}}{\cosh b} T_{a \text{ in}} + (\beta + \epsilon) \frac{\tanh b}{b} T_{b \text{ in}} \quad (4.14a)$$

$$T_{b \text{ out}} = \frac{1}{1 + (\beta + \tau D) \frac{\tanh b}{b}} (\beta + \epsilon) \frac{\tanh b}{b} T_{a \text{ in}} \frac{e^{\epsilon + \delta D}}{\cosh b} T_{b \text{ in}} \quad (4.14b)$$

where:

$$\beta = \frac{\alpha_a + \alpha_b}{2}$$

$$\epsilon = \frac{\alpha_a - \alpha_b}{2}$$

$$\tau = \frac{\tau_a + \tau_b}{2}$$

$$\delta = \frac{\tau_a - \tau_b}{2}$$

$$b = \sqrt{\epsilon^2 + 2\beta\tau D + \tau^2 D^2}$$

From these transfer functions, frequency response can be directly established by letting the time domain operator  $D = \frac{\partial}{\partial t}$  equal  $j\omega$ . The Laplace transformation of the unit impulse response is found by letting the Laplace variable,  $S$ , equal  $D$  (provided initial conditions are taken as zero).

For the intermediate exchanger the equations can be simplified slightly since  $\epsilon = 0$ .

For the boiler  $\alpha_b = 0$  and  $\tau_b = 0$

$$T_{a \text{ out}} = e^{-\alpha_a - \tau_a D} T_{a \text{ in}} + G_{ab} T_{b \text{ in}} \quad (4.15)$$

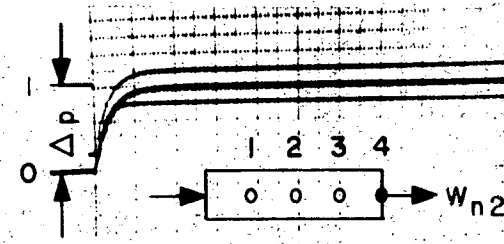
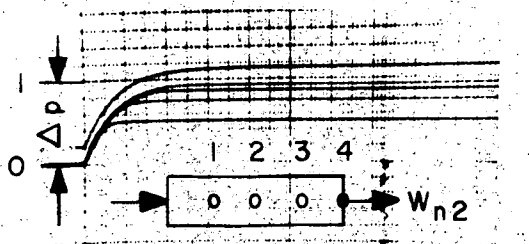
# BOILER UNCOUPLED TRANSIENT RESPONSES

FINAL STEADY  
STATE TEMPERATURE-  
DISTANCE PROFILES

100% LOAD LEVEL

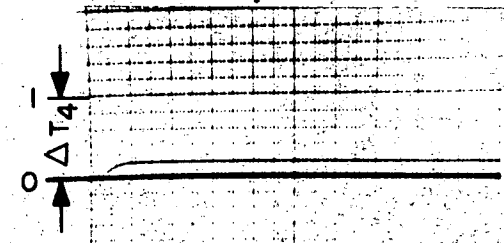
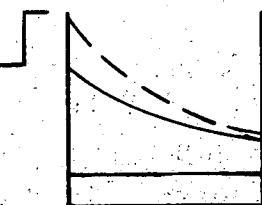
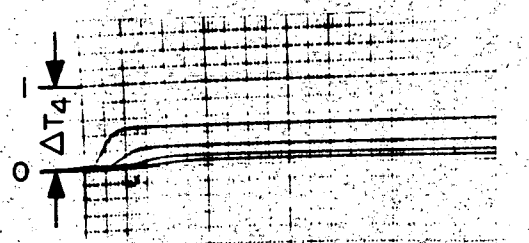
20% LOAD LEVEL

STEP IN  
EFFECTIVENESS  
SODIUM TEMPERATURE  
STEAM PRESSURE



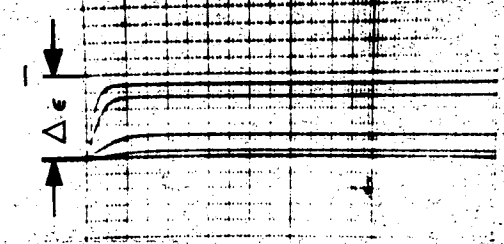
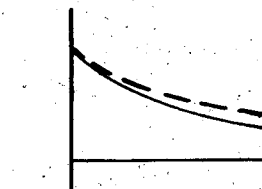
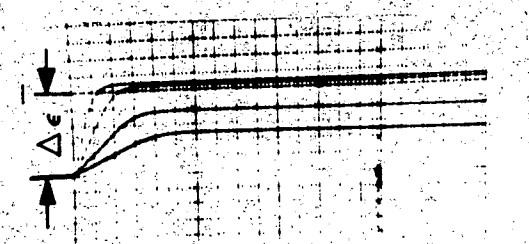
432

STEP IN  
EFFECTIVENESS  
SODIUM TEMPERATURE  
STEAM PRESSURE



234

STEP IN  
EFFECTIVENESS  
SODIUM TEMPERATURE  
STEAM PRESSURE



234

TEMPERATURE CHANGES ( $\Delta T$ ) RECORDED

FIGURE 4.2

$$\frac{Q}{W_a C_{pa}} = G_{ab} T_{a \text{ in}} - \left[ \frac{\tau_a D + G_{ab}}{1 + \frac{\tau_a}{\alpha_a} D} \right] T_b \quad (4.16)$$

where:

$$G_{ab} = \frac{1 - e^{-(\alpha_a + \tau_a D)}}{1 + \frac{\tau_a}{\alpha_a} D} \frac{1 - e^{-\alpha_a}}{1 + \left( \frac{1}{\alpha_a} - \frac{e^{-\alpha_a}}{1 - e^{-\alpha_a}} \right) \tau_a D} \quad (4.17)$$

Because the boiler effectiveness,  $1 - e^{-\alpha_a}$ , is nearly unity,  $T_{a \text{ out}}$  and  $\frac{W}{W_a C_{pa}}$

do not depend directly on sodium flow rate,  $W_a$ . The operator  $G_{ab}$  is very nearly a simple lag as is shown from computer step response Figure 4.2 and from frequency plots Reference 12.

Pipe transport is characterized by the same dynamic operation as applies for the boiler self-term, the transport delay. A more exact solution including the wall charging and steady-state heat leakage to the surroundings is given by:

$$T_{a \text{ out}} = e^{-(\alpha_a - \tau_a D)} - \frac{r_b^2 \frac{C_w}{W_a C_{pa}} D}{1 - \tau_w D} T_{a \text{ in}} \quad (4.18)$$

where:

$$\tau_w = \frac{C_w}{H_a A_a H_b A_b} = \text{wall charging time}$$

$$\tau_a = \frac{M_a}{W_a}$$

For sodium pipe flow,  $\tau_w$  is very small as is  $r_a$ .

Therefore:

$$T_{a \text{ out}} = e^{(-\alpha - \tau_a' D)} \quad (4.19)$$

where:

$$\tau_a' = \frac{M_a C_{pa} + r_b^2 C_w}{W_a C_{pa}} \approx \frac{M_a C_{pa} + C_w}{W_a C_{pa}}$$

For steam pipe flow,  $\tau_a$  is very small and  $\tau_w$  may be large because of the low superheat film coefficient. Hence it is assumed that:

$$T_{a \text{ out}} \approx T_{a \text{ in}}$$

The analytical solutions of the previous paragraphs are not sufficient to completely determine each heat exchanger's transient behavior. First of all, no solutions are given for the most important input; namely, fluid flow rate variation. This input causes the parameters of the differential equations (4.13a and b) to vary. When the flow changes are specified in advance, the equations are still linear but with non-constant coefficients. This feature is exploited in a later section to determine uncoupled step responses for large flow changes using a linear computer model. However, when the system is controlled, the flow changes are dependent on heat exchanger's behavior. Hence the system behaves non-linearly with respect to large disturbances.

Second, analytical transfer function solutions are not convenient even for linearized analysis of interconnected systems with natural and control feedback paths. Algebraic complications make examination of the effect of parameter variations extremely difficult. Hence selection of the controllers' parameters would be virtually impossible. A simple but approximate technique is available (Reference 10.) for single control loops. Where possible, this method has been exploited to achieve approximate controller settings and to

achieve an understanding of the importance of process parameter values on the controlled dynamic performance. These results have been confirmed by the analog computer study.

Third, the transfer function enables fairly easy determination of the frequency response by substitution of  $j\omega$  for  $D$ . There are algebraic complications arising from the necessity to convert terms from real and imaginary notation, which is useful for summations, to gain and phase, which is convenient for multiplications, and vice versa. Exact determination of the transient response from the transfer function is much more difficult for infinite or very high order systems. Furthermore, it is not clear that the exact response to an arbitrary disturbance (e. g., a step change in inlet temperature) would provide a particularly valuable piece of information for either control or thermal stress determinations. Far simpler but approximate methods might suffice equally as well. It would seem that the simpler method suggested by Paynter (Reference 5), which matches quantitatively the low frequency behavior and qualitatively the high frequency behavior, would provide adequate information for either problem. In addition, Paynter's method is useful in determining the approximate behavior of any point in the heat exchanger fluid path, tube wall, outside shell, or tube sheet from the analog computer results of the terminal fluid temperature transients.

#### 4.2.2. Non-Linear Computer Models

The methods of the previous section were shown to fall short of the mark on three counts. These objections can be overcome using an analog computer approach. Exact computer or analytical representation of any real physical system (except the computer itself) is impossible. Thus, all mathematical and computer analysis of physical problems is in reality analysis of idealized models which hopefully behave in certain important respects like the real physical system they represent. An important aspect of analysis, which is often overlooked, is the criterion for judging the acceptability of a model.

Dynamic models may be judged on the basis of frequency band, amplitude range, and spatial correspondence. No model is perfect over an infinite input frequency spectrum. Typically models fail at very high frequency where the usual assumptions (e. g. continuum mechanics) fail to hold. However, response at these high frequencies is generally highly attenuated and therefore of no practical consequence. In order to determine accurately stability of a feedback loop, the model of the open loop process (including controller and compensation) must be valid in the neighborhood of frequencies producing  $180^\circ$  of phase lag. Lower frequency behavior is important in establishing optimum control settings approximate closed loop transient response and steady-state behavior. Hence it is desirable for the model to match the real system behavior for frequencies from zero out to that producing an open loop phase shift of  $180^\circ$ . Beyond this frequency only a qualitative match is required. Thus, added sophistication in frequency modeling is required when lead compensation is employed and less sophistication when lag compensation is employed.

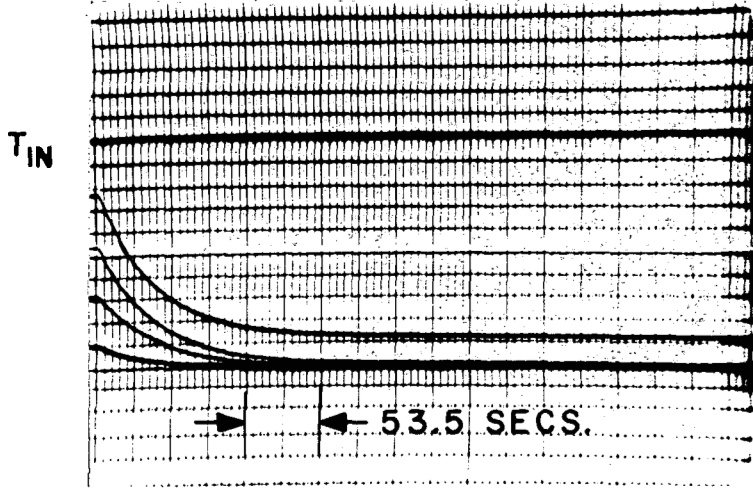
In order to match high frequency behavior using practical computational methods, it is necessary to make the system more linear, hence restricting the allowable range of input amplitudes. Occasionally a transformation of variables will enable linear analysis to apply for a large range of input amplitudes. This is the case in the present problem provided good control is achieved in which thermodynamic states in the sodium and steam loops are maintained nearly constant over the useful load range. Then, as shown in Sections 4.1.1 and 4.1.2, the heat exchangers behave linearly with respect to variations in temperatures and the logarithms of flow rates provided a variable time scale inversely proportional to the load level is employed. Some other important system components behave linearly with respect to these variables. These components include the turbine nozzle and piping, but exclude the reactor, turbine speed control loop, and the voltage control loop, as well as time constants of fixed parameter controllers in the thermodynamic

# INTERMEDIATE HEAT EXCHANGER TEMPERATURE RESPONSES TO LARGE FLOW VARIATIONS TEMPERATURE CHANGES ( $\Delta T$ ) RECORDED

## PRIMARY STREAM RESPONSE

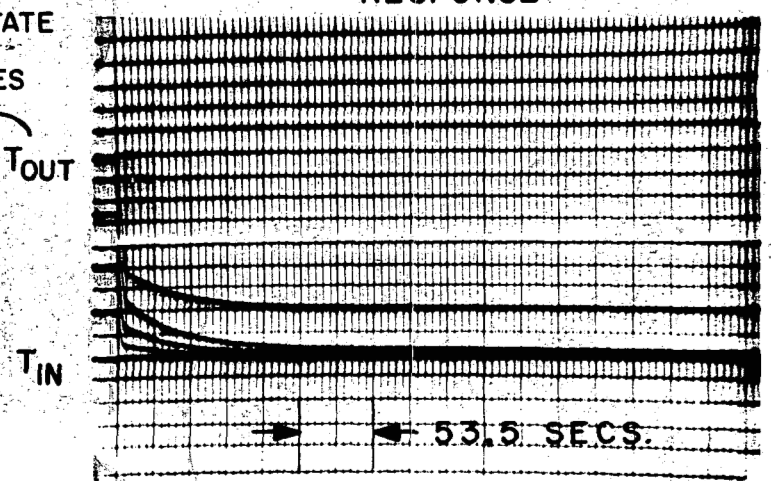
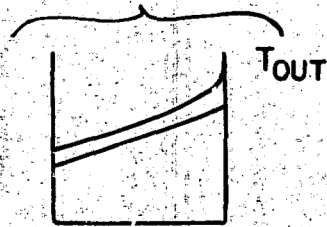
## SECONDARY STREAM RESPONSE

100% TO 20% STEP IN  
PRIMARY FLOW RATE



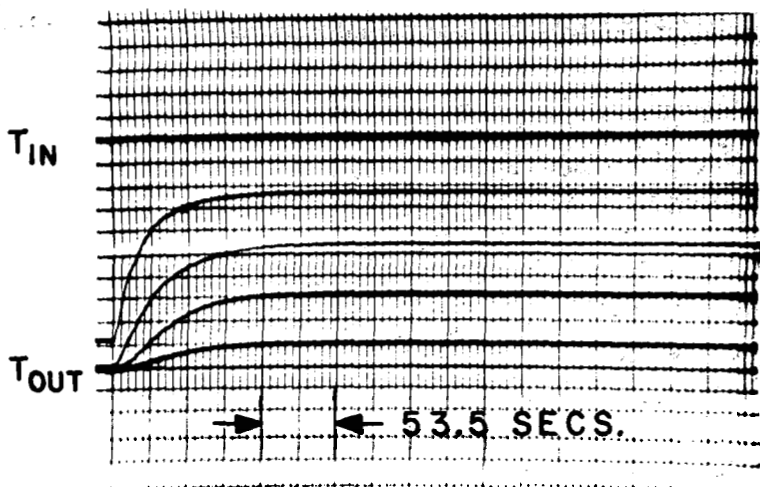
A

FINAL STEADY STATE  
TEMPERATURE  
DISTANCE PROFILES

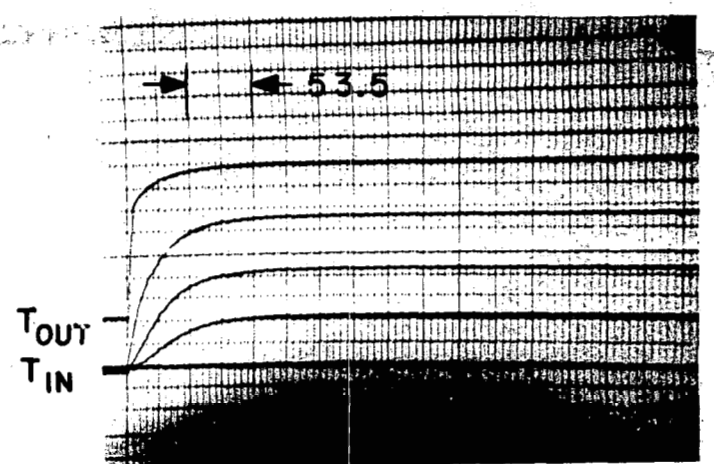
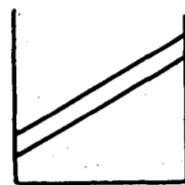


B

20% TO 100% STEP IN  
PRIMARY FLOW RATE

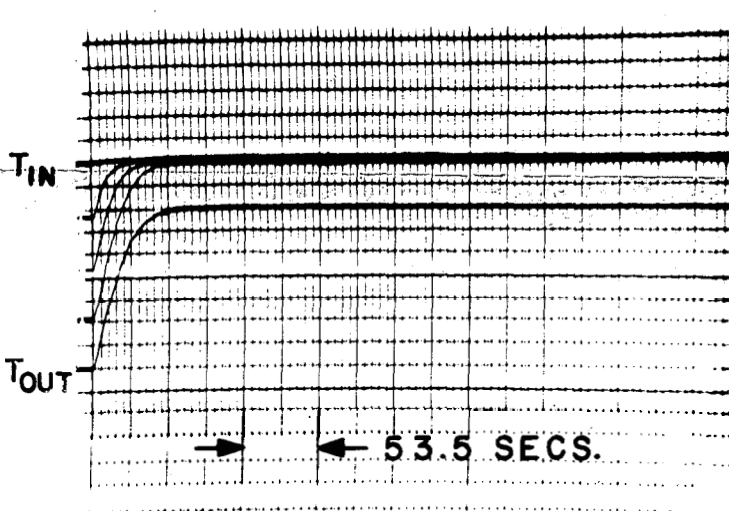


C

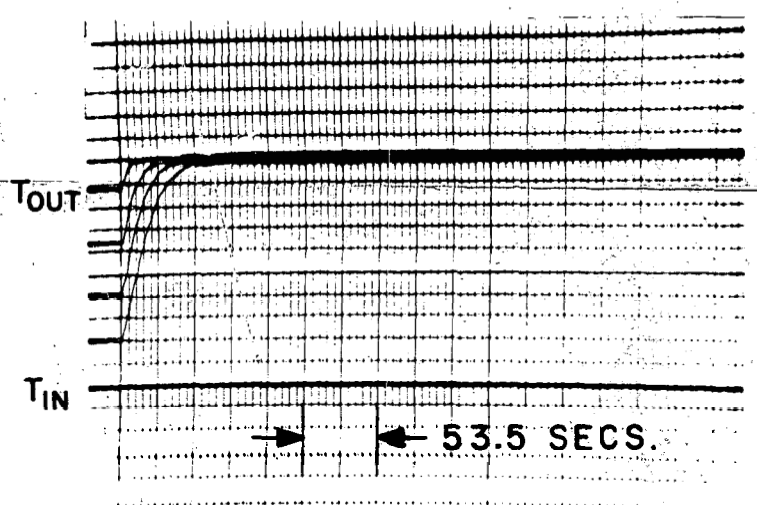
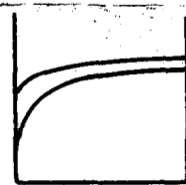


D

100% TO 20% STEP  
IN SECONDARY FLOW RATE

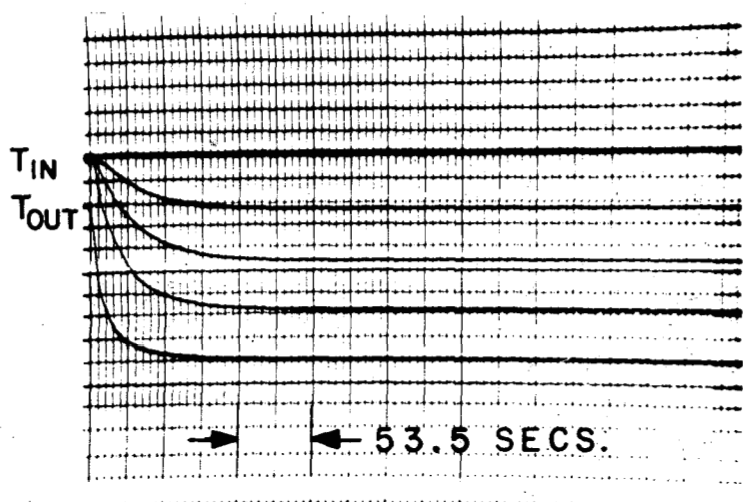


E

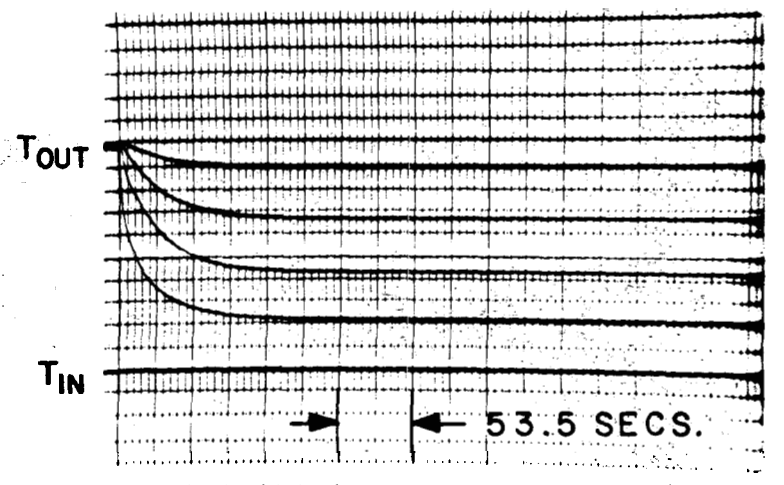
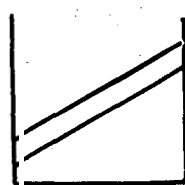


F

20% TO 100% STEP  
IN SECONDARY FLOW RATE



G



H

FIGURE 4.3



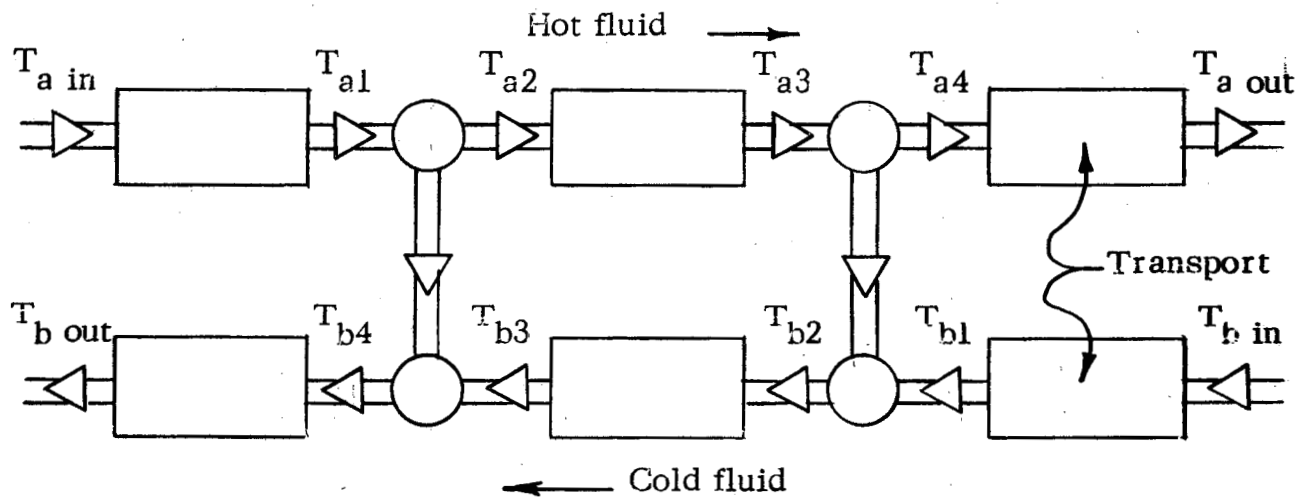
system. By exploiting the linearity with respect to the new variables, nearly uniform control is achieved over the entire useful load range. For convenience in interpreting analog data, a real time base is employed and linear rather than logarithmic variations in flow rates are plotted. This accentuates the differences in behavior at different local levels and makes the system appear much more non-linear than it really is.

If no control is employed, the system as a whole behaves non-linearly in response to large disturbances. However, because of the pipe transport delays, the non-linear interactions do not immediately affect the intermediate heat exchanger (IHx) following a step change in sodium flow. Hence the initial part of step responses of this exchanger can be determined using a linear model having a step-wise parameter variation to start the transient (see Figure 4.3). The transients in the boiler and superheater cannot be accurately determined using the same technique because the steam flow rate is not an independent variable. However, the same method in which coupling is neglected was used to study the superheater behavior (see Figure 4.7). The initial parts of these transients at least gives an idea of the type of response to be expected with no control.

Non-linear computations were not made for two reasons. First, under the casualty control scheme outlined in the previous chapter, it appears that the system always behaves quasi-linearly when using logarithmic flow and load varying time scale variables. Hence there is a need for non-linear computation only when poor or no casualty control exists. Second, because of the distributed nature of thermal systems accurate, high frequency, large amplitude non-linear modeling is not feasible with the available analog computing hardware. The following paragraphs indicate the difficulties involved.

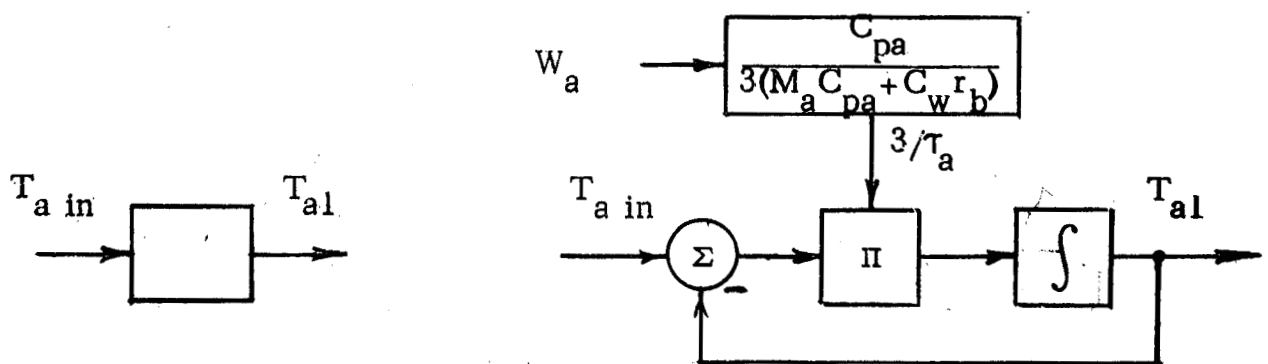
Consider a single counterflow heat exchanger. The simplest dynamic analog model which can take into account some of the natural feedback interaction associated with the counterflow configuration has two heat transfer nodes.

As was pointed out in Section 4.1.1, statics can be matched exactly with any number of nodes. In order to get good dynamic performance from the model, it has been shown in Reference 10 that three equal transport operators for each stream should be employed. An energy flow diagram is shown in Figure 4.4.



Energy Flow Diagram for a Counterflow Heat Exchanger

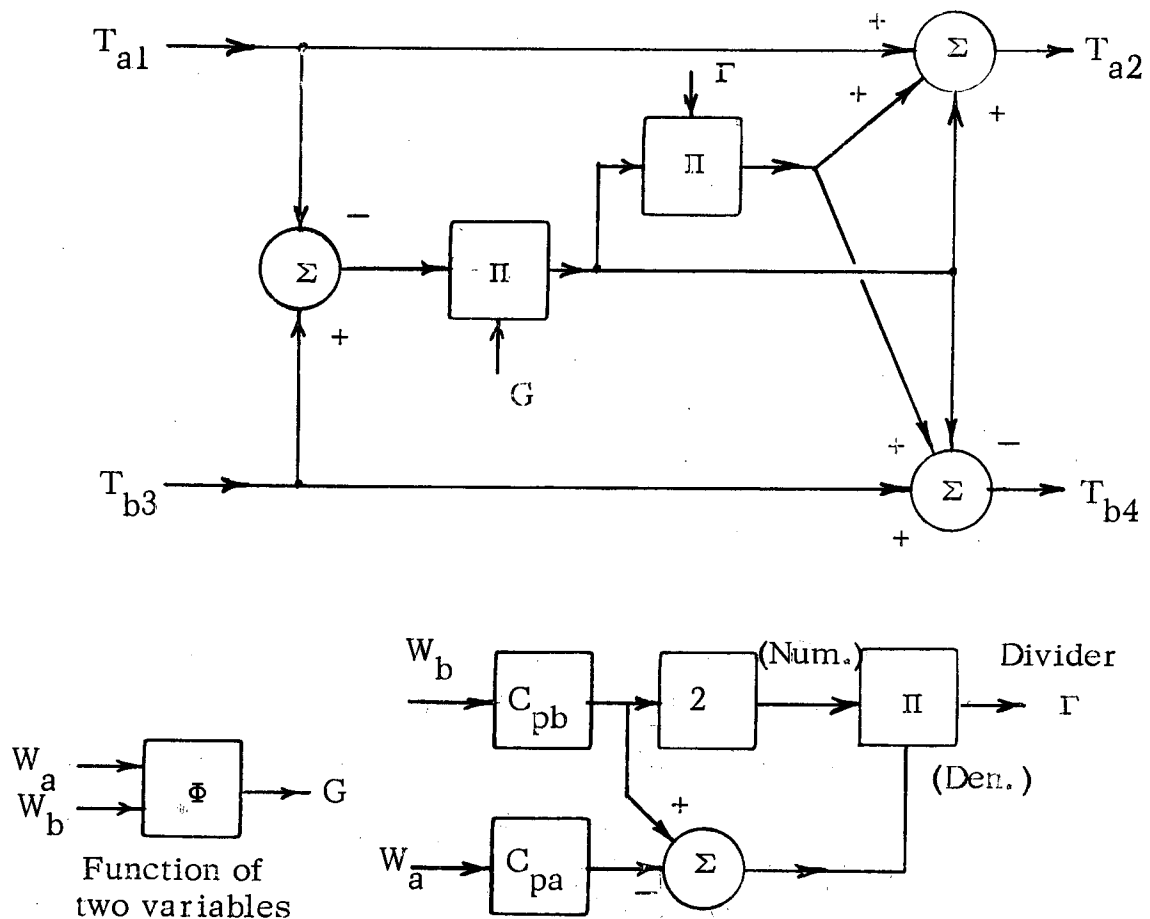
Figure 4.4



Transport Operator Analog Representation

Figure 4.5

One multiplier per operator is necessary with this scheme. Tapped variable time delay lines such as the "bucket brigade" (Reference 4.5) could be used to eliminate the multipliers but much more linear equipment would be required to achieve good accuracy. Multipliers are denoted by the symbol  $\Pi$  (for product) in the computer diagrams.



Heat Transfer Node Analog Representation

Figure 4.6

The heat transfer node representation is shown in Figure 4.6. Two multipliers are required per node. Also a function of two variables and a divider are required per heat exchanger. There are other ways of modeling the heat transfer node but none are particularly economical with either linear or non-linear equipment. Hence, it is apparent that non-linear modeling of the complete system including three heat exchangers, piping, variable turbine nozzle, reactor, and control, and sodium pump characteristics, would be a very difficult task. It would appear that all or most of the non-linearities would be important without a casualty control system.

#### 4.2.3. Linear Computer Models and Results

Linear heat exchanger behavior can be modeled using the same schemes as shown in Figures 4.4, 4.5, and 4.6. The differences are: (1) that more heat transfer nodes and transport operators may be used, (2) the transport time is assumed constant corresponding to the final load levels, and (3)  $G$  is assumed constant at the final load level value and  $\Gamma$  variations are linearized.  $\Gamma_o$ ,  $W_{bo}$ ,  $W_{ao}$ , are taken as the steady-state final values.

$$\Delta \Gamma = (1 - \Gamma_o^2) \left( \frac{\Delta W_b}{W_{bo}} - \frac{\Delta W_a}{W_{ao}} \right)$$

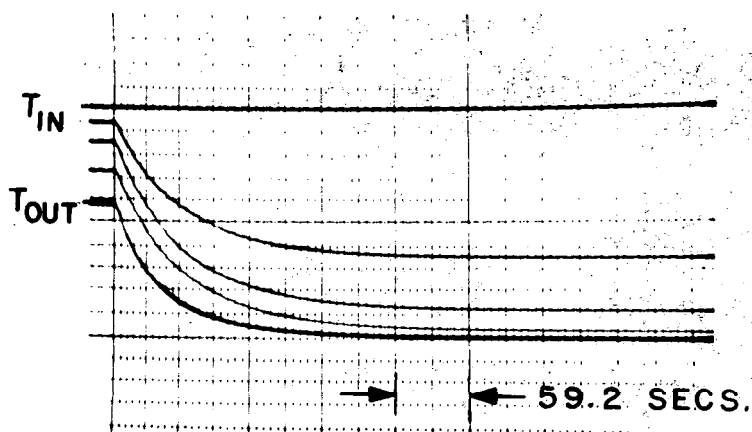
Detailed uncoupled studies of the boiler, superheater, and IHX have been performed. Four nodes and five transport operators per stream are employed. The principal objective of this study was to determine simplified input-output models for use in the complete coupled system study. Also recorded were intermediate temperatures leaving each transport operator such as  $T_{a1}$ ,  $T_{a3}$ ,  $\dots$ , and  $T_{b1}$ ,  $T_{b3}$ ,  $\dots$  as shown in Figure 4.4. The model is designed to give good input-output behavior without regard to the internal spatial correspondence. Hence the internal temperature traces are principally included to achieve a qualitative understanding of the transient behavior of the

# SUPERHEATER TEMPERATURE RESPONSES TO LARGE FLOW VARIATIONS TEMPERATURE CHANGES ( $\Delta T$ ) RECORDED

## SECONDARY RESPONSE

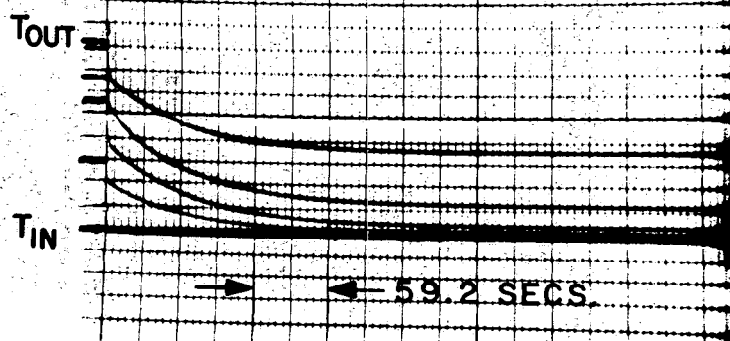
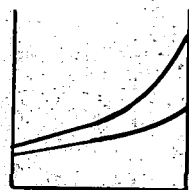
## STEAM RESPONSE

100% TO 20% STEP  
IN SECONDARY FLOW RATE



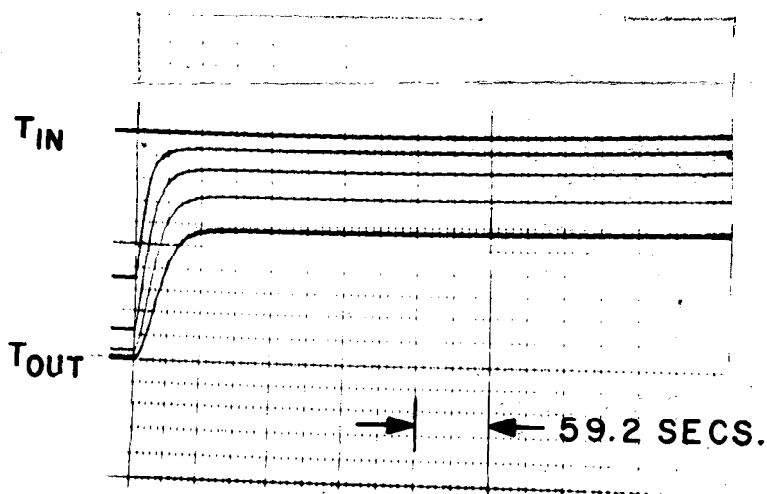
A

FINAL STEADY STATE  
TEMPERATURE-  
POSITION PROFILES

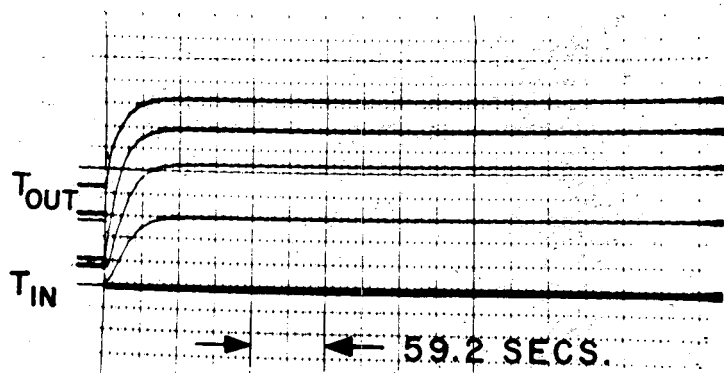
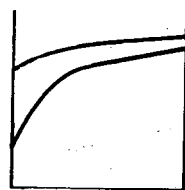


B

20% TO 100% STEP  
IN SECONDARY FLOW RATE

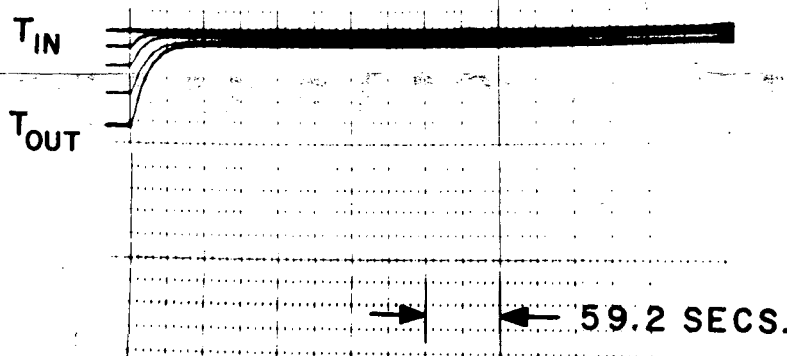


C

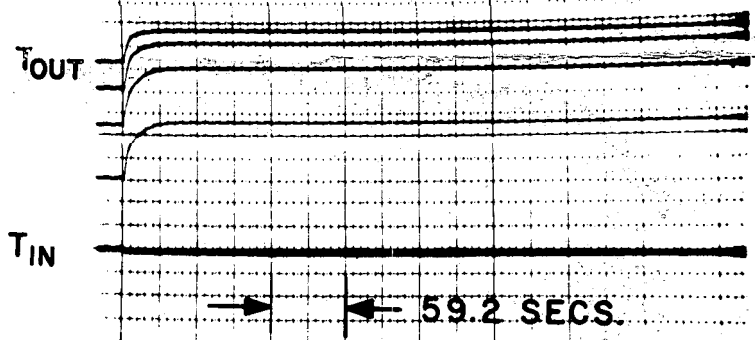
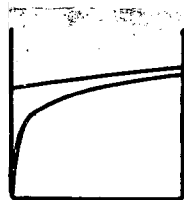


D

100% TO 20% STEP IN  
STEAM FLOW RATE

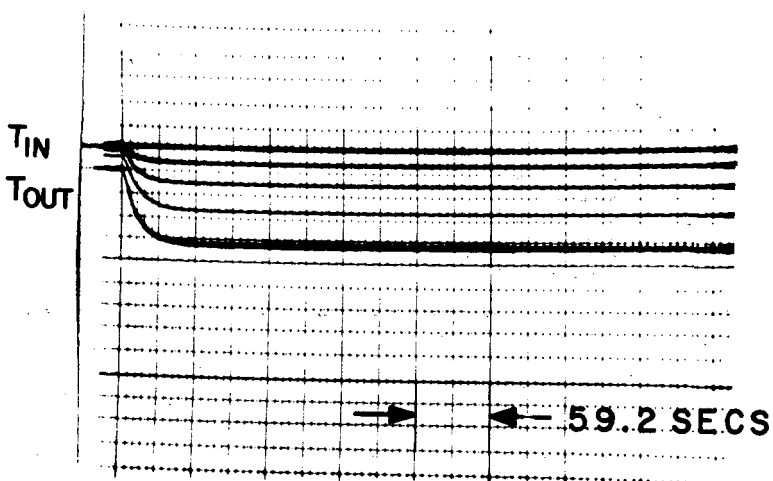


E

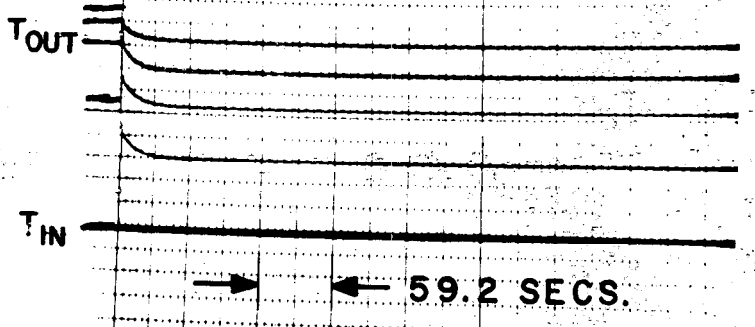
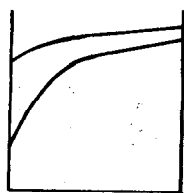


F

20% TO 100% STEP IN  
STEAM FLOW RATE



G



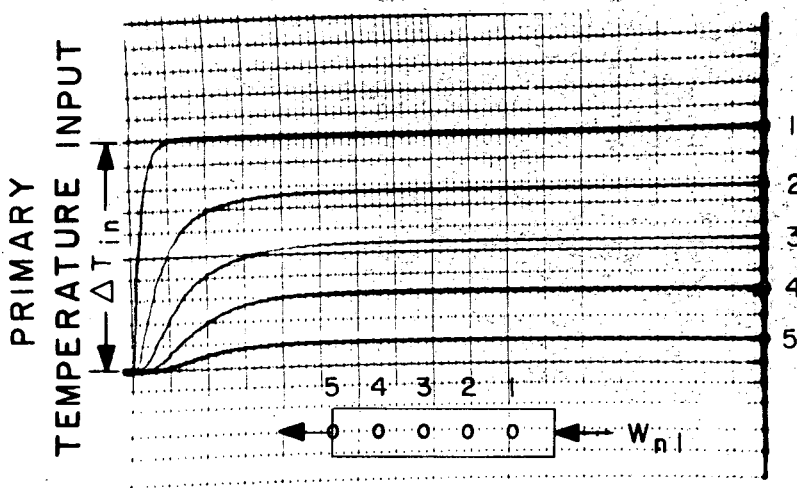
H

FIGURE 4.7

# INTERMEDIATE HEAT EXCHANGER TEMPERATURE RESPONSES TO TEMPERATURE INPUTS TEMPERATURE CHANGES ( $\Delta T$ ) RECORDED

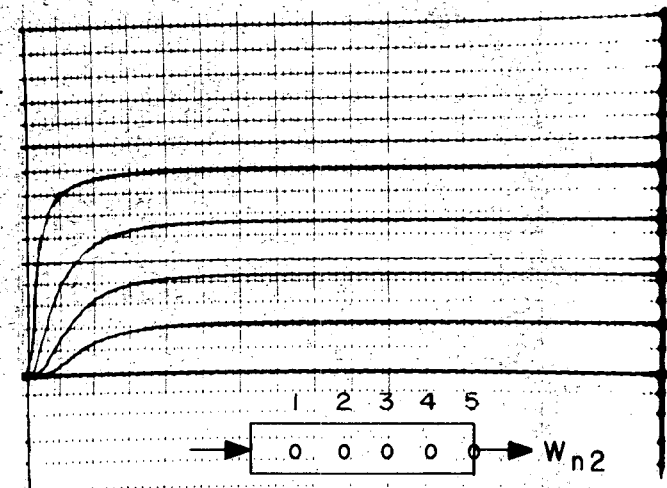
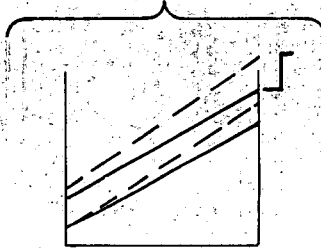
## PRIMARY SODIUM RESPONSE

## SECONDARY SODIUM RESPONSE

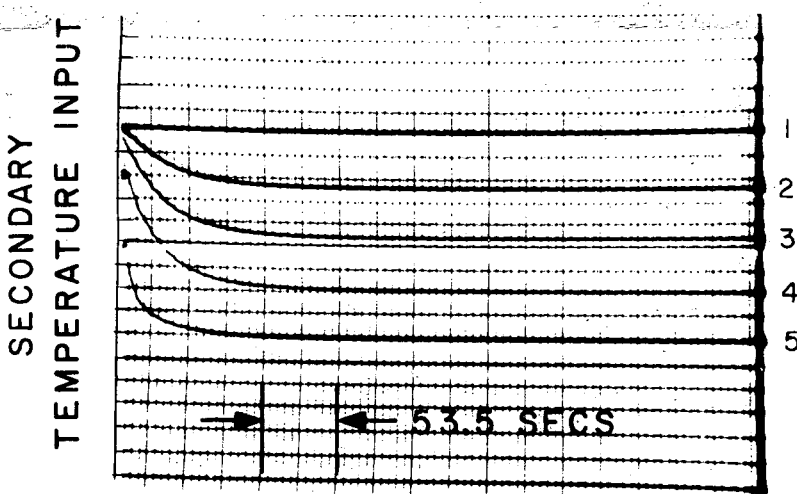


A

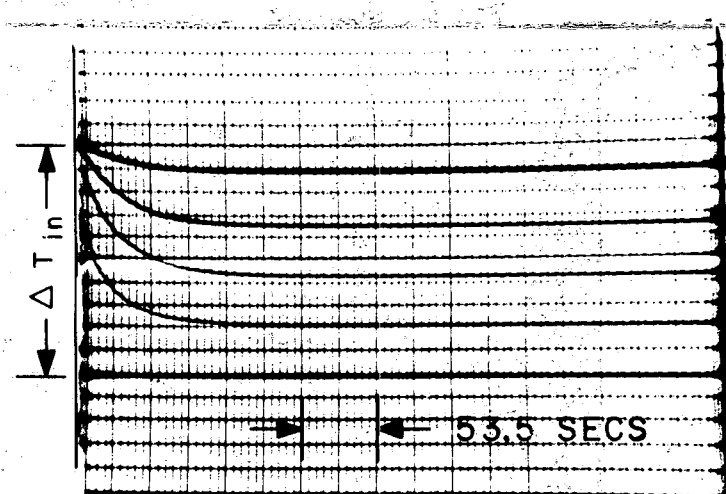
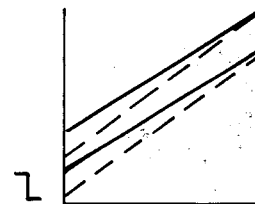
FINAL STEADY  
STATE TEMPERATURE-  
DISTANCE PROFILES



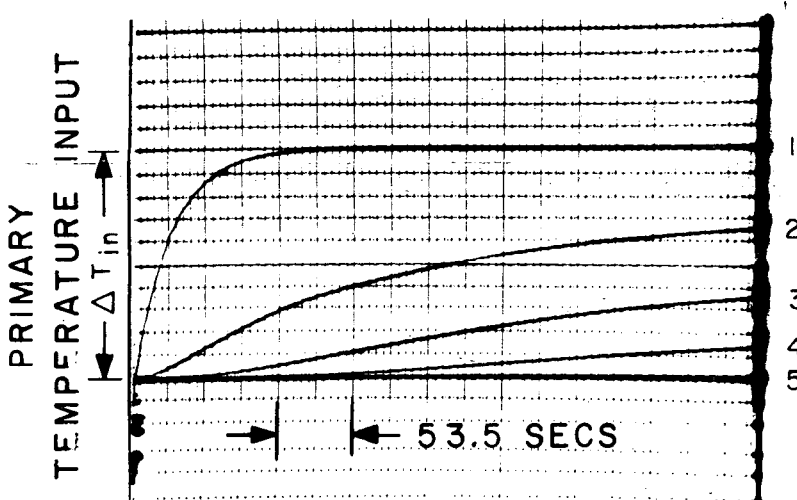
B



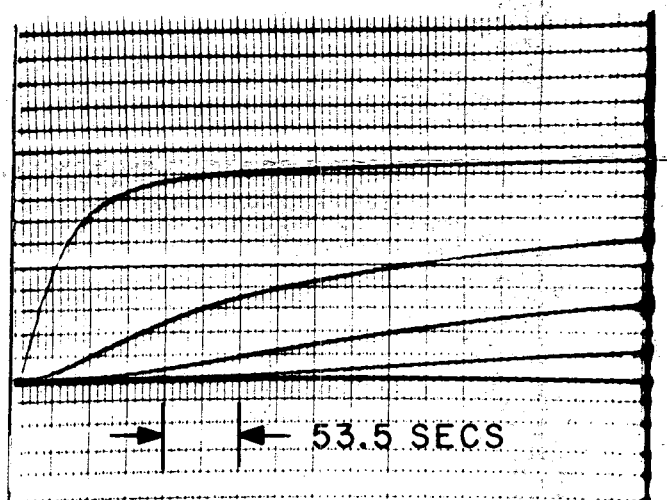
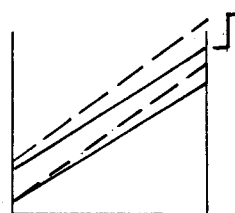
C



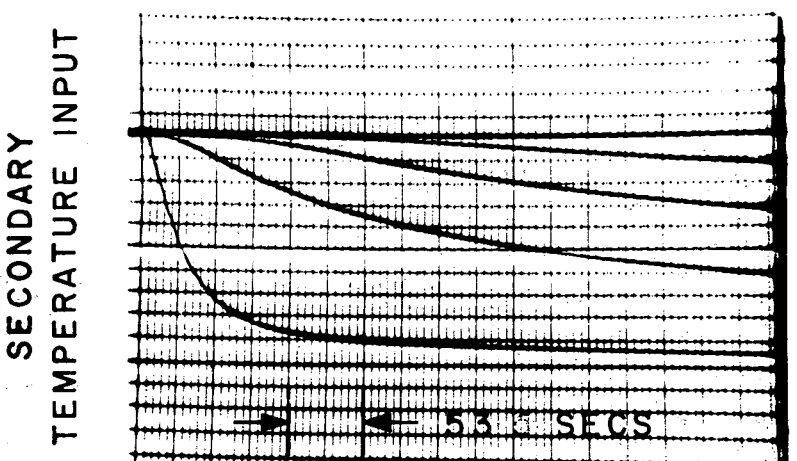
D



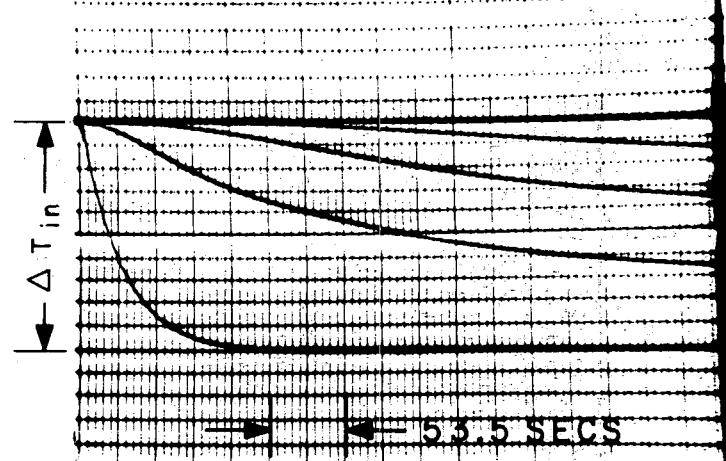
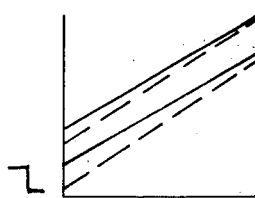
E



F



G



H

FIGURE 4.8

100% LOAD LEVEL

20% LOAD LEVEL

129 082

# SUPERHEATER TEMPERATURE RESPONSE TO TEMPERATURE INPUTS TEMPERATURE CHANGES ( $\Delta T$ ) RECORDED

SECONDARY RESPONSE

STEAM RESPONSE

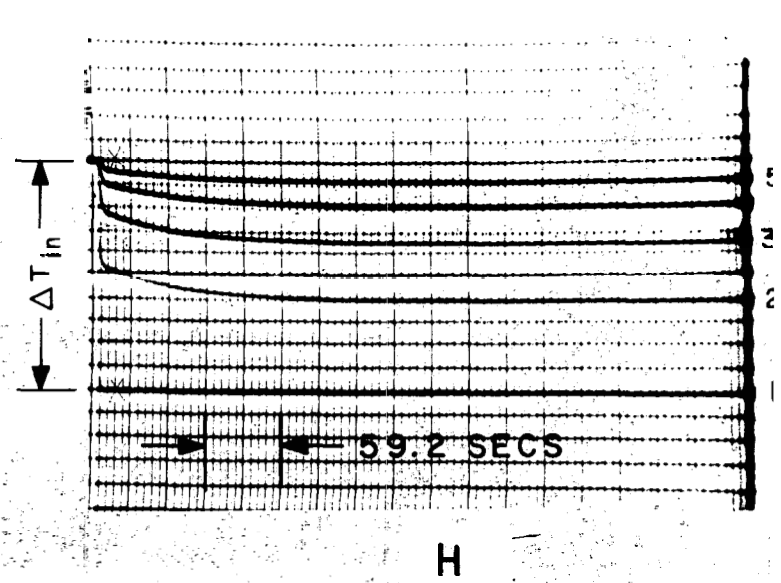
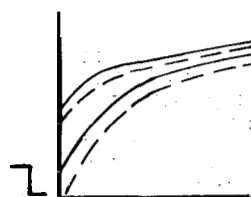
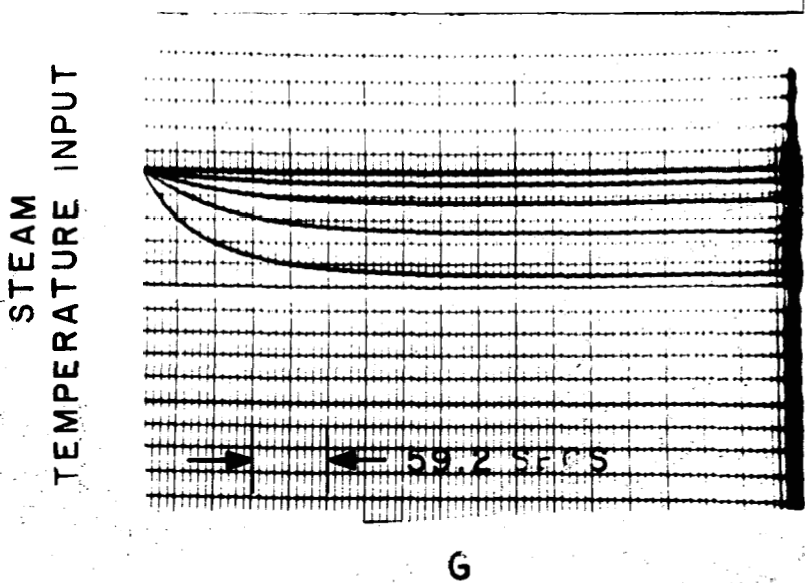
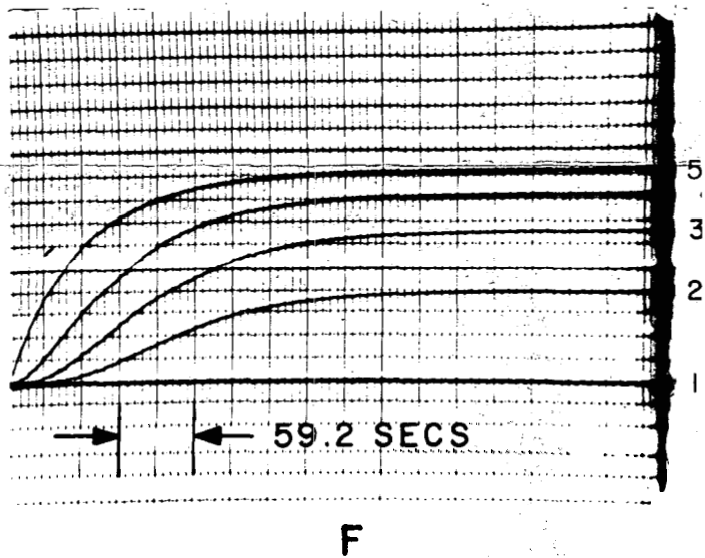
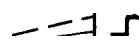
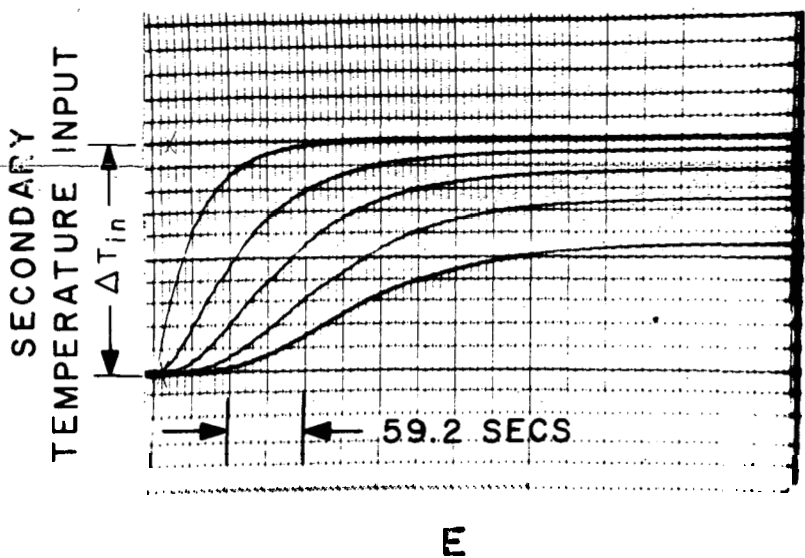
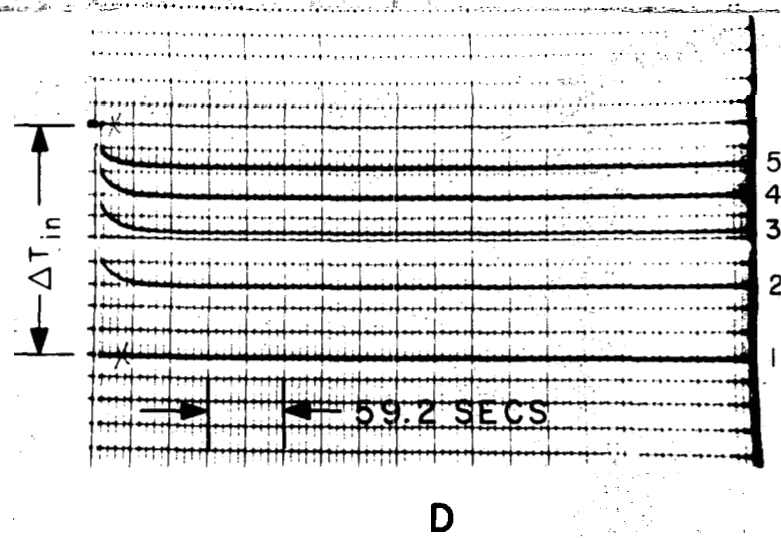
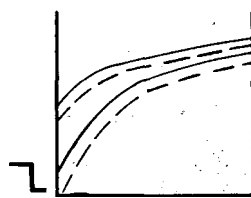
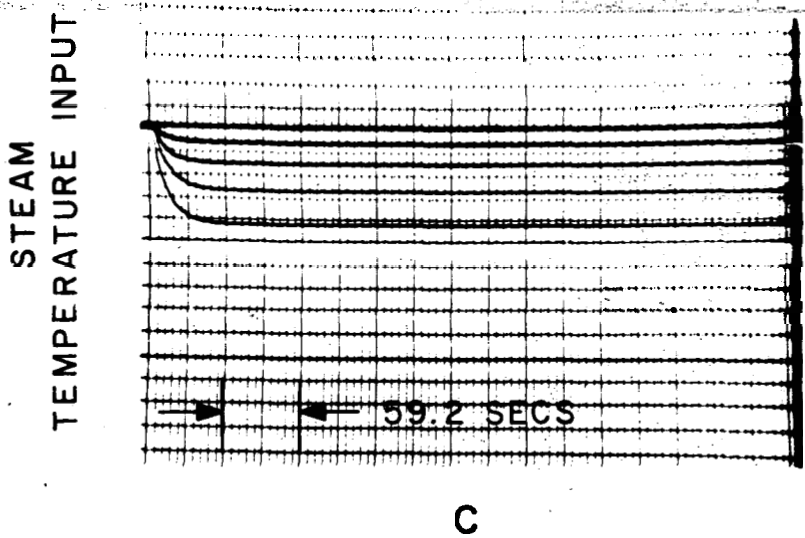
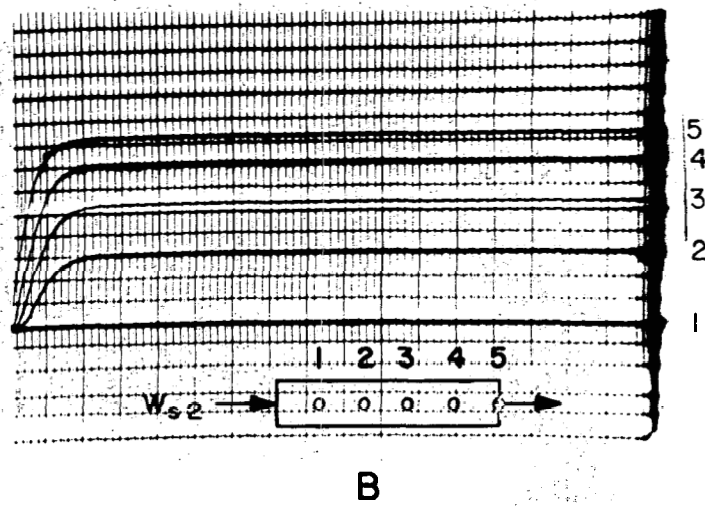
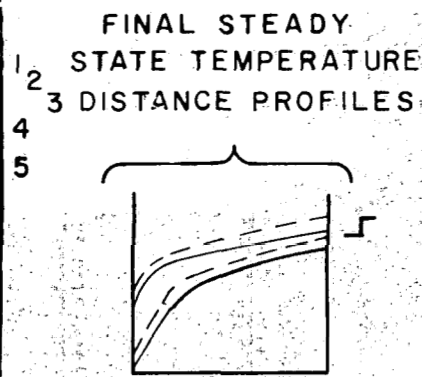
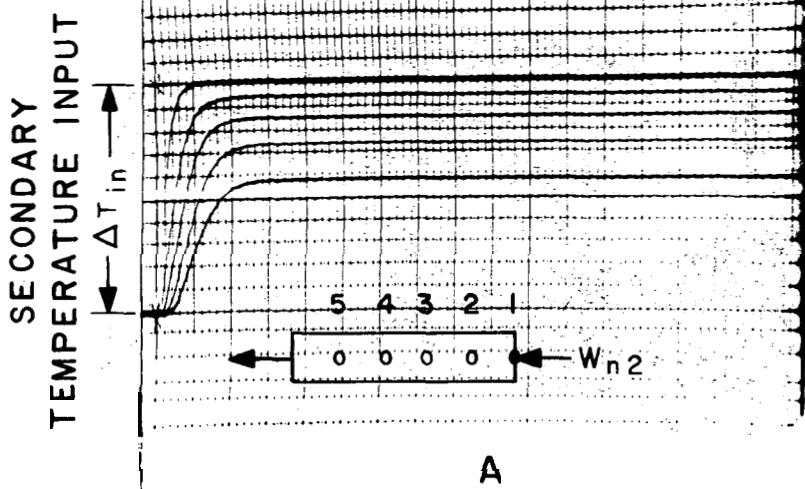
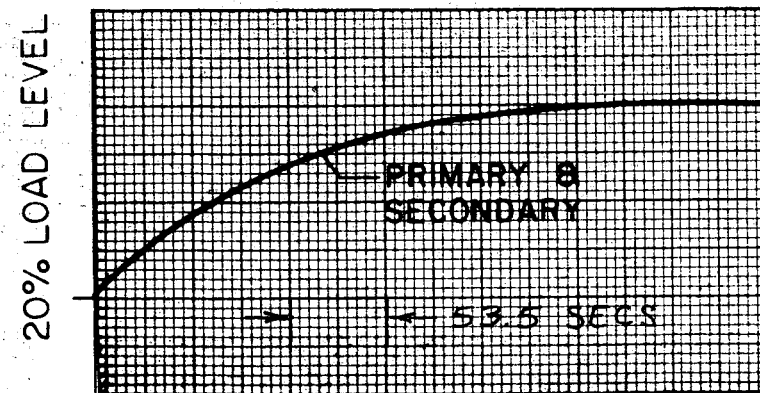
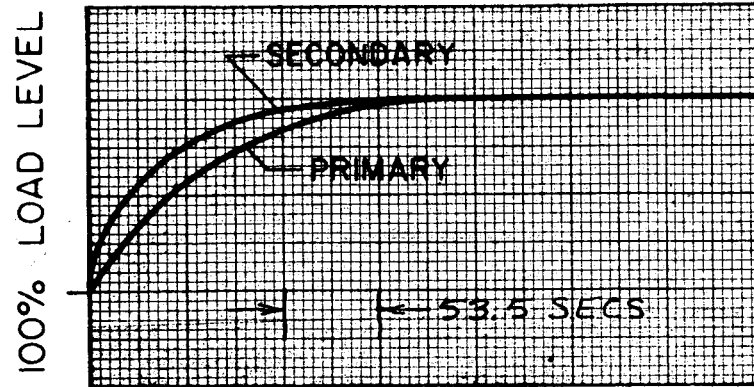


FIGURE 4.3

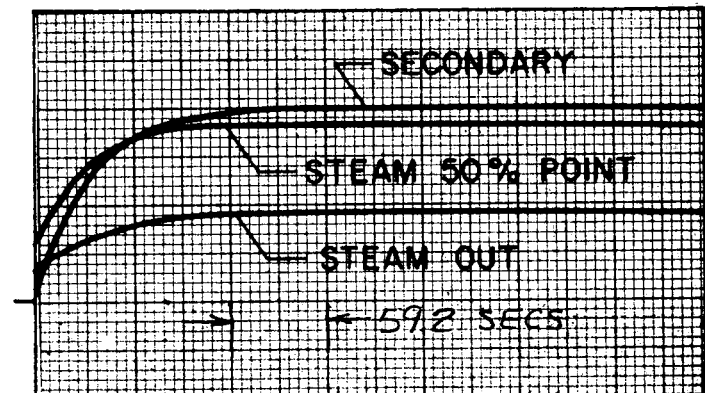
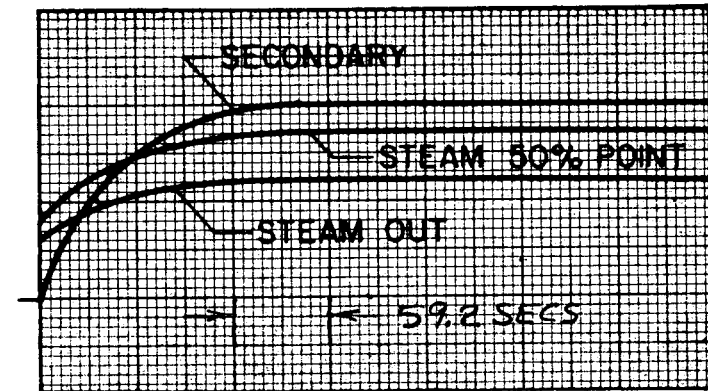


# TEMPERATURE CHANGES ( $\Delta T$ ) RECORDED

## INTERMEDIATE HEAT EXCHANGER



## SUPER HEATER



## LINEARIZED EXCHANGER TERMINAL FLOW RESPONSES

FIGURE 4.10



heat exchanger. Nominally these internal temperatures correspond to .2, .4, .6, .8 subdivisions for transport but to 0, .25, .5, .75 subdivisions for heat transfer. Hence the spatial correspondence at the last two internal points is better than for the first two.

The transient behavior of the superheater and IHX (Figures 4.3, 4.7, 4.8, 4.9, 4.10) is largely governed by the shell side transport times. The tube side plenum lags are lumped with the interconnecting piping and are not included in these figures. All of the step responses are monotonic (i.e. non-decreasing). The terminal variations are not always greater in magnitude than the internal variations for flow rate inputs as is shown in Figures 4.10 and 4.2. Further detail which may aid in the interpretation of these responses is included in Appendix 8.

#### 4.3. Assumptions

A number of assumptions have been made in this analysis. The most important of these are listed below. Most of these are discussed in detail elsewhere.

##### 4.3.1. Single-Phase Heat Exchanger Representation

- (a) All fluids are assumed to have one dimensional velocity and temperature profiles.
- (b) Axial conduction is neglected.

Note: (a) and (b) are compensated by using lags as transport operators.

- (c) Heat loss to the surroundings is neglected.
- (d) Wall charging time is neglected.
- (e) Low frequency models suffice in consideration of the effect of heat exchanger dynamics on controlled system behavior.
- (f) Variation of  $G$  is neglected.
- (g) Variation of transport time vs  $\beta$  relationship is neglected.

#### 4.3.2. Two-Phase System Behavior

- (a) Fog flow is assumed in the riser.
- (b) Low frequency modeling is adequate for pressure behavior.
- (c) Distributed riser pressure drop is lumped at the exit.
- (d) Riser inertia is neglected.
- (e) Bubble volume in the drum and in the tray is neglected.
- (f) The steam pipe transmission time is assumed negligible.  
Resistance in the superheater and in the nozzle is assumed adequate to rapidly damp the pressure wave reflections.
- (g) The effect of spatial steam pressure variations on thermodynamic states is neglected.

#### 4.3.3. Other Components

- (a) The turbine nozzle is assumed to be a choked flow restriction.
- (b) The reactor wall and fluid energy storages are neglected.
- (c) The electrical transients in the sodium pump motor drive are neglected.

## LIST OF REFERENCES

1. "Intermediate Heat Exchanger Preliminary Design", Report APAE #41, Volume I, by ALCO Products, Inc., Schenectady, N. Y., Feb. 28, 1959.
2. "Steam Generator Preliminary Design", Report APAE #41, Volume II, by ALCO Products, Inc., Schenectady, N. Y., Feb. 28, 1959.
3. Phone Conversation with General Electric, Schenectady, N. Y. Representative Concerning Type M-900 Wound Rotor Induction Motor.
4. "Supplemental Agreement Between ALCO Products, Inc., and the U. S. Atomic Energy Commission", Modification #3 - Supplemental Agreement to Contract No. AT(11-1)-666.
5. "On an Analogy Between Stochastic Processes and Monotone Dynamic Systems", by H. Paynter, Paper Presented at the International Conference on Automatic Control, Heidelberg, Germany, September 1956, Published in "Regelungstechnik : Moderne Theorien und Ihre Verwendbarkeit", Verlag R. Oldenbourg, Munich, Germany, 1957.
6. "A Study of Voltage and Frequency Transients in the SM-2 (APPR-16) Nuclear Reactor Power Plant", by Z. J. J. Stekly, P. D. Hansen, and J. H. Eaton, Report #125, Microtech Research Company, Cambridge, Mass., April 15, 1959.
7. "Principles of Turbo-Machinery", D. G. Shepherd, The MacMillan Co., New York, N. Y., 1956.
8. "The Dynamics and Thermodynamics of Compressible Fluid Flow", Volume I, Ascher H. Shapiro, The Ronald Press Co., New York, N. Y., 1953.
9. "Principles of Nuclear Reactor Engineering", Samuel Glasstone, D. VanNostrand Co., Inc., New York, N. Y., 1955.

LIST OF REFERENCES (Concl)

10. "The Dynamics of Heat Exchange Processes", P. D. Hansen, ScD Thesis, Mechanical Engineering Department, M. I. T., Cambridge, Mass., Scheduled for Presentation January 1960.
11. "Compact Heat Exchangers", W. M. Kays and A. L. London, McGraw-Hill Book Company, Inc., New York, N. Y., 1958.
12. "Control of Shell and Tube Heat Exchangers", Allan R. Catheron, Samuel H. Goudhue, and Peter D. Hansen, ASME Paper 59-IRD-14, ASME Instrument and Regulators Conference, Cleveland, Ohio, March 29 - April 1959.
13. Conversation with the Bailey Meter Company's Boston, Massachusetts Sales Office and Engineering Sales Representative.
14. "Water Hammer Analysis", John Parmakian, Prentice-Hall, Inc., New York, N. Y., 1955

## APPENDIX 1 - DYNAMICS OF TWO-PHASE FLUIDS

## A.1.1. Energy Storage

With relatively few restrictive assumptions, a general energy storage equation for two-phase liquid-vapor systems may be written.

These assumptions which imply reversible thermodynamic equilibrium at each instant are:

1. All stored liquid is saturated.
2. All stored vapor is saturated.
3. Pressure and therefore temperature are uniform at any instant.

Although the resulting energy storage equation is quite simple, the derivation is somewhat involved. For this reason, the actual derivation is set apart as Figure A.1. and the procedure described verbally here.

A control volume within which all liquid is saturated liquid and all vapor is saturated vapor is defined. Spatial pressure and temperature gradients within this volume are assumed non-existent. Also there is assumed to be no non-condensable gas present. The fluid entering the control volume may be slightly sub-cooled or two-phase, while the fluid leaving may be slightly superheated or two-phase for a boiler or evaporator, and vice-versa for a condenser. This control volume may be either infinitesimal or finite in size.

Continuity is applied separately to all the liquid and to all the vapor (1 and 2). The time rates of change of the vapor and liquid volumes are eliminated to achieve an equation for the evaporation rate (. 5). This equation may be interpreted as a volume balance.

### A.1.2

These equations are used to eliminate the  $\frac{dm_L}{dt}$  and  $\frac{dm_V}{dt}$  terms in the energy equation ( 6) to achieve ( 9). Through equations 10a and 10b, small amounts of superheating and sub-cooling may be included in the steady state heat balance. If there is a sizeable transport time associated with these single phase effects, they should be treated separately. After recognizing pressure dependencies equations, 12a and 12b result.

There are several possibilities for defining pressure dependent terms such as A, B, and C. These are selected because A and C are nearly constant over the complete range of pressures from zero to critical. B becomes infinite at the critical pressure indicating that the critical state is achieved with a rate approaching zero from a state within the two-phase region. Thus, it may be expected that equilibrium at the critical state is reached very slowly compared to other two-phase states. For this reason, irreversible metastable effects may become more pronounced near the critical point violating the instantaneous reversible thermodynamic equilibrium assumption implied in this derivation.

A, B, and C are plotted vs.  $\ln p$  in Figure A.1.2 for steam. The values are likely to be similar for other fluids since reduced properties are used in the formulation.

The most difficult quantity to determine in the dynamic energy equation, either theoretically or experimentally, is the hold-up volume quality,  $\gamma_H$ . This quantity depends on the slip velocity between vapor and liquid. Two extreme conditions can be considered in order to estimate  $\gamma_H$ . For infinite drag coefficient between liquid and vapor, no slip, the local flowing mass quality is equal to the local hold-up mass quality. For zero drag coefficient between liquid and vapor, uniform cross-sectional area, and liquid completely filling the cross-section at the entrance (or exit for a condenser), the local hold-up

volume quality may be shown to equal the flowing mass quality, resulting in spatially uniform liquid and vapor velocities at any instant. The steady-state flowing mass quality at any point may be easily determined if the total flow is known since the vapor flow rate is given by:

$$W_{vz} = \frac{Q_z}{h_{fg}}$$

where  $Q_z$  is the total rate of heat transfer between the point where  $W_{vz}$  is measured and the point the flow is all liquid. Since the hold-up volume quality is a function of the hold-up mass quality and pressure (see Figure A.1.3), bounding estimates of the local volume quality may be easily established. The difference between these bounding estimates is very large at low pressures, decreasing to zero at the critical point.

At low pressures, the uniform phase velocity (zero drag coefficient) model is probably closer to the correct answer because of the relatively large slip between vapor and liquid. At high pressure which includes the 2200 psi system slip is very small and the fog flow assumption is expected to yield a very good estimate. Slip velocity can be shown to vary approximately inversely with the square root of pressure.

#### A.1.2. Two-Phase Mass Storage

In order to account for mass storage, the hold-up density is assumed to depend on pressure and the flowing mass quality. Either of the two bounding estimates of the hold-up volume quality mentioned in the previous section lead to this type of dependence.

The continuity equation applied to infinitesimal control volume becomes:

$$-\frac{\partial w}{\partial z} = \frac{\partial \rho_h A_c}{\partial t} = \rho_h \frac{\partial A_c}{\partial t} + A_c \frac{\partial \rho_h}{\partial t} \quad (\text{A.1.1})$$

Assuming hold-up density dependence on flowing quality and pressure:

$$\frac{1}{\rho_h} \frac{\partial \rho_h}{\partial t} = -K_x \frac{1}{x_f} \frac{\partial x_f}{\partial t} + K_p \frac{1}{p} \frac{dp}{dt} \quad (\text{A. 1. 2})$$

where

$$K_x \equiv \frac{x_F}{\rho_h} \frac{\partial \rho_h}{\partial x_F} = \frac{x_F v_{fg}}{v_F + x_1 v_{fg}} \quad \begin{array}{l} \text{infinite drag} \\ \text{(fog flow)} \end{array} \quad \frac{\rho_h \rho_{fg}}{\rho_h} \quad \begin{array}{l} \text{zero drag} \\ \text{(uniform phase velocity)} \end{array}$$

$$K_p \equiv \frac{p}{\rho_h} \frac{\partial \rho_h}{\partial p} = \frac{\rho_h}{\rho_f} \left( \frac{p}{v_f} \frac{dv_f}{dp} \right) + \left( 1 - \frac{\rho_h}{\rho_f} \right) \left( - \frac{p}{v_{fg}} \frac{dv_{fg}}{dp} \right) + \left( \frac{p}{\rho_{fg}} \frac{d\rho_{fg}}{dp} \right) \left( \frac{\rho_f}{\rho_h} - 1 \right)$$

and

$$\frac{1}{x_f} \frac{dx_f}{dt} = \frac{1}{W_v} \frac{\partial W_v}{\partial t} - \frac{1}{W} \frac{\partial W}{\partial t} \quad (\text{A. 1. 3})$$

Hence:

$$\frac{\partial W}{\partial z} + K_x \frac{\rho_h A_c}{W} \frac{\partial W}{\partial t} = \frac{K_x}{x_f} \frac{\rho_h A_c}{W} \frac{\partial W_v}{\partial t} + K_p \frac{\rho_h A_c}{p} \frac{dp}{dt} \quad (\text{A. 1. 4})$$

Equation 12a of Figure A.1 may be used to eliminate  $\frac{dW_v}{dt}$ . For the special case of a fixed control volume, no shear power, no subcooling, and no superheating:

$$Q_z = W_{vz} h_{fg} + (W_z - W_1) \frac{v_f}{v_{fg}} h_{fg} + \tau_{Bz} \frac{1}{p} \frac{dp}{dt} \quad (\text{A. 1. 5})$$



where:

$$\tau_B = p_c V_z \left\{ (1 - \gamma_{hz}) A + B + \frac{r_a C_{wz}}{V_z} C \right\} \frac{1}{p} \frac{dp}{dt}$$

and  $z$  is the distance from the point where the flow is all liquid to any point in the two-phase flow measured along the flow path. Subscript 2 indicates properties at the latter point, subscript 1, the former.

Taking the first derivative of A.1.5 with respect to  $\tau$  and solving for  $\frac{dW_v}{dt}$ :

$$\frac{dW_{vz}}{dt} = \frac{1}{h_{fg}} \frac{dQ_z}{dt} - \frac{v_f}{v_{fg}} \left( \frac{dW_z}{dt} - \frac{dW_1}{dt} \right) - W_v \left( \frac{p}{h_{fg}} \frac{dh_{fg}}{dp} \right) \frac{1}{p} \frac{dp}{dt} + \tau_{Bz} \frac{1}{p} \frac{d^2 p}{dt^2} \quad (A.1.6)$$

Derivatives of quantities multiplied by factors which are zero in steady-state are neglected. This limits Equation A.1.6 to small excursions from a steady condition.

Substituting A.1.6 into A.1.4 results in:

$$L \frac{\partial W_z}{\partial z} + \gamma_t DW_z = \tau_t \frac{v_f}{v_z} DW_1 + \tau_t \frac{v_{fg}}{v_z} \left\{ \frac{1}{h_{fg}} DQ_z + \left[ W_v \left( -\frac{p}{h_{fg}} \frac{\partial h_{fg}}{\partial p} \right) + \frac{K_p}{K_x} \right] \frac{1}{p} Dp + \tau_{Bz} \frac{1}{p} D^2 p \right\} \quad (A.1.7)$$

where:

$$\tau_t = \frac{K_x v_z}{x_{Fz} v_{fg}} \frac{\rho_h LA_c}{W}$$

$$\tau_t = -\frac{\rho_h LA_c}{W} \text{ for fog flow}$$

$$\tau_t = \left[ y_h \rho_f + (1 - y_h) \rho_g \right] \frac{LA_c}{W} \text{ for uniform phase vel.}$$

$$v_z = v_f + x_{Fz} v_{fg}$$

$$D = \frac{\partial}{\partial t}$$

Equation A.1.7 is integrated over a length,  $L_i$   $z_{i+1} - z_i$ , small enough that  $\tau_t$  and the right hand side may be assumed independent of  $z$ .

$$\Delta W_{i+1} = e^{-\tau_{ti} D} \Delta W_i + (1 - e^{-\tau_{ti} D}) \left\{ \frac{v_f}{v_i} \Delta W_i + \frac{v_{fg}}{v_i h_{fg}} \Delta Q_i + W_{vi} \frac{v_{fg}}{v_i} \right. \\ \left. \left[ \left( - \frac{p}{h_{fg}} \frac{h_{fg}}{p} \right) + \left( \frac{K_p}{K_x} \right)_i + \tau_{Bz} D \right] \frac{\Delta p}{p_i} \right\} \quad (\text{A.1.8})$$

Where the subscript  $i$  replaces  $z$  of the previous equations.

The notation is employed to indicate variations from a steady-state condition. When there are changes in quality over the control volume, it is necessary to sub-divide into many sections such that the variation in parameters within any section is negligible. This makes Equation A.1.8 linear.

Functions of pressure,  $\left( + \frac{p}{h_{fg}} \frac{dh_f}{dp} \right)$ ,  $\left( \frac{p}{h_{fg}} \frac{dh_g}{dp} \right)$ ,  $\left( - \frac{p}{v_{fg}} \frac{\partial v_{fg}}{\partial p} \right)$ ,

$\left( - \frac{p}{\rho_{fg}} \frac{\partial \rho_{fg}}{\partial p} \right)$ ,  $\left( \frac{p}{v_f} \frac{dv_f}{dp} \right)$ ,  $\frac{v_g}{v_{fg}}$ , and  $\left( - \frac{p}{v_g} \frac{\partial v_g}{\partial p} \right)$  are plotted against

pressure for water in Figures A.1.4 and A.1.5. Some of these also approach infinity at the critical point again indicating that pressure cannot change rapidly through thermodynamic equilibrium states near the critical point.

Boiler liquid level studies require a model of boiler circulation. Boiler circulation depends upon the riser continuity relation, two-phase mass storage, and the circulation loop pressure drop equation. The differential equation of A.1.1 has been solved. The solution is a one-dimensional flow-in, flow-out relationship for a two-phase mass storage region. This solution however includes the two-phase energy equation of Equation 12a in Figure A.1.1. Equation A.1.8 is not the most convenient relationship for computer studies. A more convenient form follows.

Start with the assumptions and analysis leading to Equation A.1.4.

$$\frac{\partial W}{\partial z} + K_x \frac{\rho_k A_c}{W} \frac{\partial W}{\partial t} = \frac{K_x}{x_f} \frac{\rho_h A_c}{W} \frac{\partial W_c}{\partial t} + K_p \frac{\rho_h A_c}{p} \frac{\partial p}{\partial t} \quad (\text{A.1.4})$$

Define:

$$\tau_i' = K_x \frac{\rho_h \gamma_i}{W}$$

Instead of introducing the two-phase energy equation, solve Equation A.1.4 directly.

$$\frac{\Delta W_{i+1}}{W_o} = \frac{\Delta W_i}{W_o} e^{-\tau_i' D} + (1 - e^{-\tau_i' D}) \left( \frac{\Delta W_v}{W} + \frac{K_p}{K_x} \frac{1}{p} \Delta p \right) \quad (\text{A.1.9})$$

or

$$\frac{\Delta W_i}{W_o} - \frac{\Delta W_{i+1}}{W_o} = \frac{\rho_h \gamma_i}{W_o} D \frac{\Delta \rho_h}{\rho_h} = (1 - e^{-\tau_i' D}) \left( -\frac{\Delta W_v}{W_v} - \frac{K_p}{K_x} \frac{\Delta p}{p} + \frac{\Delta W_i}{W_o} \right)$$

For a small section that is  $i$  to  $i+1$ , the operator  $(1 - e^{-\tau_i' D})$  may be satisfactorily approximated by the first order term of a Taylor's expansion leading to

$$\frac{\Delta \rho_h}{\rho_h} = K_x \left( \frac{\Delta W_i}{W_o} - \frac{\Delta W_v}{W_v} \right) - K_p \frac{\Delta p}{p} \quad (\text{A.1.10})$$

Equations A. 1. 9 and A. 1. 10 are used in the boiler circulation model.

### A. 1. 3. Stability of Forced and Natural Circulation Loops in Steam Generators

Instability in boiler circulation loops may result from a long unheated riser section having a large fraction of the loop frictional pressure drop or from a low downcomer inertia. The criterion for stability in these cases is derived from a momentum equation applied to the entire loop. The sum of all spatial pressure differences around the loop must be zero at any instant.

Changes in the total flow at any point give rise to small pressure changes which are very important in determining stability, but these changes are generally negligible in mass and energy storage and heat transfer considerations. For this reason, the heat transfer and pressure terms in Equation A. 1. 8 are neglected in the circulation loop stability analysis. These terms cannot alter stability but may excite oscillations if the terms themselves are already oscillatory. For this case, A. 1. 8 becomes:

$$\Delta W_{i+1} = e^{-\tau_{ti} D} \Delta W_i + (1 - e^{-\tau_{ti} D}) \frac{\rho_i}{\rho_f} \Delta W_1 \quad (\text{A. 1. 11a})$$

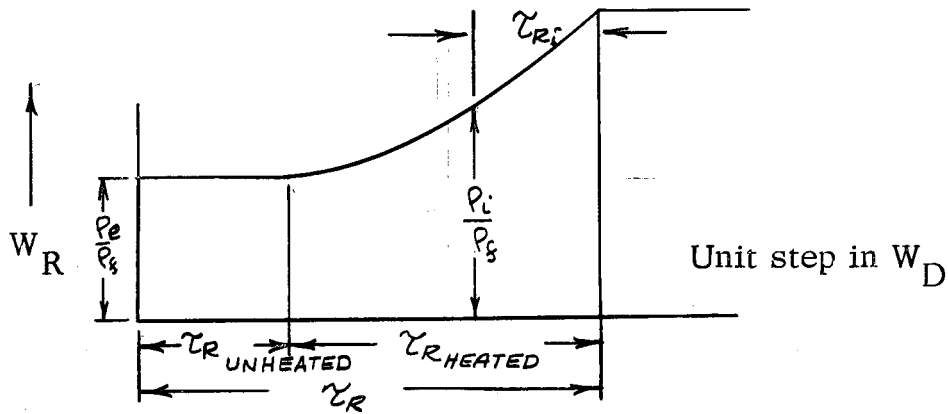
For a typical variation of  $\tau_{ti}$  and  $x_F$  with position, the solution of an infinite cascade of equations of the form A. 11 is sketched in Figure A. 5. The input is a unit step in the downcomer flow,  $\Delta W_D = \Delta W_1$ . The output, the riser outflow,  $W_R$ , has the shape of the flowing density vs distance from the exit with the distance scale stretched according to the local transport times. By merely shifting the zero of the line axis, the step response of any intermediate riser mass flow rate results. In equation form:

$$\Delta W_i = \left[ \frac{\rho_i}{\rho_f} + \sum (1 - \frac{\rho_i}{\rho_f}) e^{-\tau_{ti} D} \right] \Delta W_1 \quad (\text{A. 1. 11b})$$

where

$$\tau_{ri} = \sum_{i=0}^i \tau_{ti}$$

This equation is entirely equivalent to a cascade of equations of the form (A.1.11a).



Riser Outflow Response to a Step In Downcomer Flow Rate

Figure A.1.6

The local densities do not change instantaneously following a step change in inlet flow. It is shown using Equations A.1.3, A.1.11, and 12.4 of Figure A.1.1 that the dynamic operator relating density to inflow is the transport delay.

Conservation of mass on the  $i$ 'th section requires:

$$\Delta W_i - \Delta W_{i+1} = D \Delta (\rho \gamma_i)$$

Neglecting pressure heat transfer and volume changes there results:

$$\Delta W_i (1 - e^{-\tau_{ti} D}) - (1 - e^{-\tau_{ti} D}) \left[ \frac{v_f}{v_i} \Delta W_D \right] = W_o \tau_{ti} D \frac{\Delta \rho_i}{\rho_i}$$

For small  $\tau_{ti} D (\tau_{ti} \omega)$ , this becomes:

$$\frac{\Delta W_i}{W_o} - \frac{v_f}{v_i} \frac{\Delta W_D}{W_o} = \frac{\Delta \rho_i}{\rho_i}$$

and substituting A.1.11b there results:

$$\sum \left(1 - \frac{\rho_i}{\rho_f}\right) e^{-\tau_{ri} D} \frac{\Delta W_D}{W_o} = \frac{\Delta \rho_i}{\rho_i}$$

The pressure drop equation becomes:

$$\Delta P_{\text{pump}} + \Delta P_{\text{frict}} + \Delta P_{\text{inertie}} + \Delta P_{\text{bouyant}} = 0$$

Where the momentum drop is of the same from as and is therefore lumped with the friction term.

$$\Delta P_{\text{frict downcomer}} = f_D \frac{W_D^2}{\rho_f} \quad (\text{A.12a})$$

$$\Delta P_{\text{frict riser}} = \sum f_{ri} \frac{W_i^2}{\rho_i} \quad (\text{A.12b})$$

$$\Delta P_{\text{inertia downcomer}} = \frac{1}{g_o} \left( \sum \frac{L}{A} \right)_D \frac{dW_D}{dt} \quad (\text{A.12c})$$

$$\Delta P_{\text{inertia riser}} = \frac{1}{g_o} \sum \left( \frac{L}{A} \right)_i \frac{dW_i}{dt} \quad (\text{A.12d})$$

$$\Delta P_{\text{bouyant}} = \sum \frac{g}{g_o} L_i \rho_i - \frac{g}{g_o} L_D \rho_f \quad (\text{A.12e})$$

$$\Delta P_{\text{pump}} = -f(W_D) \quad (\text{A.12f})$$

The downcomer flow,  $W_D$ , is assumed the same as  $W_1$ .

These pressure drops are out of phase when the downcomer flow is varied sinusoidally, since the flow and density at each point in the riser lags the

In order that the system be marginally stable at a particular frequency, the resultant must be zero. In order to go unstable, the resultant must pass below and to the left of the origin as frequency increases. In order to be stable, the resultant must pass to the right and above the origin as frequency increases. This stability criterion is closely related to the Hyquist criterion\* and can be proven in a similar way. An assumption is made for the sake of



Figure A.1.7

In order that the system be marginally stable at a particular frequency, the resultant must be zero. In order to go unstable, the resultant must pass below and to the left of the origin as frequency increases. In order to be stable, the resultant must pass to the right and above the origin as frequency increases. This stability criterion is closely related to the Hyquist criterion\* and can be proven in a similar way. An assumption is made for the sake of

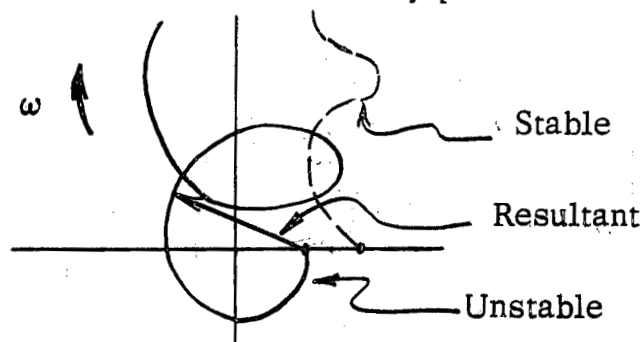
using feedback system notation.

$$1 + \frac{1}{G(\omega)}$$

using feedback system notation.

Hence, the 0,0 point of Figure A.6 has the same significance as the (-1,0) point of the Nyquist plane. Also, since  $G(\omega)$  goes to zero at infinite frequency,  $1 + \frac{1}{G(\omega)}$  goes to infinity.

simplifying the analysis and the resulting criterion. It is noted the conservative results occur when all riser inertia is neglected since the presence of the inertia term tends to cause the resultant trajectory to cross the real axis sooner. As an alternative assumption, it is probably conservative to lump the riser inertia with the downcomer since any phase shift that would actually



Vector Diagram Showing Stability

Figure A.1.8

occur would tend to make the real axis crossing occur further to the right. It is likely that the riser inertia is small. However, when a large downcomer cross-section is employed, validity of either of the alternative assumptions may be questionable.

The resultant of all of the non-inertial terms is a monotone function of the downcomer flow rate, having a non-decreasing step response. Thus, the pressure drop equation is re-written in a linearized form to test for the stability of small perturbations:

$$I_L D W_D + G_D W_D = 0 \quad (\text{A.1.13})$$

where:

$$I_L = \text{downcomer or loop inertia} = \frac{1}{g_0} \sum \frac{L}{A}$$

$G_D$  = linearized monotone operator



$$\mathbb{G}_D W_D = \alpha_D W_D + \sum \alpha_{Ri} W_i + \sum \alpha_{\rho i} \left( -\frac{\partial W}{\partial \rho} \right) \rho_i = \left[ \alpha_D + \sum \frac{\rho_i}{\rho_f} \alpha_{Ri} + \sum \left( 1 - \frac{\rho_i}{\rho_f} \right) \alpha_{Ri} e^{-\tau_{Ri} D} + \sum \alpha_{\rho i} e^{-\tau_{Ri} D} \right] W_D \quad (\text{A.1.14})$$

$$\alpha_D = 2 \Delta P_{\text{frict}_D} \frac{1}{W_D} + \left( -\frac{\partial \Delta P_{\text{pump}}}{\partial W} \right)$$

$$\alpha_{Ri} = 2 \frac{\Delta P_{\text{frict}_i}}{W_D}$$

$$\alpha_{\rho i} = \left( \frac{gL_i}{g_0} - \frac{\Delta P_{\text{frict}_i}}{\rho_i} \right) \left( -\frac{\partial \rho_i}{\partial W} \right)$$

$$\left( -\frac{W}{\rho_i} \right) \frac{\partial \rho_i}{\partial W} = \left( 1 - \frac{\rho_i}{\rho_f} \right) \text{ for fog flow}$$

$$= \left( \frac{\rho_f}{\rho_h} - 1 \right) \text{ for uniform phase velocity}$$

The worst case results when the density change in the heated section is concentrated spatially, followed by a constant density region.

Then

(A.1.15)

$$I_L DW_D + \left( \alpha_D + \alpha_R \frac{\rho_e}{\rho_f} \right) W_D + \left[ \left( 1 - \frac{\rho_e}{\rho_f} \right) \alpha_R + \alpha_{\rho i} \right] e^{-\tau_R D} W_D = 0$$

For sinusoidal variations in  $W_D$ , the operator  $D$  may be replaced by  $j\omega$ , and there results:

$$\left\{ \alpha_D + \alpha_R \frac{\rho_e}{\rho_f} + \left[ \left( 1 - \frac{\rho_e}{\rho_f} \right) \alpha_R + \alpha_{\rho} \right] \cos \tau_R \omega \right\} W_D + j \left\{ \omega I_L - \left[ \left( 1 - \frac{\rho_e}{\rho_f} \right) \alpha_R + \alpha_{\rho} \right] \sin \tau_R \omega \right\} W_D = 0 \quad (\text{A.1.16})$$

At the point of incipient instability,  $W_D$  may be finite and yet the equation is satisfied. Setting the imaginary term to zero gives an implicit equation for  $\omega_N$ :

$$I_l \omega_N = \left[ \left(1 - \frac{\rho_e}{\rho_f}\right) \alpha_R + \alpha_\rho \right] \sin \tau_R \omega_N \quad (\text{A.1.17})$$

When the real coefficient is positive at this frequency the system is stable because net energy is being removed per cycle. Conversely, the system is unstable when the real coefficient is negative at  $\omega = \omega_N^*$ . Thus, the system is stable at any frequency if:

$$\alpha_D + \alpha_R \frac{\rho_e}{\rho_f} > \left(1 - \frac{\rho_e}{\rho_f}\right) \alpha_R + \alpha_\rho$$

or:

$$\boxed{\alpha_D > \left(1 - 2 \frac{\rho_e}{\rho_f}\right) \alpha_R + \alpha_\rho} \quad (\text{A.1.18})$$

The most unfavorable condition results when:

$$\alpha_D + \alpha_R \frac{\rho_e}{\rho_f} = 0$$

then for stability:

$$\cos \tau_R \omega_N > 0$$

since:

$$\left(1 - \frac{\rho_e}{\rho_f}\right) \alpha_R + \alpha_\rho > 0$$

---

\*A more rigorous derivation of the condition for stability follows the approach taken in the proof of Nyquist criterion.

therefore:

$$\tau_R \omega_N < \frac{\pi}{2}$$

and

$$\sin \tau_R \omega_N < 1$$

At incipient instability:

$$\frac{I_\ell}{\tau_R} - \frac{\pi}{2} = \left[ \left(1 - \frac{\rho_e}{\rho_f}\right) \alpha_R + \alpha_\rho \right]$$

Thus, the system is stable, if:

$$\boxed{\frac{I_\ell}{\tau_R \left[ \left(1 - \frac{\rho_e}{\rho_f}\right) \alpha_R + \alpha_\rho \right]} > \frac{2}{\pi}} \quad (\text{A. 1. 19})$$

Not much of the conservation of the preceeding statement can be shaved without involving tedious calculations or graphical constructions. Taking into account the distributed density distribution in the riser shaves a little; however, in this case, the system is stable if:

$$\frac{I_\ell}{\sum \left[ \left(1 - \frac{\rho_i}{\rho_f}\right) \alpha_{Ri} + \alpha_{\rho i} \right] \tau_{Ri}} > \frac{2}{\pi} \quad (\text{A. 1. 20a})$$

or:

$$\alpha_D > \sum \left[ \left(1 - 2 \frac{\rho_i}{\rho_f}\right) \alpha_{Ri} + \alpha_{\rho i} \right] \quad (\text{A. 1. 20b})$$

If neither of these is satisfied, the system may be stable or unstable.

The condition for .7 damping is much easier to predict accurately than the condition for 0 damping (stability). With virtually no approximation, except either zero or lumped riser inertia, a method first suggested by H. M. Paynter (Reference 5) yields:

$$\frac{I_l}{\sum (1 - \frac{\rho_i}{\rho_f}) \alpha_{Ri} + \alpha_{\rho i} \tau_{Ri}} = 2 \quad (\text{A.1.21})$$

for approximately .7 damping of the lowest frequency pair of oscillatory roots.\* This value is independent of  $\alpha_D$ . Hence, even though  $\alpha_D$  may be large enough to satisfy A.1.20b, the system may be lightly damped unless A.1.21 is also satisfied.

For this system using the values of Appendix 5, and the criteria A.1.18 and A.1.19, the stability ratios are calculated as follows:

	<u>100%</u>	<u>20%</u>
1. $\frac{(1 - 2 \frac{\rho_e}{\rho_f}) \alpha_R + \alpha_\rho}{\alpha_D}$	.36	.31
2. $\frac{I_l}{\tau_R \left[ (1 - \frac{\rho_e}{\rho_f}) \alpha_R + \alpha_\rho \right]}$	.44	.37

The first of these indicates that the down-comer friction is large enough to insure stability. The second condition indicates that the system may be unstable and is likely to be lightly damped.

\*This is established by analogy to the feedback control of a monotone process,  $G(D)$ , with a floating controller having an integral or reset time of  $I_l$  which was an identical characteristic equation. The lowest frequency roots for this situation are the only roots which might give rise to instability. The criterion imposed assures that the closed loop control system frequency response amplitude has no curvature at zero frequency implying that the closed loop system has no amplitude ratio greater than that of zero frequency. This condition forces the lowest frequency roots to be approximately .7 damped.

Figure A.1 - Two-Phase Energy Storage Derivation

## Mass Storage Liquid Phase

$$\underbrace{W_1 (1 - x_{F1})}_{\text{liquid inflow}} - \underbrace{W_e}_{\text{evaporation}} - \underbrace{W_2 (1 - x_{F2})}_{\text{liquid outflow}} = \underbrace{\frac{dm_L}{dt}}_{\text{rate of liquid storage}} \quad (1)$$

where

$$\frac{dm_L}{dt} = \frac{d\rho_f \gamma_L}{dt} = \gamma_L \frac{d\rho_f}{dt} + \rho_f \frac{d\gamma_L}{dt} \quad (2)$$

and the flowing mass quality is:

$$x_{F1} = \frac{W_{v1}}{W_1} = 1 - \frac{W_{L1}}{W_1}; \quad x_{F2} = \frac{W_{v2}}{W_2} = 1 - \frac{W_{L2}}{W_2}$$

## Mass Storage Vapor Phase

$$\underbrace{W_1 x_{F1}}_{\text{vapor inflow}} + \underbrace{W_e}_{\text{evaporation rate}} - \underbrace{W_2 x_{F2}}_{\text{vapor outflow}} = \underbrace{\frac{dm_v}{dt}}_{\text{rate of vapor storage}} \quad (3)$$

$$\frac{dm_v}{dt} = \frac{d\rho_g \gamma_v}{dt} = \gamma_v \frac{d\rho_v}{dt} + \rho_g \frac{d\gamma_v}{dt} \quad (4)$$

combining 1, 2, 3, and 4 and employing:

$$\frac{d\gamma_v}{dt} + \frac{d\gamma_L}{dt} = \frac{d\gamma}{dt}$$

there results a volume storage equation:

$$\underbrace{W_e v_{fg}}_{\text{"volume generated"}} = \underbrace{W_2(v_f + x_{F2} v_{fg})}_{\text{volume outflow}} - \underbrace{W_1(v_f - x_{F2} v_{fg})}_{\text{volume inflow}} + \underbrace{\gamma_L \frac{1}{\rho_f} \frac{d\rho_f}{dt} + \gamma_v \frac{1}{\rho_g} \frac{d\rho_g}{dt}}_{\text{compressibility}} + \underbrace{\frac{d\gamma}{dt}}_{\text{expansion}}$$

Energy Storage, the First Law of Thermodynamics

(6)

$$\underbrace{Q}_{\text{rate of heat transfer}} - \underbrace{P}_{\text{power inputs other than expansion}} - \underbrace{p \frac{d\gamma}{dt}}_{\text{expansion power}} = \underbrace{W_2 h_2}_{\text{energy inflow}} - \underbrace{W_1 h_1}_{\text{energy outflow}} + \underbrace{\frac{d(mh - p\gamma)}{dt}}_{\text{rate of liquid energy storage}} + \underbrace{r_a C_w \frac{dT}{dt}}_{\text{rate of wall energy storage*}}$$

\*A portion,  $r_a$ , of the total wall capacity,  $C_w$ , is lumped with the fluid if the wall charging time  $\tau_w$ , is negligible. This is usually the case because of the large two-phase film conductance.

$$r_a \equiv \frac{UA}{H_a A_a} = \frac{H_b A_b}{H_a A_a + H_b A_b}$$

$$\tau_w \equiv \frac{C_w}{H_a A_a + H_b A_b}$$

where the subscript b refers to the two-phase fluid and the subscript a to the other fluid.

where:

$$\frac{d(mh)}{dt} = \frac{d(m_L h_f + m_v h_g)}{dt} = m_L \frac{dh_f}{dt} + m_v \frac{dh_g}{dt} + h_f \frac{dm_L}{dt} + h_v \frac{dm_v}{dt} \quad (7)$$

and employing 1, 2, and 5 together with 7 yields:

$$\begin{aligned} \frac{d(mh)}{dt} = & m_L \frac{dh_f}{dt} + m_v \frac{dh_g}{dt} + W_1 (h_f + x_{F1} h_{fg}) - W_2 (h_f + x_{F2} h_{fg}) + \\ & \frac{h_{fg}}{v_{fg}} \left\{ W_2 (v_f + x_{F2} v_{fg}) - W_1 (v_f + x_{F1} v_{fg}) + \gamma_L \frac{1}{\rho_f} \frac{d\rho_f}{dt} + \gamma_v \frac{1}{\rho_g} \frac{d\rho_g}{dt} + \frac{d\gamma}{dt} \right\} \end{aligned} \quad (8)$$

and simplifying:

$$\begin{aligned} \frac{d(mh)}{dt} = & \gamma_L \left[ \rho_f \frac{dh_f}{dt} + \frac{h_{fg}}{v_{fg}} \left( \frac{1}{\rho_f} \frac{d\rho_f}{dt} \right) \right] + \gamma_v \left[ \rho_g \frac{dh_g}{dt} + \right. \\ & \left. \frac{h_{fg}}{v_{fg}} \left( \frac{1}{\rho_g} \frac{d\rho_g}{dt} \right) \right] + (W_1 - W_2) \left[ h_f - \frac{v_f}{v_{fg}} h_{fg} \right] + \frac{h_{fg}}{v_{fg}} \frac{d\gamma}{dt} \end{aligned} \quad (9)$$

In Equation 6 let:

$$h_2 = h_f + x_2 h_{fg} + \underbrace{\Delta h_{s.h.}}_{\text{superheat}} \quad (10a)$$

(zero unless  $x_2 = 1$ )

$$h_1 = h_f + x_1 h_{fg} - \underbrace{\Delta h_{s.c.}}_{\text{subcooling}} \quad (10b)$$

(zero unless  $x_1 = 0$ )

substituting 9, 10a, and 10b into 6 yields:

$$\begin{aligned}
 Q - P = & W_2 \left[ x_2 h_{fg} + \frac{v_f}{v_{fg}} h_{fg} + \Delta h_{s.h.} \right] - W_1 \left[ x_1 h_{fg} + \frac{v_f}{v_{fg}} h_{fg} - \Delta h_{s.c.} \right] + \\
 & \gamma_L \left[ \rho_f \frac{dh_f}{dt} + \frac{h_{fg}}{v_{fg}} \left( \frac{1}{\rho_f} \frac{d\rho_f}{dt} \right) \right] + \gamma_v \left[ \rho_g \frac{dh_g}{dt} + \frac{h_{fg}}{v_{fg}} \left( \frac{1}{\rho_g} \frac{d\rho_g}{dt} \right) \right] + \\
 & \frac{h_{fg}}{v_{fg}} \frac{d\gamma}{dt} - \gamma \frac{dp}{dt} = r_a C_w \frac{dT}{dt} \quad (11)
 \end{aligned}$$

Define the hold-up volume quality as:

$$y_h \equiv \frac{\gamma_v}{\gamma} = 1 - \frac{\gamma_L}{\gamma} \quad (12)$$

Also  $h_f$ ,  $h_g$ ,  $\rho_f$ ,  $\rho_g$ , and  $T$  are functions of pressure only. Thus, the three functions A, B, and C, defined below, are also functions of pressure only.

$$\begin{aligned}
 A &= \left\{ \frac{1}{v_f} \frac{dh_f}{dp} + \frac{h_{fg}}{pv_{fg}} \left( \frac{p}{\rho_f} \frac{d\rho_f}{dp} \right) \right\} \frac{p}{p_c} \\
 B &= \left\{ \frac{1}{v_f} \frac{dh_g}{dp} - \frac{1}{v_f} \frac{dh_f}{dp} + \frac{h_{fg}}{pv_{fg}} \left( \frac{p}{\rho_g} \frac{d\rho_g}{dp} - \frac{p}{\rho_f} \frac{d\rho_f}{dp} \right) - 1 \right\} \frac{p}{p_c} \\
 C &= \left\{ \frac{v_{fg}}{s_{fg}} \right\} \frac{p}{p_c}
 \end{aligned}$$

where  $p_c$  is arbitrarily selected as the critical pressure. Equation 11 then becomes:

$$\begin{aligned}
 Q - P = & (W_{v2} - W_{v1}) h_{fg} + (W_2 - W_1) \frac{v_f}{v_{fg}} h_{fg} + W_2 \Delta h_{s.h.} + W_1 \Delta h_{s.c.} + \\
 & p_c \gamma \left\{ (1 - y_h) A + B + \frac{r_a C_w}{\gamma} C \right\} \frac{1}{p} \frac{dp}{dt} + \frac{h_{fg}}{v_{fg}} \frac{d\gamma}{dt} \quad (12a)
 \end{aligned}$$



or

$$Q - P = (W_2 v_2 - W_1 v_1) \frac{h_{fg}}{v_{fg}} + W_2 \Delta h_{s.h.} + W_1 \Delta h_{s.c.} + p_c \gamma \left\{ (1 - y_h) A + B + \frac{r_a C_w}{\gamma} C \right\} \frac{1}{p} \frac{dp}{dt} + \frac{h_{fg}}{v_{fg}} \frac{d\gamma}{dt} \quad (12b)$$

where

$$v_2 = v_f + x_2 v_{fg}$$

$$v_1 = v_f + x_1 v_{fg}$$

When there is no subcooling or superheating, the infinitesimal form of Equation 12a is:

$$\frac{\partial}{\partial z} (Q - P) = h_{fg} \frac{\partial W_v}{\partial z} + \frac{v_f}{v_{fg}} h_{fg} \frac{\partial W}{\partial z} + p_c A_c \left\{ (1 - y_h) A + B + \frac{r_a C_w}{\gamma} C \right\} \frac{1}{p} \frac{dp}{dt} + \frac{h_{fg}}{v_{fg}} \frac{dA_c}{dt} \quad (13)$$

where  $A_c$  is the cross-sectional area,  $y_h$  and  $\frac{r_a C_w}{\gamma}$  are local values, and  $z$  is the axial position coordinate.

# TWO PHASE ENERGY STORAGE

$$\frac{Q}{Q_0} = \frac{W_a \left[ \frac{h_{sg}}{\Delta h_o} + \frac{\Delta h_{sw}}{\Delta h_o} \right] \frac{W_i}{W_o} \left[ \frac{h_{sg}}{\Delta h_o} - \frac{\Delta h_{se}}{\Delta h_o} \right] + \tau \frac{dp}{dt}}{\frac{W_a \left[ \frac{h_{sg}}{\Delta h_o} + \frac{\Delta h_{sw}}{\Delta h_o} \right] \frac{W_i}{W_o} \left[ \frac{h_{sg}}{\Delta h_o} - \frac{\Delta h_{se}}{\Delta h_o} \right] + \tau \frac{dp}{dt}}$$

WHERE:

$$Q_0 = W_o \Delta h_o$$

$$\tau_B = \left[ A(1-y) + B + C \frac{r_a C_w}{\gamma} \right] \frac{P_c V}{Q_0}$$

FIGURE A.1.2

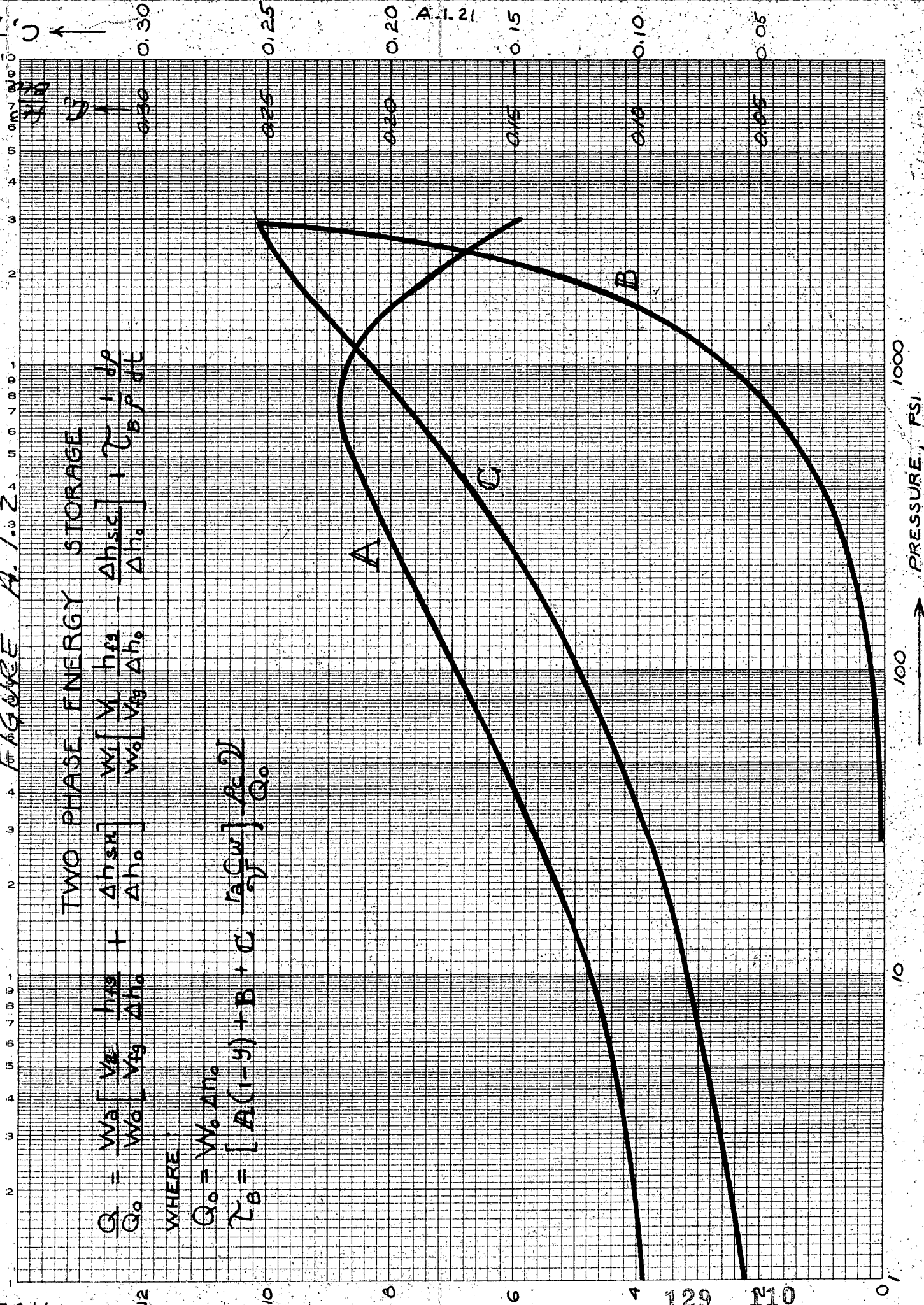


FIGURE A.1.3

4 CYCLES X 10 DIVISIONS PER INCH

GEN. ENG. PAPER

SEMI-LOGARITHMIC

10 DIVISIONS PER INCH

10 DIVISIONS PER INCH

10 DIVISIONS PER INCH

10 DIVISIONS PER INCH

10 DIVISIONS PER INCH

10 DIVISIONS PER INCH

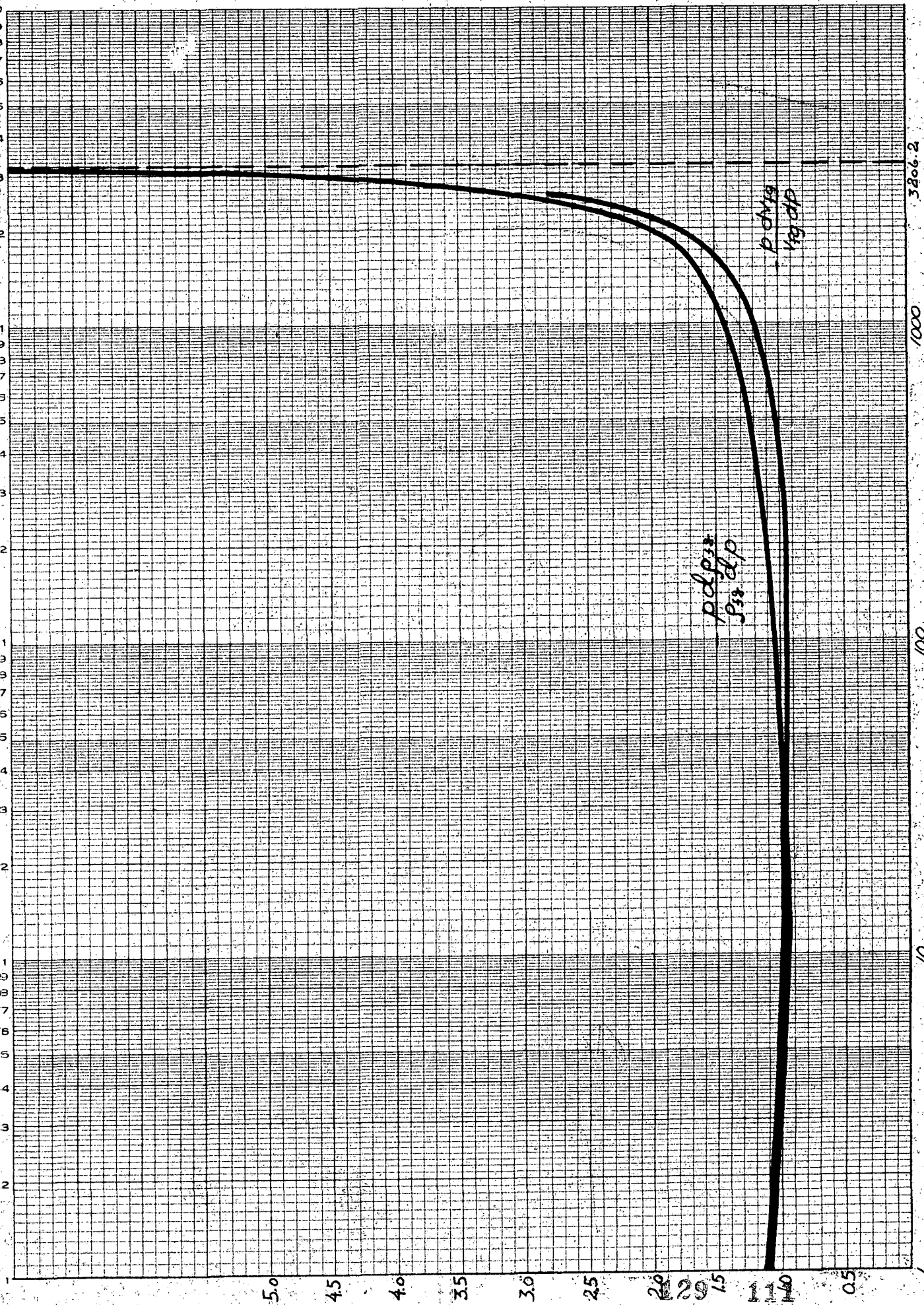


FIGURE A.1.4

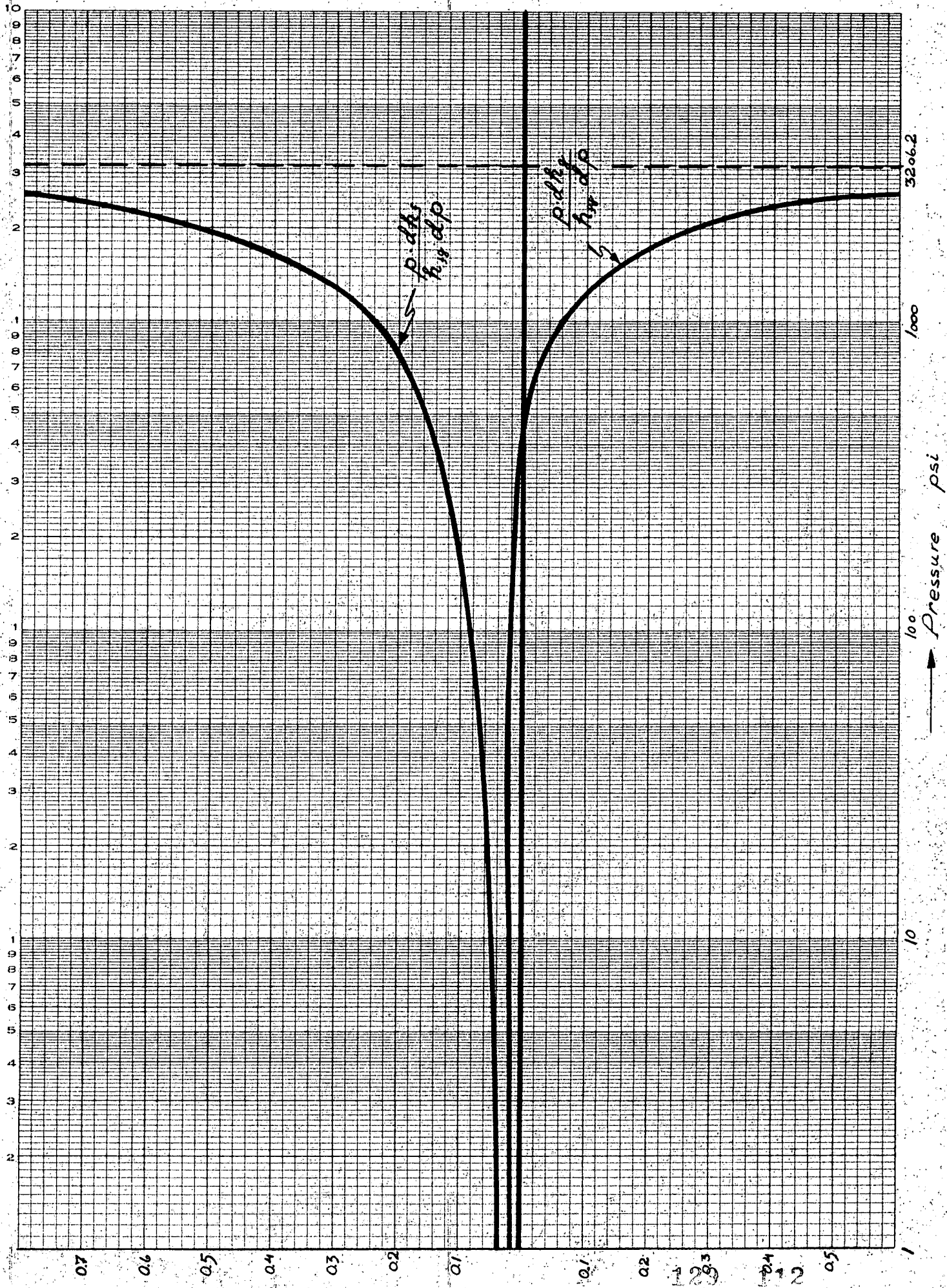
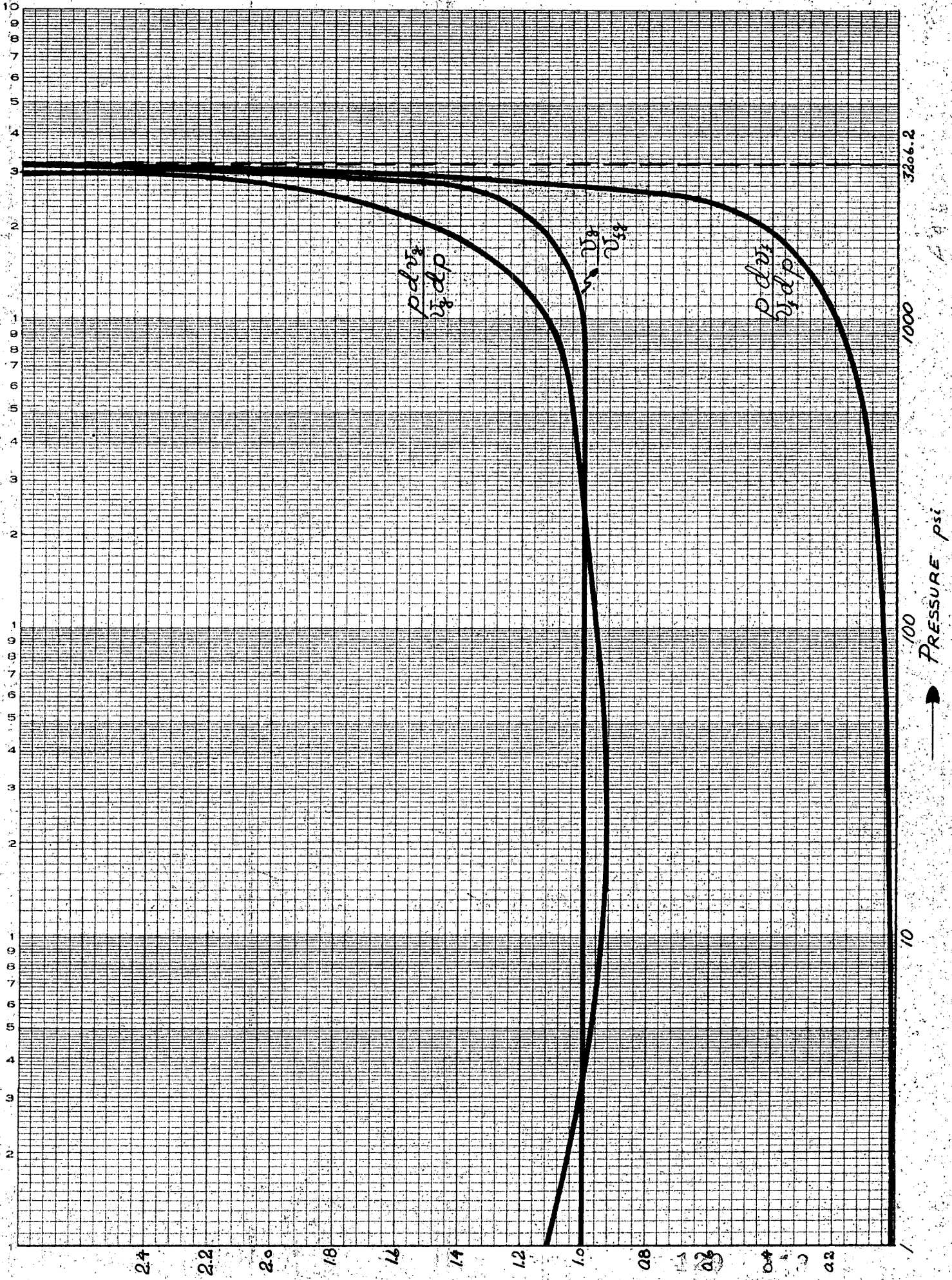




FIGURE A.1.5



## APPENDIX A. 2 - COUNTERFLOW EXCHANGER

The analysis associated with exchangers, and in particular the counterflow exchangers, is in Chapter 4. Two of the exchangers in this system qualify as counterflow, the intermediate exchanger and the superheater. Two studies are performed on these exchangers. The first considers the uncoupled exchanger temperature responses to flow and temperature inputs. The second study considers the coupled responses of the exchangers for flow and temperature variations.

## A. 2. 1. Uncoupled Responses

Chapter 4 presents an analysis of the counterflow exchanger. Equations 4.14a and 4.14b are the solutions to the exchanger terminal temperatures. These equations however may be written in the following form.

For small lumps, that is, short exchangers

$$T_{a \text{ out}} = \Delta_a \left\{ 1 - G(1+\Gamma) T_{a \text{ in}} + G(1+\Gamma) T_{b \text{ in}} \right\} \quad (\text{A. 2. 1})$$

$$T_{b \text{ out}} = \Delta_b \left\{ G(1-\Gamma) T_{a \text{ in}} + 1 - G(1-\Gamma) T_{b \text{ in}} \right\} \quad (\text{A. 2. 2})$$

$$\text{Where } \Delta = \text{unit gain dynamic operator} \quad (\text{A. 2. 3})$$

$$G = \frac{\tanh \beta \Gamma}{\Gamma + \tanh \beta \Gamma} \quad (\text{A. 2. 4})$$

$$\Gamma = \frac{W_b C_{pb} - W_a C_{pa}}{W_b C_{pb} + W_a C_{pa}} \quad (\text{A. 2. 5})$$

$$\beta = \frac{UA}{2} \left( \frac{1}{W_a C_{pa}} + \frac{1}{W_b C_{pb}} \right) \quad (\text{A. 2. 6})$$

Figure A. 2. 1 presents the uncoupled reticulated exchanger model block diagram. This diagram models each stream with five transport operators and four transfer nodes. The evaluation of  $\beta$  is based upon the static analysis in References 1 and 2. A discussion of the unity gain operator  $\Delta$  is in Chapter

## A. 2. 2

4. The computer model uses simple lag approximations to these dynamic operators. Each of the five transport operator times equal one-fifth of the total effective transport time as defined in Equation A. 2. 7.

$$\tau_a = \frac{M_a C_{pa} + C_w r_a}{W_a C_{pa}} \quad (\text{A. 2. 7})$$

where

$r_a$  = a side fraction of heat transfer resistance

$C_w$  = wall capacity (A. 2. 8)

$M_a$  = stored fluid mass (A. 2. 9)

$W_a$  = mass flow rate (A. 2. 10)

$C_{pa}$  = specific heat (A. 2. 11)

and similarly for stream b.

The total transport times for both streams in both exchangers are

<u>100% Load Level</u>	
IHX	
Primary	53.5 secs.
Secondary	6.59 secs.
S. H.	
Secondary	59.2 secs.
Steam	2.12 secs.

Table A. 2. 1 presents the coefficient values used for the computer solution of Figure A. 2. 1.

### A. 2. 3

Small flow variations can be analyzed by a linear model. The solutions of Chapter 4 are valid for flow variations; however, they are algebraically non-linear. Linearization of the equivalent Equations A. 2. 1 and A. 2. 2 lead to an additional term to each equation of the form.

$$G (T_{a \text{ local}} - T_{b \text{ local}}) \frac{1}{2} (1-\Gamma) (\Delta W_b - \Delta W_a) \quad (\text{A. 2. 12})$$

The model used in this analysis divides the exchanger into equal  $\beta$  lumps. Therefore, the only variation from node to node in the coefficient of Equation A. 2. 12 is the local heat transfer temperature difference  $T_{a \text{ local}} - T_{b \text{ local}}$ . The coefficient used at each node is  $G_{wij}$ . In the actual computer solution voltages corresponding to the local temperature difference were measured and used to scale the coefficients of the  $\Gamma$  terms proportionally. The purpose of this solution is to evaluate the effective response time constants and illustrate the nature of small flow variations. The gain between flow and temperature can be evaluated through Equation A. 2. 12.

Large flow variation dependence is not satisfactorily established by the linear model. A technique peculiar to the computer provides a non-linear solution from the linear model. A steady-state temperature solution at one flow configuration is held in the computer. In this hold mode, the computer coefficient settings are adjusted to the new flow configuration. The hold mode is released and the transient solution ensues.

#### A. 2. 2. Coupled Responses

The computer model presented in the uncoupled analysis provides accurate terminal temperature histories and less accurate histories at intermediate locations. This model, however, requires considerable more computation equipment than is available or necessary for a total systems analysis. A method presented in Appendix A. 7 provides a means of approximating the terminal to terminal behavior of the exchanger with a minimum of computer



operations. In this instance, the terminal response solutions to the uncoupled exchangers are approximated through the technique of Equations A. 7. 2 and A. 7. 3. These equations determine the characteristic times of the response. This method is significant in that a group of simple lags can be selected and coupled to provide the same terminal-to-terminal responses as governed by Equations A. 7. 2 and A. 7. 3.

The terminal-to-terminal and linear model equations are

$$T_{2a} = (1 - G_x) \Delta_{21} T_{1b} + G_x \Delta_{25} T_{5b} - \Delta_{2w} \Delta \Gamma \quad (\text{A. 2. 13})$$

$$T_{3a} = (G_x) \Delta_{31} T_{1b} + (1 - G_x) \Delta_{25} T_{5b} - \Delta_{3w} \Delta \Gamma \quad (\text{A. 2. 14})$$

For the intermediate exchanger and

$$T_{4a} = \left[ 1 - G_s (1 - \Gamma_s) \right] \Delta_{43} T_{3b} + G_s (1 + \Gamma_s) \Delta_{47} T_7 + G_{FN} \Delta_{4w} \Delta \Gamma_s \quad (\text{A. 2. 15})$$

$$T_8 = G_s (1 - \Gamma_s) \Delta_{83} T_{3b} + \left[ 1 - G_s (1 - \Gamma_s) \right] \Delta_{87} T_7 + G_{FS} \Delta_{8w} \Delta \Gamma_s \quad (\text{A. 2. 16})$$

for the superheater.

The operators  $\Delta$  are the unity gain dynamic operators developed through the methods of Appendix A. 7. The temperature input gains in these equations follow from Equations A. 2. 1 and A. 2. 2 by setting the dynamic operators equal to unity. The flow gains follow similarly from Equations A. 2. 1 and A. 2. 2.

For small perturbations, the linearized flow variation dependence in Equations A. 2. 1 and A. 2. 2 are respectively

$$\left[ G_s + (1 + \Gamma_s) \frac{\partial G_s}{\partial \Gamma_s} \right] (T_{b \text{ in}} - T_{a \text{ in}}) \quad (\text{A. 2. 17})$$

and

$$\left[ G_s - (1 - \Gamma_s) \frac{\partial G_s}{\partial \Gamma_s} \right] (T_{b \text{ in}} - T_{a \text{ in}}) \quad (\text{A. 2. 18})$$

Equations A. 2. 13 - A. 2. 16 are normalized to the reactor terminal temperature difference,  $T_{1a} - T_{2b}$ . This leads to the following definitions for the superheater flow gains.

$$G_{FN} = \left[ G_s + (1 + \Gamma_s) \frac{\partial G_s}{\partial \Gamma_s} \right] \frac{T_{3b} - T_7}{T_{1a} - T_{2b}} \quad (\text{A. 2. 19})$$

$$G_{FS} = \left[ G_s - (1 - \Gamma) \frac{\partial G_s}{\partial \Gamma_s} \right] \frac{T_{3b} - T_7}{T_{1a} - T_{2b}} \quad (\text{A. 2. 20})$$

The tabulation of the values in Table A. 2 is based upon the static analysis in the References 1 and 2.

The counterflow exchanger flow gains are unity. This may be shown by the following.

In the intermediate exchanger ( $\Gamma = 0$ ) the linearized flow dependence form is

$$(T_{5b} - T_{1a}) G \Delta \Gamma \quad (\text{A. 2. 21})$$

But from the steady-state Equations A. 2. 1 and A. 2. 2 with  $\Delta = 1$ .

$$G = \frac{T_{1b} - T_{2a}}{T_{1b} - T_{5b}} \quad (\text{A. 2. 22})$$

All of the temperatures in the control study are normalized to the temperature difference across the reactor,  $T_{1a} - T_{2b}$ . Therefore, the flow coefficients in Equations A. 2. 13 and A. 2. 14 are - 1.

The results of this modeling are presented in Tables A. 2. 2 and A. 2. 3 and Figures A. 2. 2 and A. 2. 3. A further simplification, however, is used in the closed loop or controlled system models dynamics approximation. The time constants associated with temperature inputs are assumed the same as the time constants associated with flow inputs. Since the flow input time constant

## A.2.6

is faster than the temperature input time constants, the rate of temperature changes are over-emphasized. The validity of this is proven in the computer solutions. No temperature variations during normal control were measured during transient conditions. In over-emphasizing the temperature input model, no associated temperature variations were measured. Hence, need of an accurate model is reduced.

Coupled but uncontrolled or open loop system responses were measured at the 100% and 20% load level. The computer solutions to the inlet-out terminal temperatures at the superheater and intermediate heat exchangers are presented in Figures A.2.4 and A.2.5. In these models, however, the proper temperature input time constants have been used. There are no flow inputs except at the superheater and this is the change in steam flow.

Table A.2.1

### Superheater

<u>Shell/Tube</u>	<u>100/100</u>	<u>20/20</u>	<u>100/20</u>	<u>20/100</u>
$\beta/4$	.466	.68	.5	1.09
G	.316	.40	.321	.503
$\Gamma$	-.322	-.332	-.815	+.429
$\tau_{sh1}$	59.2 secs	266.4	59.2	266.4
$\tau_{sh2}$	2.12	8.6	8.6	2.12

### Intermediate Exchanger

$\beta/4$	1.96	5.62	5.45	4.1
G	.685	.85	.597	.54
$\Gamma$	0	0	-.67	+.67
$\tau_{x1}$	53.5	159	53.5	159
$\tau_{x2}$	6.59	18.3	18.3	6.59

## PARAMETERS FOR SUPERHEATER CONTROL MODEL

Parameter	100% Load Pt.	20% Load Pt.
$G_{FN}$	.739	.942
$G_{FS}$	.430	.382
$G_S$	.616	.684
$R_N$	1.00	.200
$R_S$	1.00	.212
$\Gamma_S$	-.322	-.322

Closed Loop Model

Parameter	100% Load Pt.	20% Load Pt.
$\tau_{SH1}$	32.4	178
$\tau_{SH2}$	23.6	147.5
$\alpha_1$	1.0	1.0
$\alpha_2$	.47	.60
$\beta_1$	1.0	1.0
$\beta_2$	.75	.70
$\gamma_1$	1.0	1.0
$\gamma_2$	.47	.60

Open Loop Model

Parameter	100% Load Pt.	20% Load Pt.
$\tau_{SH1}$	29.3	10.26
$\tau_{SH2}$	29.3	146.5
$\alpha_1$	1.0	1.0
$\alpha_2$	.47	.6
$\beta_1$	1.0	1.0
$\beta_2$	.75	.70
$\gamma_1$	1.0	1.0
$\gamma_2$	.47	.60

# A.2.8

## PARAMETERS FOR INTERMEDIATE HEAT EXCHANGER CONTROL MODEL

Parameter	100% Load Pt.	20% Load Pt.
$G_x$	.887	.957
$R_N$	1.00	.200

### Closed Loop Model

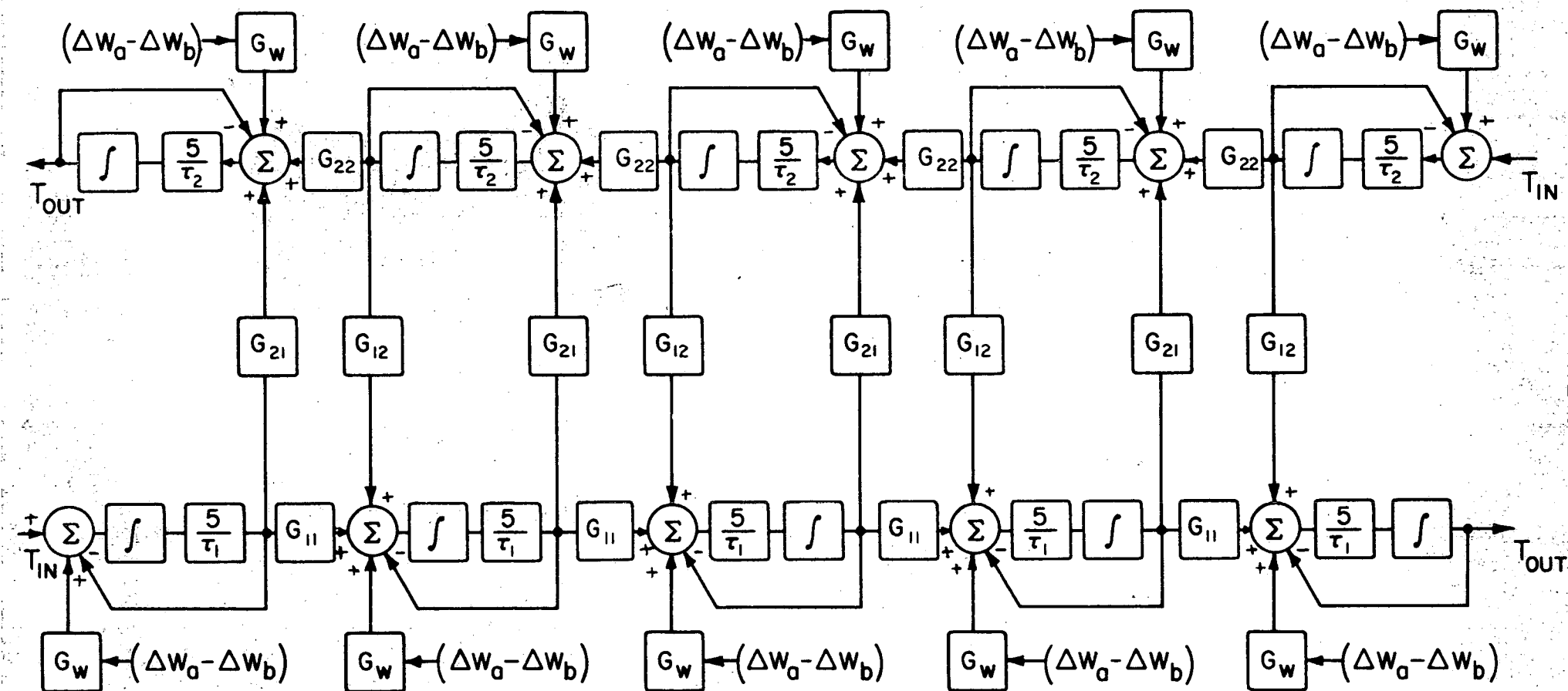
Parameter	100% Load Pt.	20% Load Pt.
$\tau_{x1}$	65.0	143.0
$\tau_{x2}$	65.0	143.0
$\alpha_1$	.10	.20
$\alpha_2$	1.0	.20
$\beta_1$	1.0	1.0
$\beta_2$	.56	.25
$r_1$	1.0	1.0
$r_2$	.89	1.0

### Open Loop Model

Parameter	100% Load Pt.	20% Load Pt.
$\tau_{x1}$	26.8	133.8
$\tau_{x2}$	37.5	268.0
$\alpha_1$	.10	.20
$\alpha_2$	1.0	.20
$\beta_1$	1.0	1.0
$\beta_2$	.56	.25
$r_1$	1.0	1.0
$r_2$	.89	1.0

Table A.2.3

# COUNTER FLOW RETICULATED HEAT EXCHANGER MODEL



$$G_{22} = [1 - G(1 - \Gamma)]$$

$$G_{21} = G(1 - \Gamma)$$

$$G_{11} = [1 - G(1 + \Gamma)]$$

$$G_{12} = G(1 + \Gamma)$$

FIGURE A.2.1

# SUPER HEATER CONTROL STUDY COMPUTER MODEL

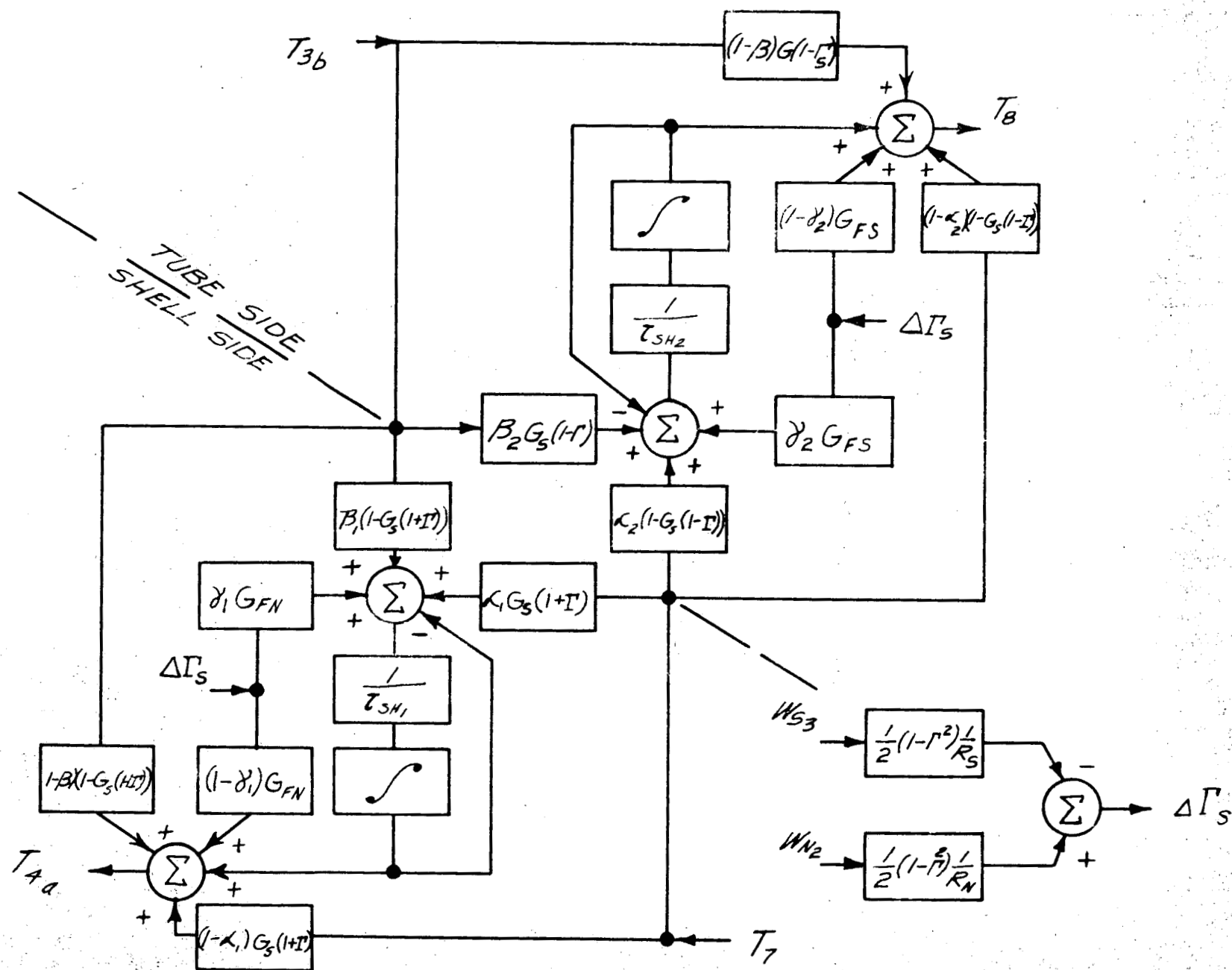


FIGURE A.2.2

# INTERMEDIATE HEAT EXCHANGER CONTROL STUDY COMPUTER MODEL

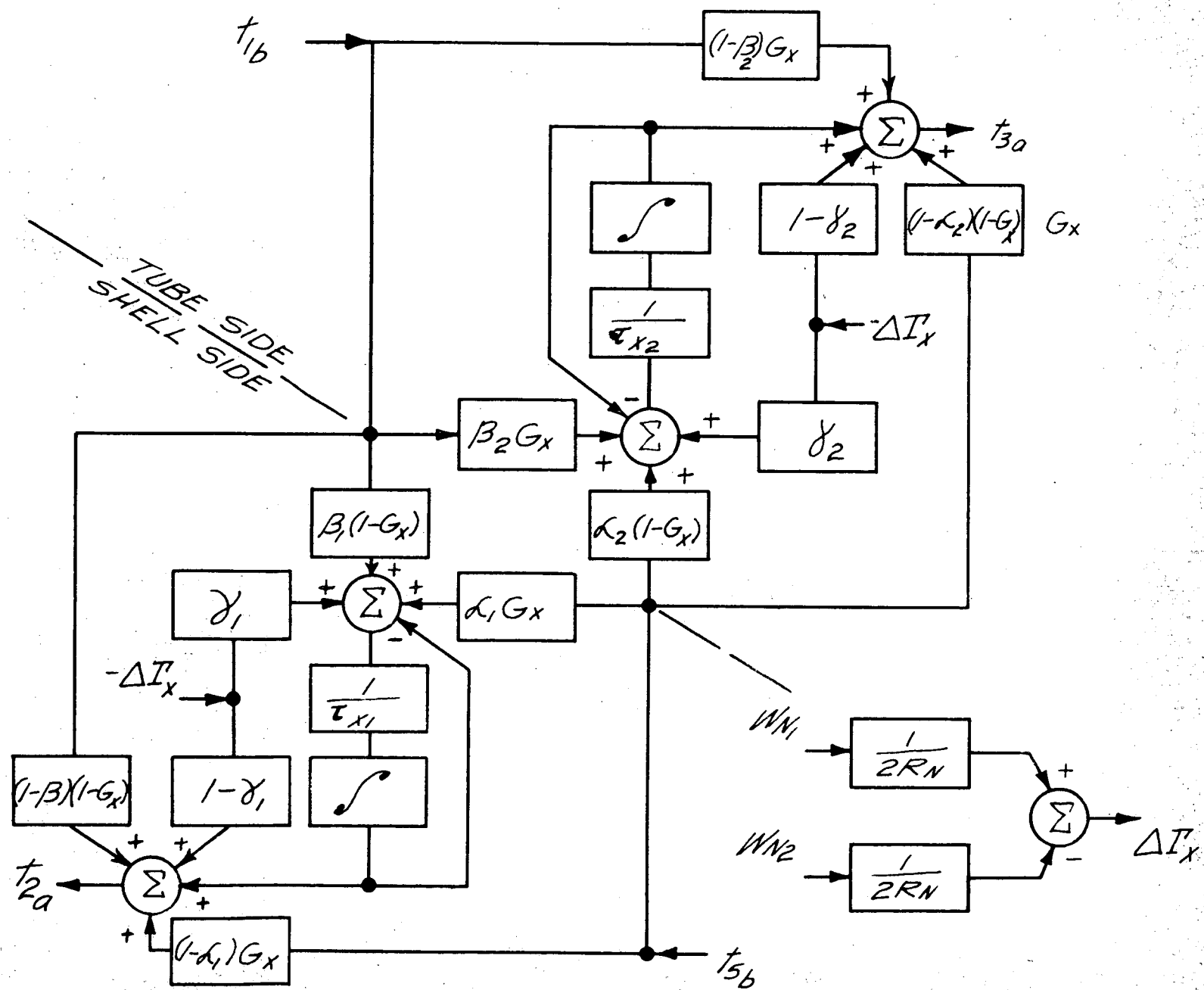
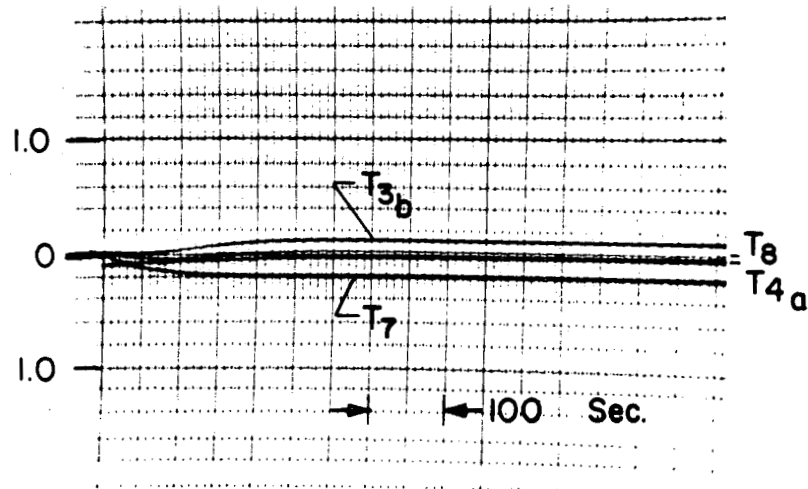


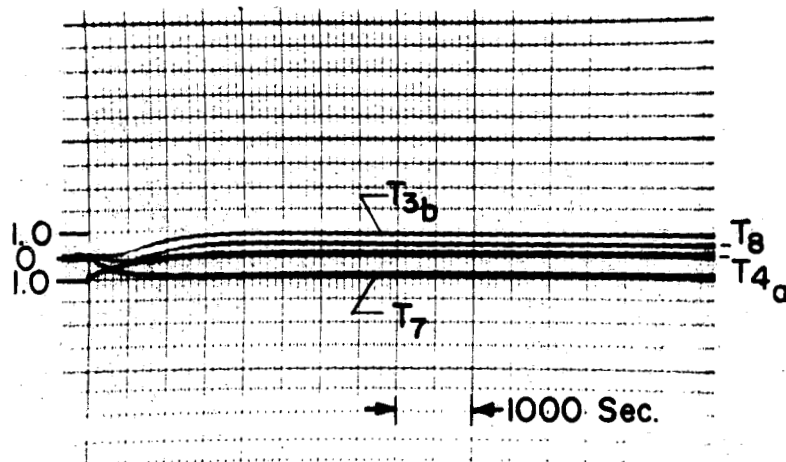
FIGURE A.2.3





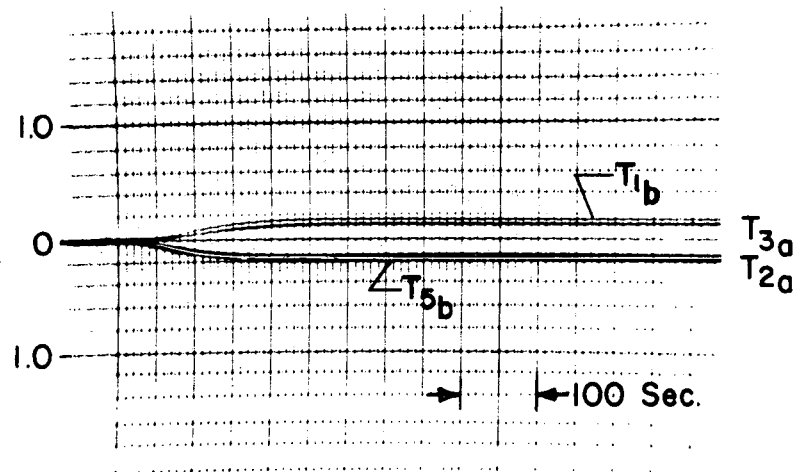
100% LOAD LEVEL

$$T = \frac{\Delta T}{(1200 - 723)^{\circ} F}$$



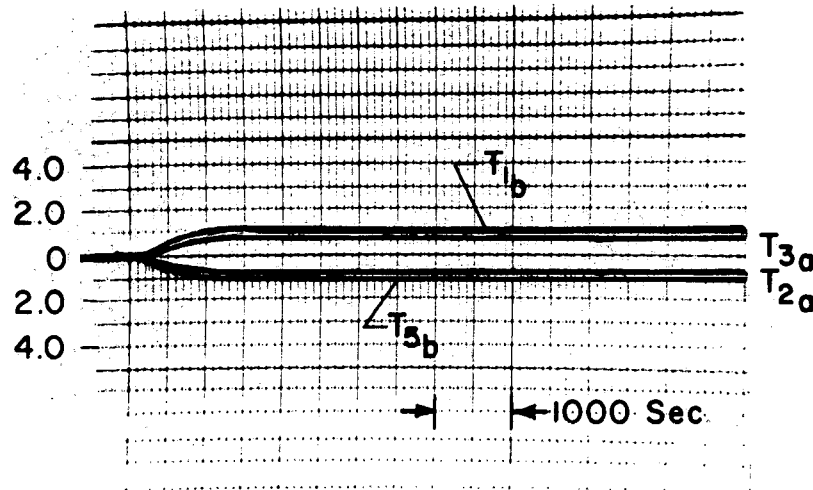
20% LOAD LEVEL

OPEN LOOP SUPERHEATER COUPLED RESPONSES  
TO STEP INCREASE IN STEAM VALVE AREA



100 % LOAD LEVEL

$$T = \frac{\Delta T}{(1200 - 723)^{\circ}F}$$



20 % LOAD LEVEL

OPEN LOOP INTERMEDIATE HEAT EXCHANGER COUPLED RESPONSES  
TO STEP INCREASE IN STEAM VALVE AREA

## APPENDIX 3 - BOILER MODEL

The boiler analysis has been presented in Chapter 4 and Appendix 1. Two separate studies have been conducted on the computer, one of the uncoupled boiler responses, and the other of the coupled or control study responses of the boiler.

### A.3.1. Uncoupled Responses

A spatially reticulated model of the boiler is used to study the uncoupled disturbance response. This model provides a temperature history of the sodium stream within the boiler and at the terminals. The model is simply an extension of the counterflow model provided in Appendix A.2 with  $\Gamma = +1$ . The boiler may be reticulated in many ways. In particular, this model divides the boiler into twenty equal  $\beta$  and transport regions. Figure A.3.1 provides a block diagram representation of the computer model. The simultaneous boiler equations are

$$T_{ai} = \Delta_{ai} \left[ (1 - 2G_i) T_{ai} + 2GT_b \right] \quad (A.3.1)$$

$$T_b = T_b \quad (A.3.2)$$

$$G_i = \frac{1 - e^{-2\beta_i}}{2} \quad (A.3.3)$$

$$\beta_i = \frac{(UA)_i}{2W_a C_{pa}} \quad (A.3.4)$$

$$\Delta_{ai} = \text{Unity gain sodium side transport delay of the } i^{\text{th}} \text{ subdivision} \quad (A.3.5)$$

The sodium stream terminal-to-terminal effective transport time is

$$\tau = \frac{M_{n2} C_{pn2} + C_{w^r b} + C_s}{W_{n2} C_{pn2}} \quad (A.3.6)$$

where

$C_w$  = tube wall capacity

$C_s$  = shell and baffle capacity

$r_b$  = steam side resistance/total resistance

The evaluation of  $\beta$  is based upon the static analysis of Reference 2. These equations provide a solution to temperature disturbances to the model; however, the effects of sodium flow variations is an algebraic non-linear dependence. For small variations in the flow rate, a linearized model may be used.

The effect of a flow variation is a change in exchanger effectiveness. The effectiveness may be determined from Equations A.3.1 and A.3.2 upon setting the dynamic operator to unity.

$$\epsilon = 2G \quad (A.3.7)$$

Therefore, the additional linearly superposed term to Equation A.3.1 for effectiveness variations is

$$2\Delta_{ai}(T_{bi} - T_{ai}) \Delta G_i$$

Linear temperature-flow variation gains depend upon the local heat transfer temperature differences.

The block diagram and computer coefficients for the uncoupled problem are presented in Figure A.3.1 and Table A.3.1. The block diagram brings to light the simple interstream coupling in the boiler as opposed to the two stream counterflow exchanger.

The entire model is a simple cascading of lags with no feedback from lag to lag. Therefore, this exchange model is quite adaptable to pencil and paper analysis. Any temperature profile within the boiler is the outlet terminal temperature of a boiler of length equal to the distance from the inlet to the point of interest. Computer results indicate that the overall response may be approximated by a single lag principally because of the near unity effectiveness.

$$T_{5a} = \frac{1}{1 + \frac{\tau_a D}{\alpha_a}} \left[ (1-\epsilon) T_{4b} + \epsilon T_7 \right] \quad (\text{A. 3. 8})$$

### A. 3. 2. Coupled Responses

The analysis of Figure A. 1. 1 provides the two-phase energy equation for the boiler. This establishes a relationship between the heat transferred to the boiler and the boiler steam generation and pressure. The analysis in Chapter 4 leading to Equations 4. 15, 4. 16, and 4. 17 provide a relation between the boiler sodium stream terminal temperatures and the heat transfer to the boiler. The linearized form of Equation 4. 16, using the lag approximation for  $G_{ab}$ , is

$$\begin{aligned} \frac{\Delta Q}{Q} &= \frac{R_q}{R_N} \frac{\Delta W_{n2}}{W_{n2}} + \frac{\epsilon R_q/B}{1 + \frac{\tau_a D}{\alpha_a}} \frac{\Delta T_4}{T_1 - T_2} - \alpha_a R_q \frac{\lambda T_7}{T_4 - T_5} \left( 1 - \frac{1}{1 + \frac{\tau_a D}{\alpha_a}} \right) \\ \frac{\Delta p}{p_0} &= \epsilon \left( \frac{1}{1 + \frac{\tau_a D}{\alpha_a}} \right)^2 \lambda \frac{T_7}{T_1 - T_2} \frac{\Delta p}{p_0} \end{aligned} \quad (\text{A. 3. 9})$$

$$R_q = \frac{Q}{Q_{\max}} \quad (\text{A. 3.10})$$

$$R_N = \frac{W_n}{W_{n \max}} \quad (\text{A. 3.11})$$

$$B = \frac{T_4 - T_5}{(T_1 - T_2)_{\max}} \quad (\text{A. 3.12})$$

$$\lambda = \frac{pv_{fg}}{h_{fg} J} \quad (\text{A. 3.13})$$

$$\alpha_a = \frac{UA}{2W_{n2} C_{pn2}} \quad (\text{A. 3.14})$$

$$\epsilon = 1 - e^{-\alpha_a} = \text{effectiveness} \quad (\text{A. 3.15})$$

In this linearization, no account is made for variations in effectiveness, because these are very small as indicated in Reference 2.

The analysis in Figure A.1.1 presents a two-phase energy equation which is quite general with respect to the inlet-outlet conditions on the control volume. The control volume chosen for the pressure control volume assumes a sub-cooled liquid entering and saturated vapor discharging. Physically an energy balance is written between feedwater in and the steam out to the superheater. This equation is

$$\frac{Q}{h_{fg}} = -W_f \frac{v_f}{v_{fg}} + W_{s2} \frac{v_g}{v_{fg}} + W_{s2} \tau_e \frac{1}{p} \frac{dp}{dt} + W_f \frac{h_{\text{sub}}}{h_{fg}} \quad (\text{A. 3.16})$$

Out of coincidence of design

$$\frac{v_f}{v_{fg}} = \frac{h_{\text{sub}}}{h_{fg}} = .2 \quad (\text{A. 3.17})$$

Linearization of equation (A. 3. 16)

$$\frac{\Delta Q}{W_{s2} h_{fg}} = -\frac{\Delta W_{s2}}{W_{s2}} \left( \frac{v_f}{v_{fg}} \right) + R_s \frac{h_g}{h_{fg}} + \tau_e D \frac{p}{p} \quad (\text{A. 3. 18})$$

where the feedwater enthalpy is assumed constant.

The good pressure control exhibited on the computer justifies neglecting variations in the vapor enthalpy with pressure for it is a small contribution in light of the fast sodium response.

There are two values of  $\tau_e$ ; one for pressure increases and the other for pressure decreases. This is a non-linear behavior. Its effect on closed loop behavior is found to be small, however). During a pressure drop, heat is transferred from the wall (drum separator and other non-heat transfer but heat storage regions) storage. Since the saturation temperature is below the wall temperature, the steam is being superheated. The superheating resistance is very large; hence the walls reach the steam temperature very slowly. For a pressure rise however, steam condenses on the walls. This mode of heat transfer is very efficient provided the liquid film drains freely and causes the drum wall temperature to be tightly coupled to the steam temperature. In the former case, the energy storage in the drum wall is neglected and in the latter the drum walls are assumed thermally lumped with the steam. (Reference 12).

The boiler is broken down into six separate regions in which the time constant, as defined in Equation 12b of Figure A.1.1, is evaluated for each and summed for the net effect. The regions are

1. Riser tubes
2. Drum separator to liquid level
3. Downcomer boiler and central
4. Vapor space below tray
5. Vapor space above tray
6. Boiler-superheater pipe

The evaluation was performed at 20%, 40%, 60%, 80%, and 100% of rated load. The time constant variation with load is very small.

The time constants for increasing pressure and decreasing pressure respectively are (flushing in the downcomer is considered in decreasing pressure transients but its effect on circulation is neglected)

$$\tau_e = 78.2 \text{ secs}$$

$$\tau_e = 62 \text{ secs}$$

For most runs, the computer model used the latter value. Results were found to be nearly the same when the former was employed. The computer block diagram and coefficient values are presented in Figure A.3.2.

The normalization values are

$$W_{n2} = 1,665,000 \text{ lbs/hr}$$

$$W_{s2} = 270,000 \text{ lbs/hr}$$

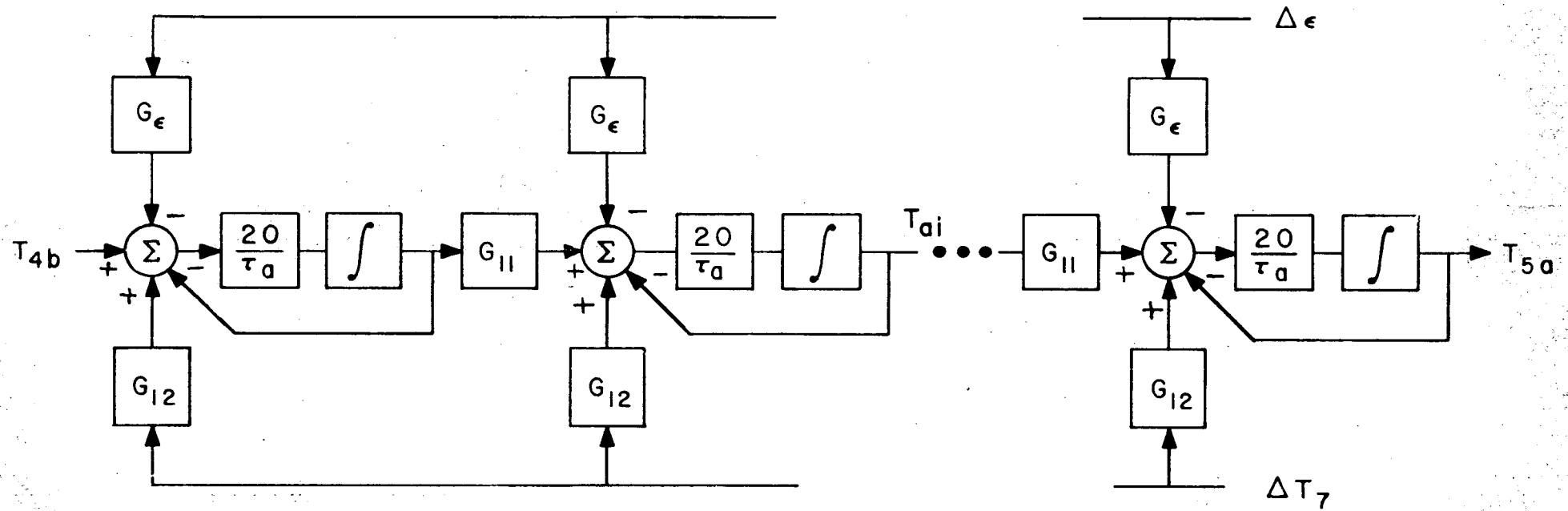
$$Q = 136,000,000 \text{ BTU/hr}$$

$$p = 2200 \text{ psi}$$

$$T_4 = T_5 = (1200 - 723) ^\circ\text{F}$$



# BOILER RETICULATED MODEL



- A.3.8 -

$$G_{11} = 1 - G(1 + \Gamma)$$

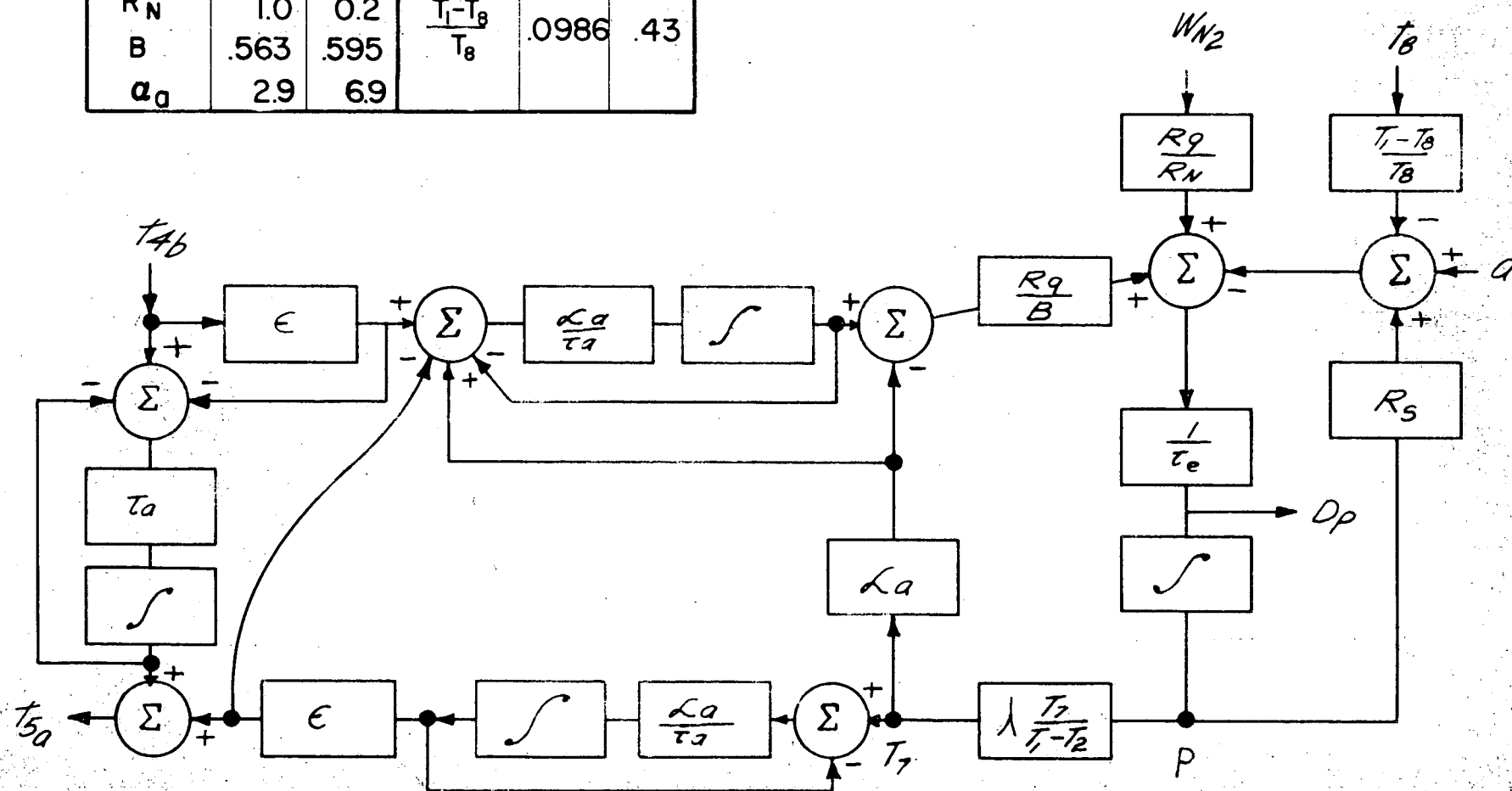
$$G_\epsilon = 2(T_{ai} - T_7)$$

$$G_{12} = G(1 + \Gamma)$$

FIGURE A.3.2

FIGURE A.3.1  
STEAM BOILER CONTROL MODEL

	100%	20%		100%	20%
$\tau_a$	73.5	367	$\tau_e$	62.0	62.0
$R_s$	1.0	.212	$\epsilon$	.943	.999
$R_q$	1.0	.2117	$\lambda \frac{T_7}{T_1 - T_2}$	.30	.28
$R_N$	1.0	0.2	$\frac{T_1 - T_8}{T_8}$	.0986	.43
$B$	.563	.595			
$a_d$	2.9	6.9			



## APPENDIX 4 - PIPE-PUMP DYNAMICS

Most fluid flow networks are basically closed loop. In fact through the conservation laws they can all be shown to be closed, that is at any point in a network mass leaving will eventually return to that point. In particular, three separate loops occur in this system each of which may be satisfactorily modeled by the following techniques.

### A. 4. 1. Sodium Pipe-Pump Loops

The momentum equation around the loop states that the sum of the forces around the loop must be zero. A satisfactory low to higher frequency model considers the flow characterized one dimensionally and environmental and system properties to be lumped in space. A diagram of such a model is presented in Figure A. 4. 1. This reticulation or sub-division occurs from obvious geometrical considerations or for a more detailed representation of distributed parameters.

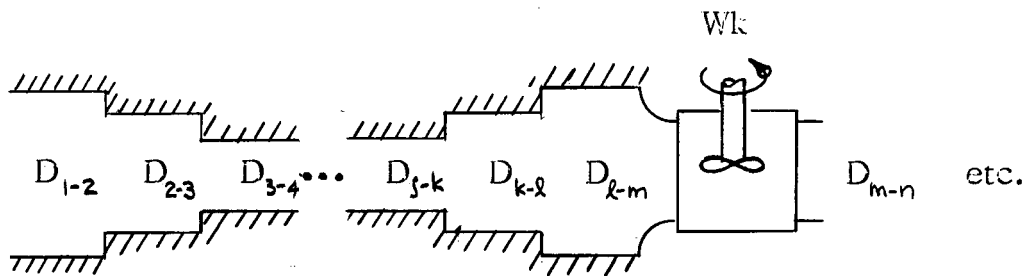


Figure A. 4. 1 - Generalized One Dimensional Pipe-Pump Model

#### A. 4. 1. 1. Pipe Model

Such a loop consists of a finite group of pipes each with constant cross section, lumped resistance at the walls and lumped parameters within the pipe, and also a power supply device such as a pump. In steady-state the pump supplies the energy dissipated through the lumped resistances. The pump must also in transient conditions account for the change in stored energy (kinetic energy

of motion) in the loop.

The unsteady momentum equation for one lump or one uniform section is (Reference 8)

$$P_a A - P_b A - \int_0^L \tau_{\text{frict}} \frac{A}{d} dL = \int_0^L \left( \frac{d}{dt} \rho A \text{vel} \right) dL \quad (\text{A. 4.1})$$

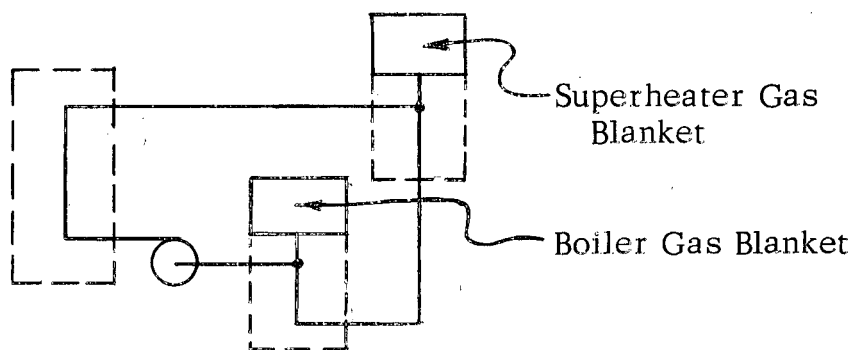
$$P_a - P_b = \left( \sum \frac{L}{A} \right) DW - \sum \delta P_{\text{frict}} \quad (\text{A. 4.2})$$

In which the terms are perfectly general for compressible as well as incompressible, flow and accuracy is limited only by the magnitude of subdivision. (To use with compressible flow however, account should also be made of mass storage). But the sum of the pressure changes around the loop must be zero; therefore,

$$\sum (P_a - P_b) = \delta P_{\text{pump}} = \left( \sum \frac{L}{A} \right) DW + \sum \delta P_{\text{frict}} \quad (\text{A. 4.3})$$

Characteristically  $\left( \sum \frac{L}{A} \right) DW$  is referred to as the inertia term and  $\sum \delta P_{\text{frict}}$  is called the dissipative term.

A schematic view of the secondary loop is in Figure A. 4. 2.



Secondary Sodium Loop Schematic

Figure A. 4. 2

Since 2 variable mass capacities exist in the system, an out-of-phase flow condition may exist between the 2 legs connecting the capacities. The pump or manipulated variable is in one leg and the boiler and superheater are in the other leg. Therefore, an additional lag exists between action and response. If just one capacity existed then there would be no capacity phase distortion introduced. Either one of the two capacities may be effectively isolated by placing a baffle between the gas blanket and sodium stream as illustrated in Figure A. 4. 3.

This baffle need not rigidly contact the tubes but should be close enough to give a maximum resistance to by-pass sodium flow. The low leakage or by-pass flow makes the secondary loop essentially a one-capacity system.

The inert gas pressurizer should be connected to the non-isolated gas blanket. This will provide the maximum sensitivity and speed of response for a pressurizer. The sodium liquid level control however should be maintained at the isolated gas blanket. The high resistance of the isolating baffle provides a large time constant for the sodium fluid charging time. This high time constant makes the level control speed of response equally slow; however, by the same token, the level cannot drift far before it is brought under control.

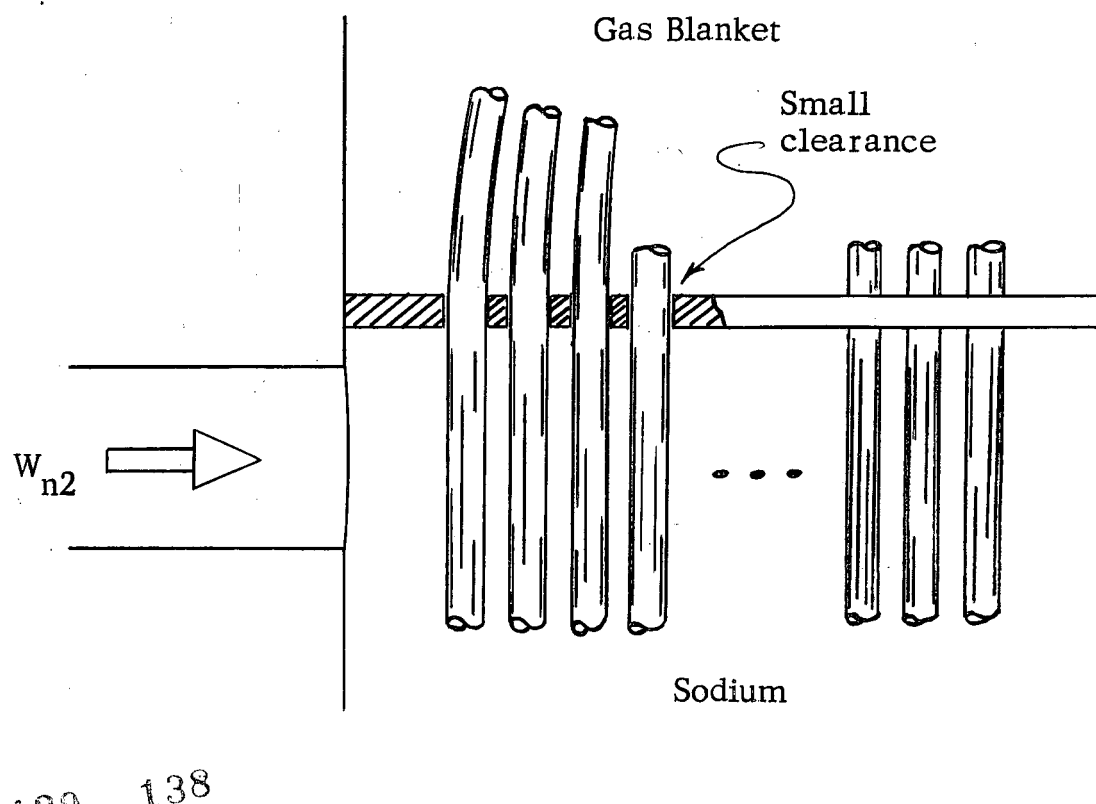
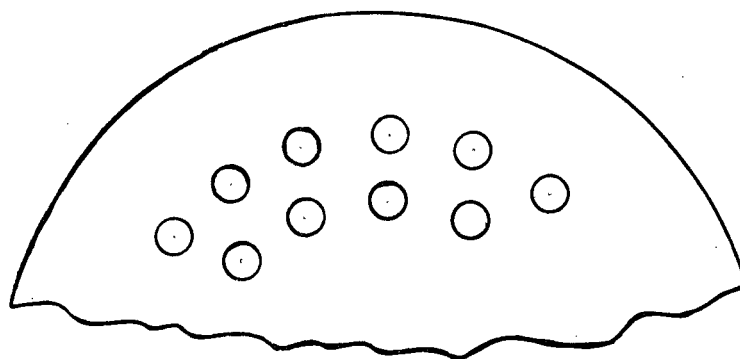
For an incompressible fluid in a system with one variable mass reservoir  $W$  is constant spacially. That is at any instant of time,  $W$  is the same throughout the loop. Linearized and non-dimensionalized Equation A.4.3 becomes:

$$\frac{\Delta \delta P_{\text{pump}}}{P_{\text{pump } 0}} = \frac{W}{g P_{\text{pump}}} \left( \sum \frac{L}{A} \right) D \frac{\Delta W}{W} + 2 \frac{\Delta W}{W} \quad (\text{A. 4. 4})$$

#### A. 4. 1. 2. Pump Model

Geometrically similar pumps can be represented by 3 dimensionless parameters for an incompressible flow. Dimensional analysis such as the Pi

-A.4.4-



129 138

A Proposed Gas Blanket Isolation

Figure A.4.3

theorem will varify the generality of the three following groupings (Reference 7).

$$\Pi_1 = (\Pi_2)^a (\Pi_3)^b \quad (\text{A. 4.5})$$

where a and b are peculiar to the chosen inter-group dependence. A common formulation is

$$\Pi_2 = \frac{W}{\rho n d^3} = \text{capacity term}$$

$$\Pi_1 = \frac{\delta P_{\text{pump}}}{\rho n^2 d^2} = \text{head term}$$

$$\Pi_3 = \frac{\mu}{\rho n d^2} = \text{Reynolds modulus}$$

The variables in each Pi group are normalized by the variables values at an arbitrary pump operating point.

Commonally the viscous effects are omitted in the pump analysis so that only 2 Pi groups are considered.

$$\frac{\delta P_{\text{pump}}}{\rho n^2 d^2} = f \left( \frac{W}{\rho n d^3} \right) \quad (\text{A. 4.6})$$

(Lower case letters are for the non-dimensionalized variables).

In perturbed form, Equation A. 4. 5 becomes:

$$\Delta \Pi_1 = f' \Delta \Pi_2 \quad (\text{A. 4.7})$$

where:

$$f' = \frac{\partial f(\Pi_2)}{\partial(\Pi_2)}$$

But:

$$\Delta \pi_1 = \frac{\Delta P}{P} - 2 \frac{\Delta N}{N} \quad (\text{A. 4. 8})$$

$$\Delta \pi_2 = \frac{\Delta W}{W} - \frac{\Delta N}{N} \quad (\text{A. 4. 9})$$

Equation A. 4. 7 reduces to:

$$\frac{\Delta \delta P}{P} - 2 \frac{\Delta N}{N} = f' \left( -\frac{\Delta W}{W} - \frac{\Delta N}{N} \right) \quad (\text{A. 4. 10})$$

In the steady-state, the pipe reflects a square law resistance; therefore:

$$\frac{\Delta \delta P_{\text{pump}}}{P_{\text{pump}}} = \frac{\Delta \delta P_{\text{pipe}}}{P_{\text{pipe}}} = 2 \frac{\Delta W}{W} \quad (\text{A. 4. 11})$$

Substitution into Equation (A. 4. 10)

$$2 \left( \frac{\Delta W}{W} - \frac{\Delta W}{N} \right) = f' \left( -\frac{\Delta W}{W} - \frac{\Delta N}{N} \right) \quad (\text{A. 4. 12})$$

This represents an identity in flow and speed. Solving for one in terms of the other

$$\frac{\Delta W}{W} = \frac{\Delta N}{N} \quad \text{in steady-state}$$

However, during transient condition, fluid inertia contributes an additional pressure drop. Equations A. 4. 4 and A. 4. 10 combined in transfer form is:

$$\Delta W = \frac{1}{1 + \tau_s D} \Delta N \quad (\text{A. 4. 13})$$

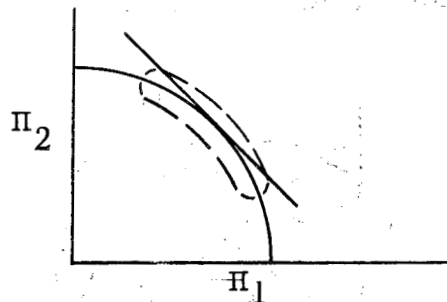
where:

$$\tau_s = \frac{W}{g P_{\text{pump}}} \sum \frac{L}{A} \quad (\text{A. 4. 14})$$



To this point, the presentation has been general. The pump evaluation has not been limited to a particular type of mechanical pump. However for the sake of the system analysis, a centrifugal pump with a variable speed induction motor drive has been chosen.

The illustration in Figure A. 4. 4 represents a typical centrifugal pump curve.



Pump Characteristic Curve

Figure A. 4. 4

The dotted line marks the region of normal operation. As a typical value, the slope equals - 1.

Consider the relationship for the torque applied to electrical rotor to torque on the pump impeller.

$$M_{\text{rotor}} - M_{\text{imp.}} = IDN \quad (\text{A. 4. 15})$$

But

$$\frac{\Delta M_{\text{imp.}}}{M} = 2 \frac{\Delta N}{N} \quad (\text{from Eulers pump and turbine equation}) \quad (\text{A. 4. 16})$$

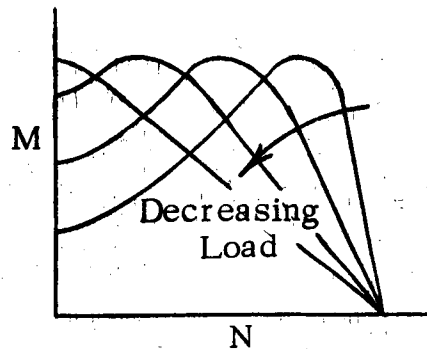
and

$$\frac{\Delta M_{\text{rotor}}}{M} = - K_N \frac{\Delta N}{N} + K_R \frac{\Delta R}{R} \quad (\text{A. 4. 17})$$

$$K_N = - \frac{\partial M}{\partial N} \frac{\Delta N}{M} \quad (\text{A. 4. 18})$$

$$K_R = \frac{\partial M}{\partial R} \frac{\Delta R}{M} \quad (\text{A. 4. 19})$$

Typical induction motor curves are presented in Figure A. 4.5.



Induction Motor Torque-Speed Curves

Figure A. 4. 5

Equation A. 4.15 expands to:

$$-K_N \frac{\Delta N}{N} + K_R \frac{\Delta R}{R} - 2 \frac{\Delta N}{N} = \frac{IN}{M} D \frac{\Delta N}{N} \quad (\text{A. 4. 20})$$

But:

$$\frac{IN}{M} \cdot \frac{N}{N} = \frac{\text{Kinetic Energy}}{\text{Power}}$$

Define

$$T_a = \frac{IN}{M} \cdot \frac{1}{K_N + 2} \quad (\text{A. 4. 21})$$

and

$$K_a = \frac{K_R}{K_N + 2} \quad (\text{A. 4. 22})$$

Then Equation A. 4. 20 becomes:

$$\frac{\Delta N}{N} = \frac{K_a}{1 + \tau_a D} \frac{\Delta R}{R} \quad (\text{A. 4. 23})$$

This derivation omits any of the magnetic induction dynamics associated with the transfer between secondary voltage and developed torques. The dynamics are quite fast (see Reference 6) and has been omitted in this analysis.

The flow controller develops a signal which reflects the motor secondary resistance. The transfer from controller to flow rate is a cascaded effect of Equations A. 4. 13 and A. 4. 23.

#### A. 4. 2. Feedwater-Pipe, Pump and Valve Model

The typical static design of the feedwater valve and pump usually matches the characteristics of the 2 elements for a linear valve stroke-flow rate relationship. This usually involves a staged constant speed centrifugal pump and a plug type control valve. Typically the pump is constant speed and there are no dynamics associated with the pump-drive as in the sodium loops. Since the condenser acts as an extremely low pass filter, only very long time variations in the system can have any coupling with the feedwater system. Therefore only the pipe from the condenser (which is treated as a constant pressure source) to the boiler is considered. The only dynamics then are associated with pipe inertia and actuator capacity. Figure A. 4. 6 gives a steady-state lumped element representation of the feedwater line pressure.

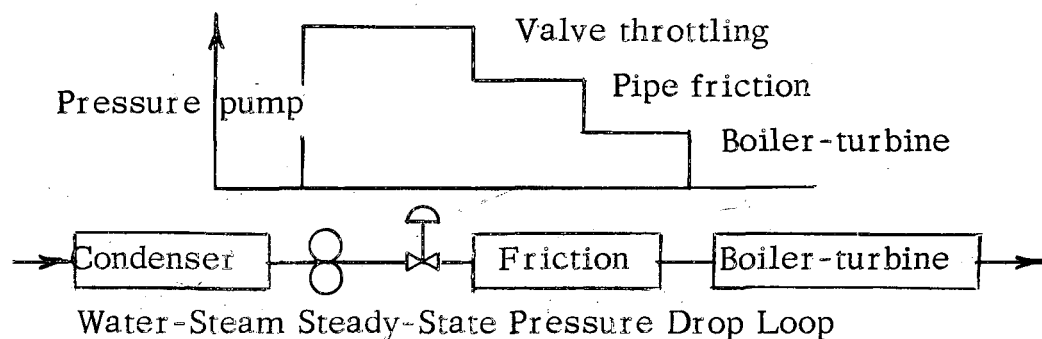


Figure A. 4. 6

However, during a transient condition, pipe inertia adds another pressure difference. The importance of the inertia drop is reflected by the time constant  $(\sum \frac{L}{A}) \frac{W}{gP_o}$ . The feedwater nozzle on the boiler separator has an area of .267 ft<sup>2</sup> (Reference 2). The normalizing pressure is boiler pressure.

$$(\sum \frac{L}{A}) \frac{1}{gP} = \frac{(75) L}{(.267) (32.2) (2200) (144)} = \frac{L}{36,300} \quad (\text{A. 4. 24})$$

Obviously for pipe dynamics to be of any significance in the feedwater circuit, the pipe must be enormously long. Consequently for the purpose of a computer model, a statically linear relationship exists between valve area and feedwater flow. However to account for residual lags in the instrumentation circuit and any actuation lag in the valve, the following provides a sufficient low to medium frequency approximation.

$$\frac{\Delta W_f}{W_f} = \frac{1}{1 + \tau_a D} \frac{\Delta M}{M} \quad (\text{A. 4. 25})$$

#### A. 4. 3. Steam Pipe Model

The steam pipe is essentially different than the other pipes in that the fluid is compressible. The flow rates at different points in space of a compressible medium can shift in phase with respect to one and another under dynamic conditions. The pipe can be principally characterized by its mass storage and inertial properties. The best model is a distributed or a one to one spatially correspondent dependence. The distributed continuity equation is:

$$L \frac{\partial W}{\partial x} = \frac{\partial}{\partial t} \rho \gamma \quad (\text{A. 4. 26})$$

In the momentum equation, omit the momentum flux contribution and consider the inertial term as dominant. This formulation is also for a frictionless pipe. A means of accounting for friction is demonstrated further on in this section. The distributed momentum equation is:

$$\frac{\partial P}{\partial x} = -\frac{1}{gA} \frac{\partial}{\partial t} W \quad (\text{A. 4. 27})$$

Make the substitution

$\left(\frac{\partial P}{\partial x}\right)_s = -\frac{1}{C^2}$  constant and non-dimensionalize with respect to the pipe length.

$$\frac{\partial W}{\partial x} = -\frac{LA}{C^2} DP \quad (\text{A. 4. 28})$$

$$\frac{\partial P}{\partial x} = -\frac{L}{Ag} DW \quad (\text{A. 4. 29})$$

The simultaneous solution of these equations can be put into the following causal form:

$$P_{\text{out}} = (\cosh \Gamma) P_{\text{in}} - Z_o (\sinh \Gamma) W_{\text{in}} \quad (\text{A. 4. 30})$$

$$W_{\text{out}} = -Y_o (\sinh \Gamma) P_{\text{in}} + (\cosh \Gamma) W_{\text{in}} \quad (\text{A. 4. 31})$$

$$\Gamma = \sqrt{\frac{L^2 D^2}{C^2 g}} \quad (\text{A. 4. 32})$$

$$Z_o = \frac{1}{Y_o} = \sqrt{\frac{C^2}{A^2 g}} \quad (\text{A. 4. 33})$$

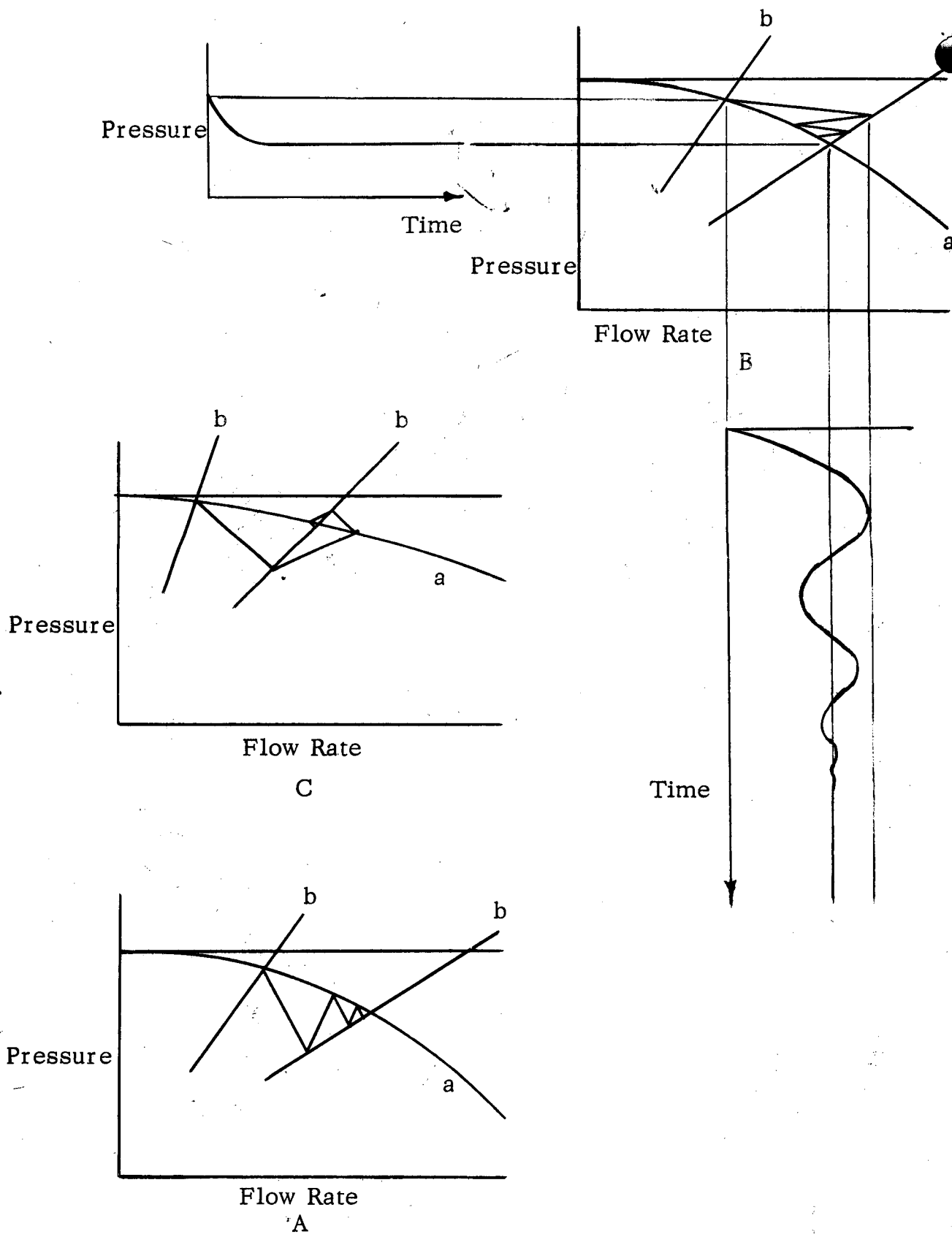
Where  $Z_o$  has the dimensions of

$$Z_o = \frac{P_o}{W_1} = \frac{\text{Sec}}{\text{Ft}^2} \quad (\text{A. 4. 34})$$

This is the line surge impedance relating instantaneously the flow and pressure changes at a termination.

A graphical presentation can facilitate the use and interpretation of Equations A. 4. 30 and A. 4. 31 (see Reference 14).

Consider a pressure-flow diagram as in Figure A. 4. 7. Curve a reflects the instantaneous impedance looking into the boiler. This curve may also reflect



a portion of the steady-state square law friction of the pipe. Likewise, curve b reflects the valve characteristics and the remaining portion of the steam pipe square law friction. The dotted line represents the data taken by the pipe variables ( $P_o$ ,  $W_o$ ) during a transient condition. This case illustrates a step increase in valve area. The 2 adjoining curves reflect the time history of the separate variables. The absolute value of the slope of the dotted line is the surge impedance  $Z_o$ . For valve manipulation responses the ideal or best pipe has an impedance which matches the impedance of curve a which reflects the superheater plus pipe friction. However, since the superheater characteristics are not linear in the pressure to flow rate relationship the impedance varies with load level. Consequently the pipe surge impedance can match the superheater at only one point. For so-called off-design performance, the curves in Figure A. 4.7 illustrate the possible modes of response. The actual choice of pipe characteristics is essentially one of design judgment.

Four types of conduit responses are possible, three of which are illustrated here. They are pressure oscillatory and flow rate monotone, A; pressure monotone and flow oscillatory, B; and both pressure and flow oscillatory, C. The period of oscillation is twice the quantity of the pipe length divided by the acoustic velocity.

The system computer model should include a representation of the steam pipe or its omission should be justified. Each line segment of Figure A. 4.7 takes half a period for completion. If 95% of the response occurs within three segments, then the time of this completion is one and a half periods. This may be and is assumed in this report to be considerably faster than any other system dynamics and therefore does not dynamically couple with the rest of the system.

## A. 4. 4. Steam Valve Model

The steam valve in this system is the throttle at the steam turbine. Most turbine throttles operate with steam in the sonic or choked region. The equation for the dimensional choked flow through a restriction (Reference 8) is:

$$A^* = \frac{1}{.532} \frac{W \sqrt{T_o}}{P_o} \quad (\text{A. 4. 35})$$

However, the valve equation when linearized and normalized to local valves becomes:

$$\frac{\Delta A}{A} = \frac{\Delta W}{W} + \frac{1}{2} \frac{\Delta T}{T} - \frac{\Delta P}{P} \quad (\text{A. 4. 36})$$

## A. 4. 5. Summary of Computer Models

The sodium loop transfer relations are in Figure A. 4. 9. The parameter values are presented in the adjoining table. Both the secondary and primary pipe-pump inertias are given by Equation A. 4. 14. The normalization values are 100% sodium flow rate and 100% pump pressure difference.

$$\delta P_{\text{pump } o} = 30 \text{ psia}$$

$$W_{no} = 1,665,000 \text{ lbs/hr}$$

$$f' = -1$$

$$g = 32.2$$

$$L_1 = 150$$

$$L_2 = 300$$

$$A_n = 1.07 \text{ sq. ft.}$$



A reticulated evaluation of the  $\sum L/A$  for the three shell sides of the three exchangers indicated the inertia effects are equivalent to about 20 to 30 feet of connecting pipe. Since the connecting pipe will likely be much larger, the above gross pipe lengths were used.

The computer model considers no steam pipe representation. Since essentially no dynamics are present in the feedwater circuit, the models are a unity gain with no dynamics from input to output. That is for the steam pipe, the steam flow out of the superheater equals steam flow at the steam valve, and for the feedwater line the feedwater flow follows valve position.

$$A_{so} = 2.19 \text{ sq. ft.}$$

$$W_{s3o} = 270,000 \text{ lbs/hr}$$

$$W_{fo} = 270,000 \text{ lbs/hr}$$

The pipe transport times used in the coupled exchanger computer model are presented below.

$$\tau_1 = \frac{6.4}{R_N}$$

$$\tau_2 = \frac{6.4}{R_N}$$

$$\tau_3 = \frac{12.8}{R_N}$$

$$\tau_4 = \frac{9.9}{R_N}$$

$$\tau_5 = \frac{12.8}{R_N}$$

Load Curve for 200 HP Wound Rotor Motor with  
Dissipative Secondary Control and Square Law Load  
(Reference 3)

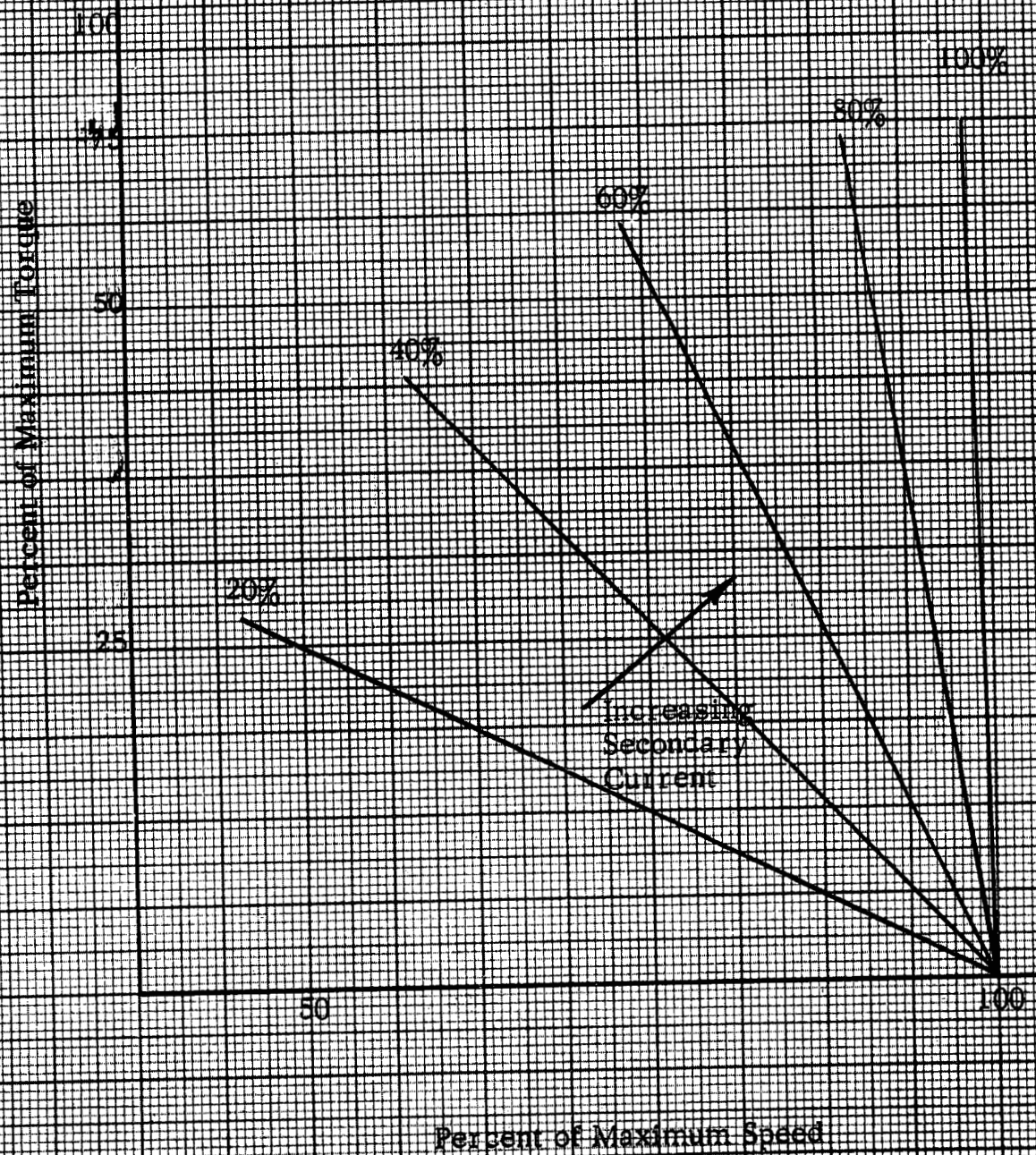
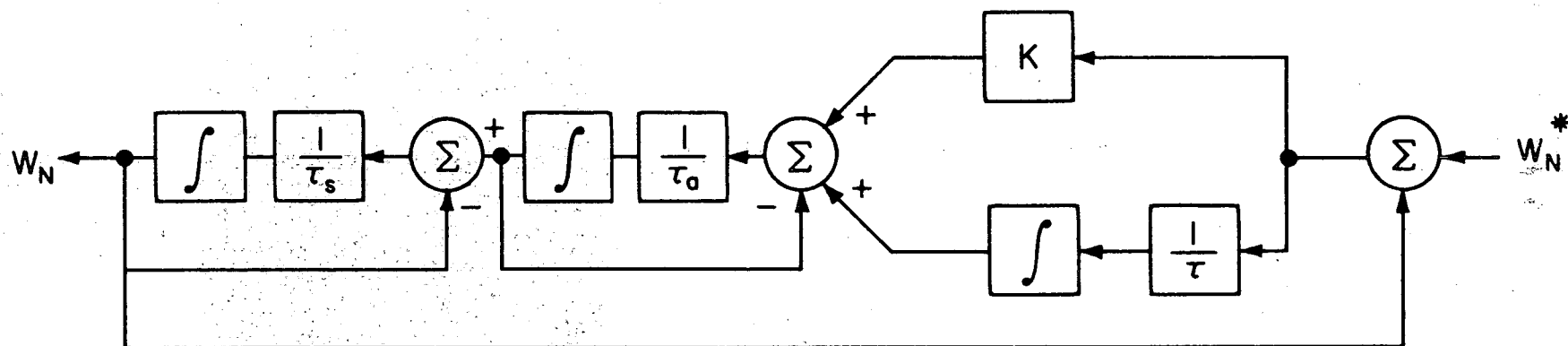


Figure A.4.8

# SODIUM CONTROL LOOP COMPUTER MODELS



	PRIMARY (1)		SECONDARY(2)	
	100 %	20 %	100 %	20 %
K	10	10	10	10
$\tau$	12.5	12.5	33	33
$\tau_0$	.0248	.0201	.0248	.0201
$\tau_s$	555	27.5	11.10	55.5

FIGURE A.4.9

## APPENDIX 5 - BOILER LEVEL CONTROL

The boiler, as a consolidated unit of boiler tubes and drum separator, is a two stream power transducer which is related statically to the rest of the system in terms of the following variables:

### Secondary Sodium System

$$W_{n2}, T_{4b}, T_{5a}$$

### Steam System

$$W_f, W_{s2}, p, T_6$$

However, the dynamical relationship requires a knowledge of the internal structure due to the relative time phase shift of the above parameters as associated with variations in energy and mass storage within this power transducer. The dynamic model of the water side of the boiler divides into essentially 3 regions; the feedwater tray (perforated deck plate), the header (region below deck plate in the separator), and the boiler tubes.

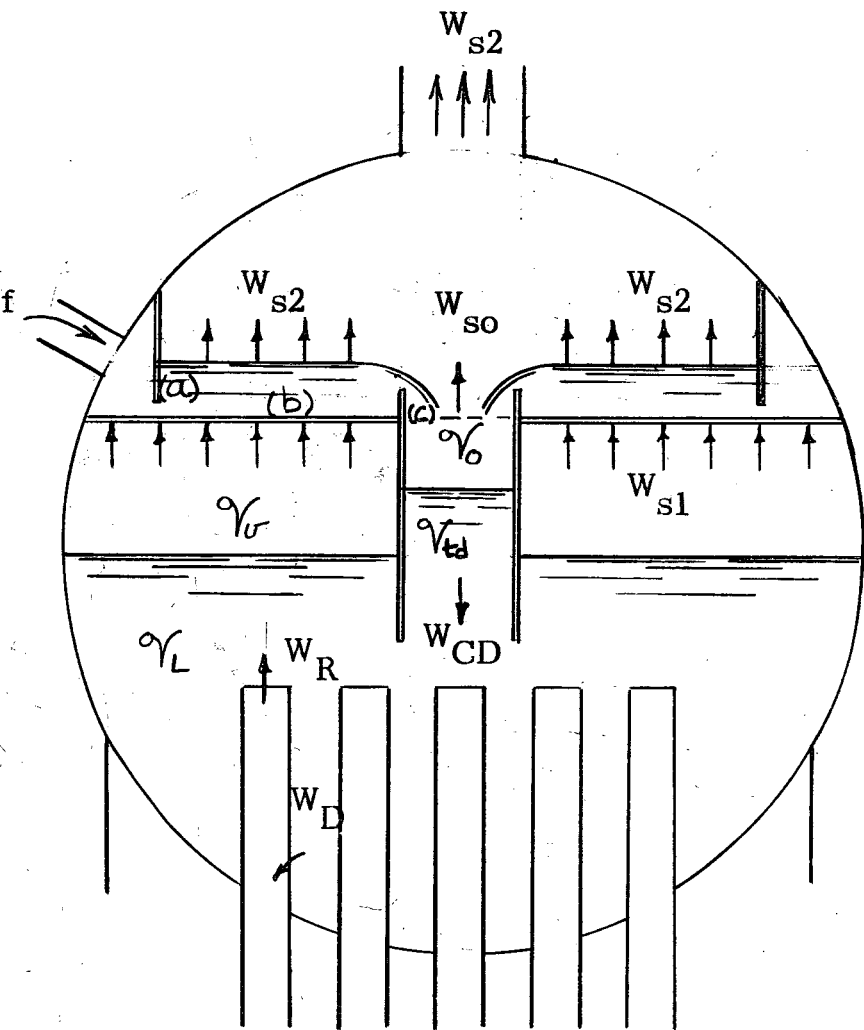
A schematic view of the boiler, Figure A. 5. 1, shows this functional partitioning of the three waterside regions.

#### A. 5. 1. Feedwater Tray

The feedwater tray consists of a sluice (a) under which the feedwater flows across the tray (b) radially to the center and over a weir (c) into the central downcomer. Steam from the header region ( $W_{s1}$ ) passes through the tray perforations, bubbles through the incoming feedwater on the tray and passes out to the superheater. Part of the steam passing through the tray condenses and raises the feedwater enthalpy up to the saturation level.

129 153

- $W_f$  = Feedwater flow rate
- $W_{td}$  = Tray weir flow rate
- $W_{CD}$  = Central downcomer Discharge flow rate
- $W_R$  = Riser discharge flow rate
- $W_D$  = Boiler tube downcomer flow rate
- $W_{s1}$  = Steam flow rate to feedwater tray
- $W_{s2}$  = Steam flow rate to superheater
- $\gamma_v$  = Vapor volume between tray and liquid level
- $\gamma_L$  = Drum volume below liquid level
- $\gamma_{td}$  = Central downcomer liquid volume above drum liquid level
- $\gamma_o$  = Central downcomer vapor volume
- $W_{so}$  = Central downcomer vapor flow rate



Schematic Representation of the Boiler Drum Separator

Figure A.5.1

A-3-2

## A.5.1.1. Feedwater Continuity and Weir Equation

For the control volume indicated, the statement of continuity follows.

$$W_f - W_{td} + W_{s1} - W_{s2} = D(\rho_t v_t) \quad (\text{A. 5.1})$$

The condensation rate is reflected by  $W_{s1} - W_{s2}$ . Presumably, the tray perforations are oriented so as to insure saturated outgoing liquid flow at all times; that is, the effective area of contact is high enough to conclude infinite or near infinite heat transfer effectiveness. In this case, the condensation rate depends upon the feedwater flow rate,  $W_f$ , temperature  $T_6$ , and rate of transport past the perforations. An additional dependence is associated with the vapor storage (hold up vapor volume) on the tray.

The mass storage term of Equation (A. 5.1) expands into

$$\rho_t D v_t + v_t D \rho_t \quad (\text{A. 5.2})$$

The product of tray area times the liquid level reflects the tray volume.

The hydraulic weir relation (Reference 2) determines the liquid height on the tray above the weir height (1 inch),  $Z_t$ .

$$W_{td} = \rho_f K Z_t^{1.4} \quad (\text{A. 5.3})$$

Perturbed and normalized Equation (A. 5.3) is

$$w_{td} = 1.4 R_s^{\frac{.4}{1.4}} z_t + R_s P_f p \quad (\text{A. 5.4})$$

or

$$z_t = \frac{1}{1.4} R_s^{-\frac{.4}{1.4}} w_{td} - P_f R_s^{\frac{1}{1.4}} p \quad (\text{A. 5.5})$$

where  $z_t$ ,  $w_{td}$ , and  $p$  are normalized with respect to their steady-state values at 100% of rated load.

$$\rho_f = \frac{p}{\rho_f} \frac{\partial \rho_f}{\partial p}; \quad \rho_{fg} = \frac{p}{\rho_{fg}} \frac{\partial \rho_{fg}}{\partial p}; \quad \rho_g = \frac{p}{\rho_g} \frac{\partial \rho_g}{\partial p} \quad (\text{A.5.6})$$

Following the reasoning in Appendix A.1, the spatially local value of steam flow rate and pressure characterizes the effective or mean density. Consequently a relation similar to that developed in Appendix A.1 for the two-phase mass storage may be used here. However since the transport time of the steam through the tray is so short, the dynamics associated with hold-up density variations are uncoupled from the main dynamics of the level control loop. Also since the perforation area to total plate area is small, the actual vapor hold-up is very small and any variations thereof are small. Consequently in the interest of the level control problem, vapor hold-up in the feedwater tray is neglected. However since liquid specific volume-pressure dependence is significant, this mode of variation is included. The mass storage term becomes

$$\frac{A \rho Z_t}{W_{fo}} (D Z_t + R_s \frac{1}{1.4} \rho_f D p) \quad (\text{A.5.7})$$

Define

$$\tau_{td} = \frac{A \rho Z_t}{W_{fo}} \quad (\text{A.5.8})$$

Then the tray continuity equation and weir equation reduce to

$$\frac{1}{\tau_l D} (w_f - 1.2 w_{td} + w_c) - .4 R_s \rho_f p = w_{td} \quad (\text{A.5.9})$$

#### A.5.1.2. Tray Condensation

Another dynamic effect is associated with the rate of change of condensation. The inlet feedwater temperature is a function of the heat transfer characteristics of the feedwater heaters and condenser pressure. In steady-state the

degree of subcooling is constant. Variations in subcooling are omitted. For the steam system under good pressure control, the likely variations in feedwater heater outlet temperature is small compared to the heat of evaporation. Therefore, the feedwater enthalpy is assumed constant.

The steady-state energy equation for the tray is

$$W_f h_{\text{sub}} = h_{\text{fg}} (W_{s1} - W_{s2}) = W_e h_{\text{fg}} \quad (\text{A. 5. 10})$$

Dynamically however, the condensation rate lags the feedwater flow rate by some fraction of the one dimensional transport time,  $\tau_{\text{td}}$ , of the feedwater through the tray. Qualitatively the dynamic dependence may be determined through the following argument. The local transport time of the feedwater on the tray varies directly as the distance from the center of the central downcomer, assuming the liquid level across the tray is constant. The effective steam to water contact also varies directly as the distance from the center. For constant steam in-flow, the increase in condensation rate following a step increase in feedwater flow rate appears similar to a simple lag or averaging operator response.

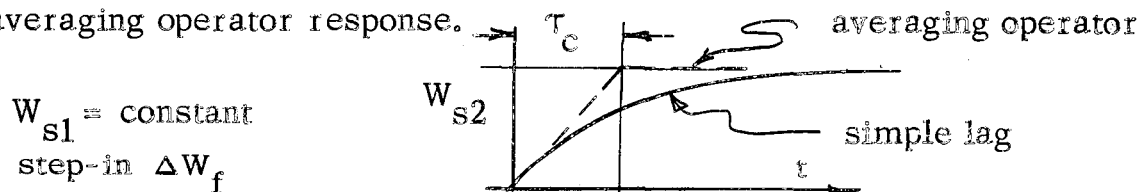


Figure A. 5. 2 - Condensation Rate Step Response

It is assumed that:

$$\Delta W_s = \frac{h_{\text{sub}}}{h_{\text{fg}}} \frac{\Delta W_f}{1 + \tau_c D}$$

where  $\tau_c$  is approximately  $\tau_{\text{td}}$ . The dashed line with  $\tau_c = \tau_{\text{td}}$  would result if there were no transient changes in the tray liquid temperature distribution since the local heat transfer surface area and local transport time are proportional.



## A.5.2. Header

This region as shown in Figure A.5.1 constitutes the space in the drum separator below the feedwater tray. A statement of the volume subdivision is as follows

$$V_H = V_L + V_v + V_{td} + V_o = \text{Constant} \quad (\text{A. 5.12})$$

$V_L$  = Volume below liquid level including central downcomer region

$V_v$  = Volume above liquid level excluding the central downcomer region and below the tray

$V_{td}$  = Liquid volume in central downcomer above header liquid level

$V_o$  = Vapor volume in central downcomer up to the tray level

The continuity expression for all of the in-flows and out-flows to the header follows. (See Figure A.5.1).

$$W_R + W_{CD} - W_D - W_{sl} - W_{so} = DM_H \quad (\text{A. 5.13})$$

and

$$M_H = \underset{(a)}{\rho_g V_H} + \underset{(b)}{\rho_{fg} V_{td}} + \underset{(c)}{(\rho_L - \rho_g) V_L} \quad (\text{A. 5.14})$$

The three terms constituting mass storage have the following significance.

Term (a) reflects the minimum mass storage or a density base in the header. Terms (b) and (c) represent density corrections over and above the equivalent vapor storage. Term (b) reflects the "stand pipe" driving head which offsets or develops the steam pressure drop across the feedwater tray. Term (c) is the liquid storage below header liquid level.

## A.5.2.1. Feedwater Tray Pressure Drop

The tray through-flow steam drops in pressure. To a first order evaluation, this pressure drop results from 2 actions; a viscous drop through the perforation and a liquid height gravity head drop.

$$\delta P_T = \delta P_F + \delta P_G = \rho_{fg} \frac{V_{td}}{A_{td}} \quad (\text{A. 5. 15})$$

where

$$\delta P_F = K \frac{W_{sl}^2}{\rho_g} \quad (\text{A. 5. 16})$$

$$\delta P_G = \left( \frac{1}{12} + Z_T \right) \rho_{fg} \quad (\text{A. 5. 17})$$

Linearized and normalized Equation A. 5. 15 results in

$$\frac{\Delta \delta P_T}{\delta P_{To}} = \frac{\delta P_{Go}}{\delta P_{To}} \frac{\Delta \delta P_G}{\delta P_{Go}} + \frac{\delta P_{Fo}}{\delta P_{To}} \frac{\Delta \delta P_F}{\delta P_{Fo}} \quad (\text{A. 5. 18})$$

$$\frac{\Delta \delta P_G}{\delta P_{Go}} = \rho_{fg} \frac{\left( \frac{1}{12} + Z_{To} R_S \frac{1}{1.4} \right)}{\delta P_{Go}} \frac{\Delta P}{P} + \frac{(\delta P_{Go} - \frac{1}{12} \rho_{fg})}{\delta P_{Go}} \frac{\Delta Z_t}{Z_{to}} \quad (\text{A. 5. 19})$$

$$\frac{\Delta \delta P_F}{\delta P_{Fo}} = 2R_S \frac{\Delta W_{sl}}{W_{sl}} - \rho_g \frac{\Delta P}{P} \quad (\text{A. 5. 20})$$

The simultaneous combination of Equations (A. 5. 15), (A. 5. 18), (A. 5. 19) and (A. 5. 20) reduces to

$$\delta P_T = K_{sl} w_{sl} - K_p p + K_{td} w_{td} \quad (\text{A. 5. 21})$$

$$K_{sl} = 2R_S \frac{\delta P_{Fo}}{\delta P_{To}} \quad (\text{A. 5. 22})$$

$$K_p = P_{fg} \frac{\left(\frac{1}{12} + Z_{To} R_S^{\frac{1}{1.4}}\right)}{\delta P_{To}} - \frac{P_f R_s^{\frac{1}{1.4}}}{P_{To}} \left(\delta P_{Go} - \frac{1}{12} \rho_{fg}\right) - \frac{P_g P_{Fo}}{P_{To}} \quad (\text{A. 5. 23})$$

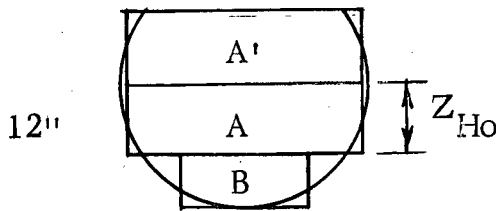
$$K_{td} = \left(\frac{\delta P_{Go} - \frac{1}{12} \rho_{fg}}{\delta P_{Go}}\right) \left(\frac{1}{1.4} R_S^{-\frac{1}{1.4}}\right) \quad (\text{A. 5. 24})$$

#### A. 5. 2. 2. Separator Level

Term (c) is a function of both the mean hold-up density below the liquid level as well as the volume occupied below the liquid level.

$$\Delta \left[ (\rho_L - \rho_g) \mathcal{V}_L \right] = \mathcal{V}_L (\Delta \rho_L - \Delta \rho_g) + (\rho_L - \rho_g) \Delta \mathcal{V}_L \quad (\text{A. 5. 25})$$

For the second term the head volume may be idealized as shown in Figure A. 5. 3.



$$\mathcal{V}_A + \mathcal{V}_{A'} + \mathcal{V}_B = \mathcal{V}_H \quad (\text{A. 5. 26})$$

$$\text{and } \mathcal{V}_A + \mathcal{V}_B = \mathcal{V}_L \quad (\text{A. 5. 27})$$

Drum Separator  
Capacity Simplification

Figure A. 5. 3

Consider  $\mathcal{V}_B$  as some fixed volume and  $\mathcal{V}_A$  and  $\mathcal{V}_{A'}$  as two depthwise small idealized cylinders. Then,

$$\Delta \mathcal{V}_A = -\Delta \mathcal{V}_{A'} \text{ and } \Delta \mathcal{V}_A = \Delta \mathcal{V}_L$$

Consider  $\mathcal{V}_A = A_H \cdot Z_H$ ;  $\Delta \mathcal{V}_A = A_H \Delta Z_H$ ,  $Z_H$  is an arbitrary length chosen to be 12 inches.

Then

$$\frac{\Delta \mathcal{V}_L}{\mathcal{V}_A} = \frac{\Delta Z_H}{Z_H} \quad (\text{A. 5. 28})$$

The first term in Equation A. 5. 25 is open to the determination of a "hold-up" density. A method similar to the relationship in Appendix A. 1. 1 should be employed. However it can be shown by the same reasoning as used for the feedwater tray that the dynamics associated with variations in hold-up density are essentially an order of magnitude faster than the other level loop control dynamics as well as being of low gain. Therefore as a first order approximation consider  $\rho_L = \rho_f$  then

$$\Delta \rho_f - \Delta \rho_g = \rho_{fg} \rho_{fg} \frac{\Delta P}{P} \quad (\text{A. 5. 29})$$

The linearized and non-dimensionalized Equation A. 5. 29 becomes

$$\frac{\Delta (\rho_{fg} \gamma_L)}{\rho_{fg} \gamma_L} = \rho_{fg} \frac{\Delta P}{P} + \frac{\gamma_A}{\gamma_L} \frac{\Delta Z_H}{Z_H} \quad (\text{A. 5. 30})$$

The mass storage term of Equation A. 5. 13 consolidates to

$$\begin{aligned} \frac{\Delta M_H}{M_H} = & \frac{\rho_g \gamma_H}{M_H} \rho_g p + \left( \frac{\rho_{fg} \gamma_{td}}{M_H} \right) (K_{sl} w_{sl} - K_p p + K_{td} w_{td}) \\ & + \frac{\rho_{fg} \gamma_L}{M_H} \left( \rho_{fg} p + \frac{\gamma_A}{\gamma_L} \frac{\Delta Z_H}{Z_H} \right) \end{aligned} \quad (\text{A. 5. 31})$$

The left hand terms of Equation A. 5. 13 constitute the in-flows and out-flows. The definitions are illustrated in Figure A. 5. 1. The 2 flows,  $W_D$  and  $W_R$  are to and from the boiler tubes respectively. The other in-flow,  $W_{CD}$ , discharges from the central downcomer. This flow can be related to the tray weir flow through a statement of continuity for the downcomer.

$$W_{td} - W_{CD} = \Delta M_{CD} = D (\rho_{fg} \gamma_{CD} + \rho_{fg} \gamma_{td}) = D (\rho_g \gamma_{CD} + \delta P_T)$$

Linearized and normalized, the mass storage term becomes

$$\frac{\Delta M_H}{M_{Ho}} = \frac{\delta P_{To}}{M_{Ho}} \frac{\Delta \delta P_T}{P_{To}} - \frac{g \gamma_{CD}}{M_{Ho}} \frac{Z_H}{Z_H} + \frac{g \gamma_{CD}}{M_{Ho}} P_g \frac{\Delta P}{P} \quad (A. 5.32)$$

The completed statement of continuity for the header is (Equations A. 5.13, A. 5.14, A. 5.21, and A. 5.31)

$$\begin{aligned} R_e \frac{\Delta W_R}{W_{Ro}} + \frac{\Delta W_{td}}{W_{tdo}} - R_e \frac{\Delta W_D}{W_{Do}} - \frac{\Delta W_{sl}}{W_{slo}} - \frac{W_{soo}}{W_{slo}} \frac{\Delta W_{so}}{W_{soo}} = \\ \frac{\rho_g \gamma_H}{W_{sl}} P_g D p + \frac{\delta P_{Ttd} A_{td}}{W_{sl}} D \left[ K_{sl} w_{sl} - K_p p + K_{TD} w_{TD} \right] \\ \frac{\rho_{fg} \gamma_L}{W_{sl}} D (P_{fg} p + \frac{\gamma_A}{\gamma_L} z_H) \end{aligned} \quad (A. 5.33)$$

Rearranged, Equation A. 5.33 becomes

$$\begin{aligned} z_H = \frac{1}{\tau_1 D} (w_{td} - w_{sl} + \frac{1}{x_e} w_R - \frac{1}{x_e} w_D) - G_p p \\ - \frac{\tau_4}{\tau_1} K_{sl} w_{sl} - \frac{\tau_4}{\tau_1} K_{td} w_{td} \end{aligned} \quad (A. 5.34)$$

$$G_p = \frac{\tau_3 + \tau_2 + \tau_4 K_p}{\tau_1} \quad (A. 5.35)$$

$$\tau_1 = \frac{\rho_{fg} A_2 Z_o}{W_{sl}} \quad (A. 5.36)$$

$$\tau_2 = \frac{\gamma_L \rho_{fg} P_{fg}}{W_{sl}} \quad (A. 5.37)$$

$$\tau_3 = \frac{\rho_g \gamma_H P_g}{W_{sl}} \quad (A. 5.38)$$

$$\tau_4 = \frac{A_1 P_{To}}{W_{sl}} \quad (\text{A. 5. 39})$$

$$R_e = \text{Reflux ratio} = \frac{1}{x_e} \quad (\text{A. 5. 40})$$

### A. 5. 3. Boiler Circulation

Determination of boiler circulation comes from the simultaneous satisfaction of the riser continuity equation and the riser-downcomer momentum equation. Appendix A.1.1, Equation A.1.1 provides a model of the riser continuity equation. This equation is

$$\frac{\Delta W_R}{W_R} = \frac{\Delta W_D}{W_D} e^{-\tau_R D} + (1 - e^{-\tau_R D}) \left( \frac{\Delta W_{sl}}{W_{sl}} + \frac{K_p}{K_x} \right) \frac{\Delta P}{P} \quad (\text{A. 5. 41})$$

The formulation of this equation presumes a hold-up density dependence of the form

$$\rho_h = f(W_R, W_s, p) \quad (\text{A. 5. 42})$$

In steady-state, the total flow is constant throughout the tube and equals the exit total flow,  $W_R$ . Since in steady-state the pressure does not vary (saturation pressure is large with respect to frictional pressure changes), this dependence is omitted. The dependence of the hold-up density upon the two flow rates depends upon the nature of drag coefficient of vapor flow relative to the liquid flow. This analysis assumes a fog flow,  $x_f = x_h$ . This amounts to assuming an infinite drag coefficient between vapor and liquid. The load vs position curves of Figure A.5.4 are also interpretable as flowing quality vs position curves.

The sum of the pressure drops around the circulation loop is zero. This is a

statement of the momentum equation

$$\delta P_{\text{frict}} + \delta P_{\text{inertia}} + \delta P_{\text{bouyant}} + \delta P_{\text{momentum}} = 0 \quad (\text{A. 5. 43})$$

The terms are defined as

$$\delta P_{\text{frict}} = \frac{f_R W_R^2}{\rho_e} + \frac{f_D W_D^2}{\rho_f} \quad (\text{A. 5. 44})$$

$$\delta P_{\text{inertia}} = \frac{1}{g_o} \left( \sum \frac{L}{A} D W_D \right) \quad (\text{A. 5. 45})$$

$$\delta P_{\text{bouyant}} = (\rho_h - \rho_f) L \quad (\text{A. 5. 46})$$

$$\delta P_{\text{expansion}} = \frac{W_R^2}{g A_R^2 \rho_e} - \frac{W_D^2}{g A_R^2 \rho_f} \quad (\text{A. 5. 47})$$

From Reference 2, p 7-D 17

$$f_R = \frac{(.017) L}{2 A_R^2 g d_R} \quad (\text{A. 5. 48})$$

$$f_D = \frac{(.017) \frac{L}{d_D} + .41}{2 A_D^2 g} \quad (\text{A. 5. 49})$$

where .017 is the friction factor and .41 the turning loss coefficient.

The bulk of riser friction is assumed to occur near the exit. Since there is an appreciable unheated region at the exit end and also most of the boiler load occurs in the first few feet, the exit density dependence is a reasonable and conservative assumption.

The cross-plot, Figure A. 5. 5, provides the recirculation rate evaluation. At a given load level, several total flow rates are assumed. The driving head or bouyant term is plotted against the remaining pressure drop terms of the momentum equation.

The dynamic control model uses a two lag one lump approximation of Equation A.1.9. In this model the pressure dependence is omitted in light of the pressure regulation achieved with this system. Likewise, system pressure dependence is omitted in the linearization of Equation A.5.43. The linearized form of the individual pressure drop contributions are

$$\frac{\Delta \delta P_{\text{frict}}}{P_{\text{go}}} = \frac{2\delta P_{\text{fR}}}{P_{\text{go}}} \frac{\Delta W_{\text{R}}}{W_{\text{R}}} + \frac{2\delta P_{\text{fD}}}{P_{\text{go}}} \frac{\Delta W_{\text{D}}}{W_{\text{D}}} - \frac{\delta P_{\text{fR}}}{P_{\text{go}}} \frac{\Delta \rho_{\text{h}}}{\rho_{\text{h}}} \quad (\text{A. 5.50})$$

$$\frac{\Delta \delta P_{\text{inertia}}}{P_{\text{go}}} = \frac{W_{\text{D}}}{P_{\text{go}} g} \left( \sum \frac{L}{A} \right) D \frac{\Delta W_{\text{D}}}{W_{\text{D}}} \quad (\text{A. 5.51})$$

$$\frac{\Delta \delta P_{\text{bouyant}}}{P_{\text{go}}} = L \rho_{\text{h}} \frac{\Delta \rho_{\text{h}}}{\rho_{\text{h}}} \quad (\text{A. 5.52})$$

$$\frac{\Delta \delta P_{\text{expansion}}}{P_{\text{go}}} = \frac{W_{\text{R}}^2}{A_{\text{R}}^2 g \rho_{\text{h}}} \left( \frac{2 \Delta W_{\text{R}}}{W_{\text{R}}} - \frac{\Delta \rho_{\text{h}}}{\rho_{\text{h}}} \right) - \frac{2 W_{\text{D}}^2}{A_{\text{D}}^2 g \rho_{\text{f}}} \frac{\Delta W_{\text{D}}}{W_{\text{D}}} \quad (\text{A. 5.53})$$

Combining:

$$\begin{aligned} & \left( 2 + \frac{4}{f_{\text{R}}} \right) \frac{\delta P_{\text{fR}}}{P_{\text{go}}} \frac{\Delta W_{\text{R}}}{W_{\text{R}}} + \frac{1}{P_{\text{go}}} \left( L \rho_{\text{h}} - 1 - \frac{2}{f_{\text{R}}} \right) \frac{\Delta \rho_{\text{h}}}{\rho_{\text{h}}} \\ & + \left[ \frac{W_{\text{D}}}{P_{\text{go}}} \left( \sum \frac{L}{A} \right) D + \left( 2 - \frac{4}{f_{\text{D}}} \right) \delta P_{\text{fD}} \right] \frac{\Delta W_{\text{D}}}{W_{\text{D}}} = 0 \end{aligned} \quad (\text{A. 5.54})$$

A block diagram simultaneous solution of Equations A.1.10, A.5.41 and A.5.54 with a two lag approximation of Equation A.5.41 is in Figure A.5.6.

#### A.5.4. Computer Models

The resulting computer models are presented in Figures A.5.6 and A.5.7. The associated parameter values and normalization values are presented below.



## NORMALIZATIONS

$$Z_{Ho} = 12''$$

$$W_{tdo} = 320,000 \text{ lbs/hr}$$

$$Z_{to} = .283'$$

$$W_{sl} = 320,000 \text{ lbs/hr}$$

$$\delta P_{Go} = 11.6 \text{ p.s.f.}$$

$$W_{s2} = 270,000 \text{ lbs/hr}$$

$$\delta P_{Fo} = 8.26 \text{ p.s.f.}$$

$$W_{s3} = 270,000 \text{ lbs/hr}$$

$$\delta P_{To} = 20.2 \text{ p.s.f.}$$

$$W_R = 1,960,000 \text{ lbs/hr}$$

$$\delta P_{go} = 193 \text{ p.s.f.}$$

$$W_D = 1,960,000 \text{ lbs/hr}$$

$$W_{CDo} = 320,000 \text{ lbs/hr}$$

$$\gamma_L = 134.0 \text{ cu. ft.}$$

$$W_{fo} = 270,000 \text{ lbs/hr}$$

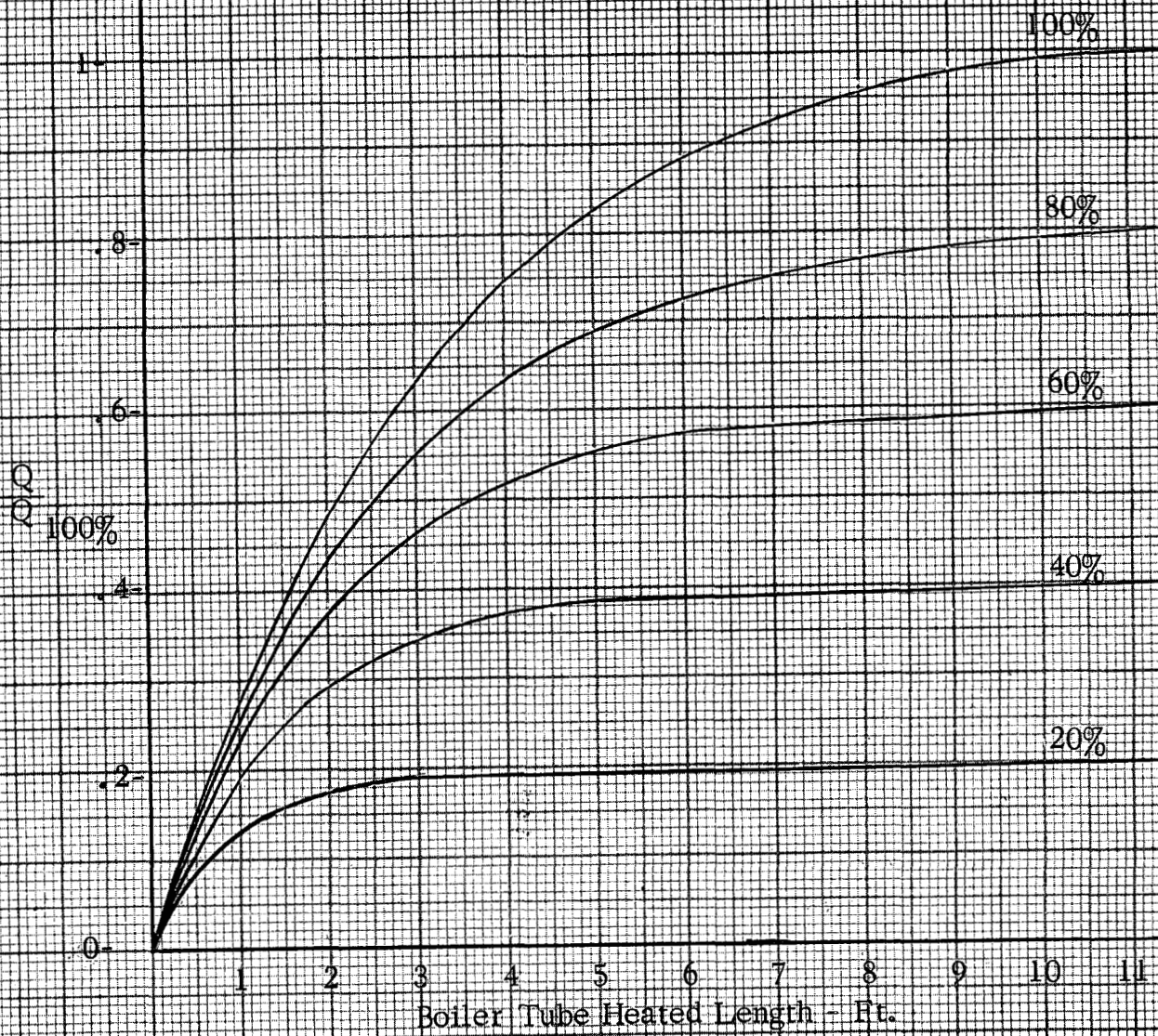
$$\gamma_H = 183.5 \text{ cu. ft.}$$

## COMPUTER PARAMETERS

<u>Parameter/Load Level</u>	<u>100%</u>	<u>20%</u>
$A_R$	.00781 sq. ft.	.00781 sq. ft.
$A_D$	.00471 sq. ft.	.00471 sq. ft.
$A_H$	50.3 sq. ft.	50.3 sq. ft.
$f_D$	4.0	4.0
$f_R$	3.6	3.6
$\frac{h_{sub}}{h_{fg}}$	.2	.2

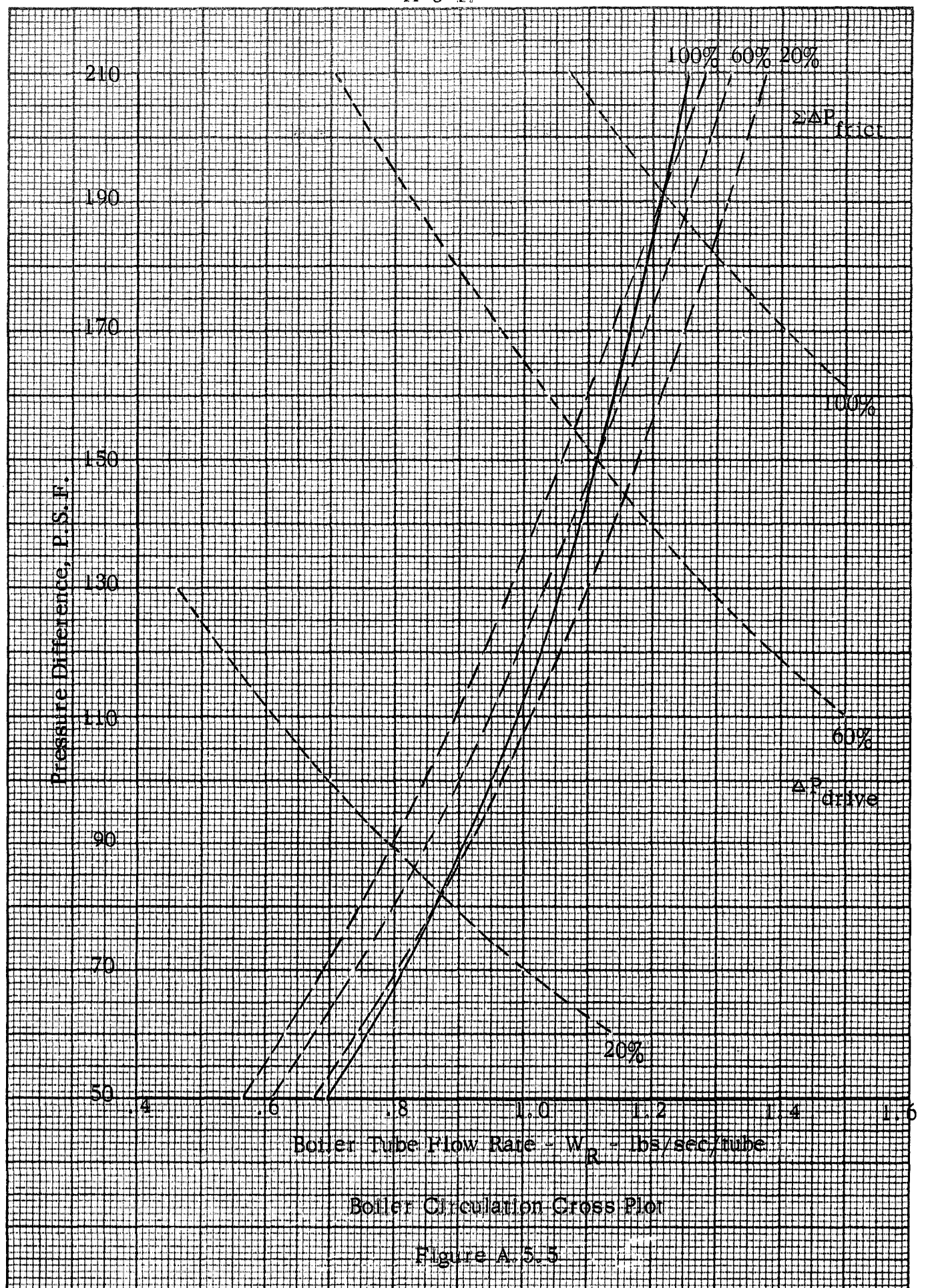
## COMPUTER PARAMETERS

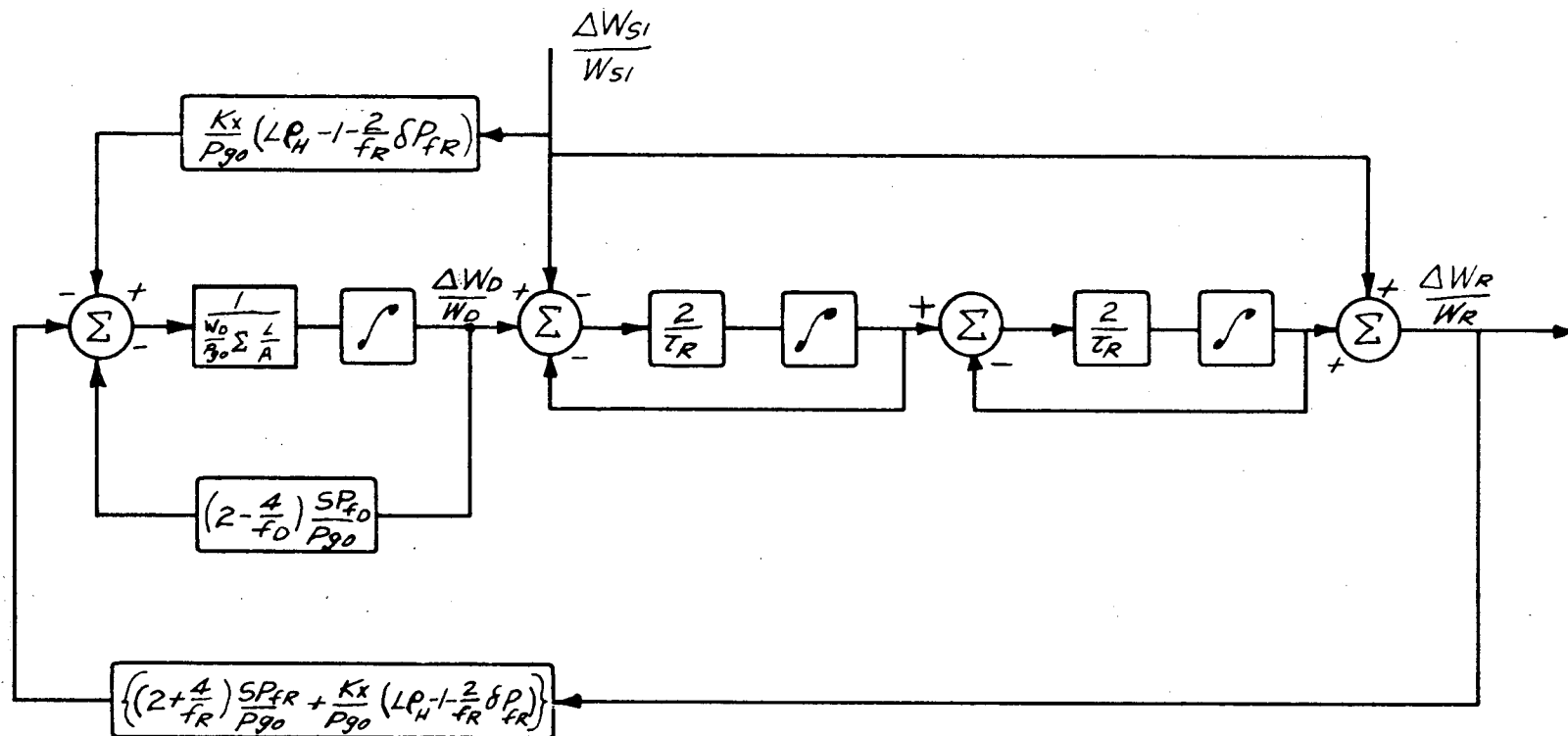
<u>Parameter/Load Levels</u>	<u>100%</u>	<u>20%</u>
$G_p$	-1.22	-1.22
$K_p$	-.51	-.762
$K_{sl}$	.174	.82
$K_x$	.447	.078
$K_{td}$	.355	.555
$L$	15 ft.	15 ft.
$\delta P_{fD}$	87.5 p. s. f.	43.5 p. s. f.
$\delta P_{fR}$	90 p. s. f.	35 p. s. f.
$R_N$	1.0	.2
$\delta P_{Fo}$	8.26 p. s. f.	
$\delta P_{Go}$	11.6 p. s. f.	
$\delta P_{To}$	20.2 p. s. f.	
$P_f$	-.5	-.5
$P_{fg}$	-.9	-.9
$P_g$	1.752	1.752
$\sum (\frac{L}{A})$	$5.11 \times 10^3/\text{ft.}$	$5.11 \times 10^3/\text{ft.}$
$X_e$	.155	.0426
$\tau_1$	16.7 secs.	16.7 secs.
$\tau_2$	-41.7 secs.	-41.7 secs.
$\tau_3$	22 secs.	22 secs.
$\tau_4$	.49 secs.	.49 secs.
$\tau_c$	5.00 secs.	5.00 secs.
$\tau_{td}$	5.05 secs.	5.26 secs.
$\tau_R$	2.38 secs.	4.25 secs.



Graph of Boiler Tube Load Vs Position

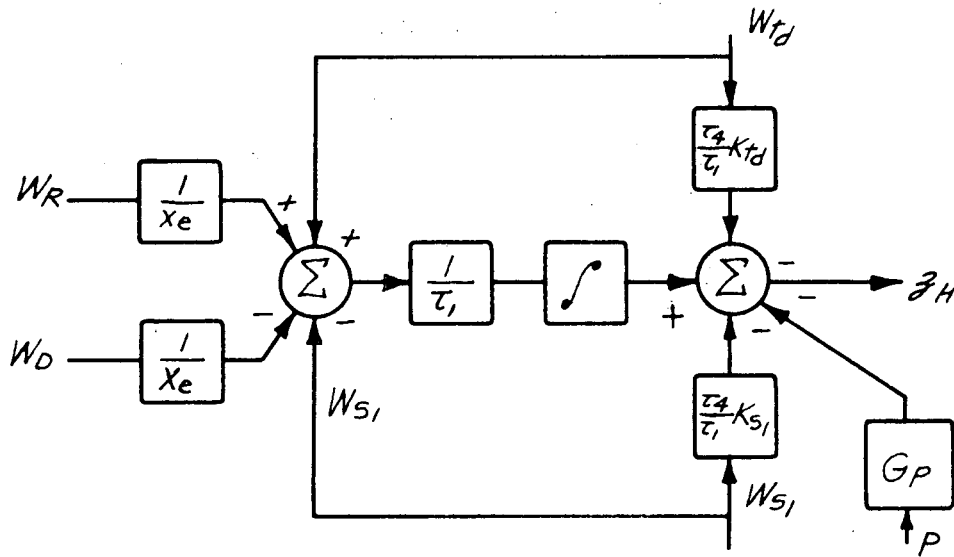
Figure A.5.4



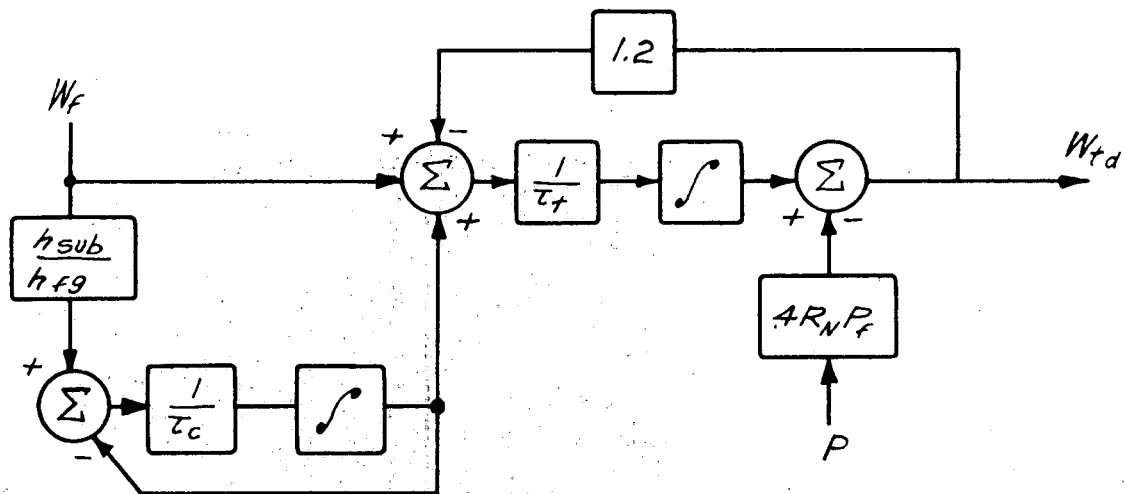


BOILER CIRCULATION BLOCK DIAGRAM

FIGURE A.5.8



BOILER LIQUID LEVEL BLOCK DIAGRAM



BOILER FEEDWATER TRAY BLOCK DIAGRAM

## APPENDIX 6 - REACTOR DYNAMICS

The reactor in this computer study is not of prime importance, therefore a model of its detailed internal structure is not required. The details of its internal mechanisms and structure are considered only so far as they effect the terminal characteristics of the reactor.

The reactor power is proportional to the neutron population and the rate of change of population is proportional to the reactivity. A statement of the neutron population dependence is in Equation A. 6. 1.

$$\frac{dn}{dt} = \frac{\Delta k}{\ell^*} n - \frac{\beta}{\ell^*} n + \sum_{i=1}^6 \lambda_i C_i \quad (\text{A. 6. 1})$$

and

$$\frac{dC_i}{dt} = \frac{\beta_i}{\ell^*} n - \lambda_i C_i \quad (\text{A. 6. 2})$$

This relation typifies the gross kinetic relationship for a thermal reactor in which six delayed neutron groups are accounted for. The detailed solution of this can be found in many standard references. However, a one delay group model gives satisfactory results for terminal modeling. Since the reactor power level is proportional to the neutron density  $n$ , then the following relation applies.

$$\frac{\Delta n}{n} = \frac{\Delta Q}{Q} \quad (\text{A. 6. 3})$$

This assumes that no dynamics or very fast dynamics exist between the flux density variations and variations in heat transfer to the fluid. This is not absolutely true for such terms as wall charging time of the fuel elements provide a dynamic distortion in  $\Delta Q/Q$ . A further discussion is provided in connection with the reactor negative temperature coefficient.

Consider one delay group and put Equations A. 6. 1 and A. 6. 2 into linearized operation form.



$$Dn = \frac{k - 1 - \beta}{\ell^*} n + \lambda C \quad (\text{A. 6. 4})$$

and

$$DC = \frac{\beta}{\ell^*} n - \lambda C \quad (\text{A. 6. 5})$$

Rearranging Equation A. 6. 5 becomes

$$\lambda C = \frac{\frac{\beta}{\ell^*} n}{\frac{1}{\lambda} D + 1} \quad (\text{A. 6. 6})$$

Introduce A. 6. 6 into A. 6. 4 then

$$\ell^* Dn = (k - 1 - \beta)n + \frac{\beta n}{\tau_n D + 1} \quad (\text{A. 6. 7})$$

where:

$$\tau_n = \frac{1}{\lambda} \quad (\text{A. 6. 8})$$

Linearized Equation A. 6. 7 becomes:

$$\ell^* D \Delta n = n_0 \Delta k - \beta \Delta n + \frac{\beta \Delta n}{\tau_n D + 1} \quad (\text{A. 6. 9})$$

Rearranging Equation A. 6. 9

$$\left( \ell^* D + \frac{\beta \tau_n D}{\tau_n D + 1} \right) \frac{\Delta n}{n} = \Delta k \quad (\text{A. 6. 10})$$

The prompt neutron lifetime,  $\ell^*$ , is considerably faster than the delayed neutron time  $\tau_n$  consequently for first order effects the prompt neutron may be neglected. Then reactivity and load are related by:

$$\frac{\beta \tau_n D}{1 + \tau_n D} \frac{\Delta Q}{Q_0} = \Delta k \quad (\text{A. 6. 11})$$



In this study, little information concerning the reactor parameters is available. The amount of thermal storage in metal walls and in the fluid is not known. For the sake of picking a model, somewhat more realistic than assuming constant reactor outlet temperature, a simplified view is taken here. All metal and fluid thermal storage is neglected or lumped with the cold leg and hot leg pipe storages. This makes possible the use of the arithmetic average of input and output temperatures in the negative temperature coefficient equations instead of the integrated average temperature. Also, a single equivalent neutron delay group is assumed. The parameters can be chosen in order to match either the very high and very low (which seems preferable) or the very low and low frequency behavior. Either reactor model behavior on the rest of the system is very small. Therefore, the crude assumptions made in this study seem justified.

$$\Delta k = f(T_m, x) \quad (\text{A.6.12})$$

where  $T_m$  mean coolant temperature and  $x$  is the rod position. At some steady-state value of  $T_m$  and  $x$ , that is values for which  $\Delta k = 0$ , Equation A.6.12 may be written in a linear form to study the effect of small changes.

$$\Delta k = a\Delta T_m + b\Delta x \quad (\text{A.6.13})$$

But arbitrarily in this formulation a hypothetical temperature  $T_c$  may be defined so as to satisfy the following relationship.

$$\Delta k = a\Delta T_m + a\Delta T_c \quad (\text{A.6.14})$$

Therefore

$$\Delta T_c = \frac{b}{a} \Delta x \quad (\text{A.6.15})$$

In normalized form

$$\Delta k = \alpha \left( \frac{-\Delta T_m}{T_{1a} - T_{2b}} + \frac{\Delta T_c}{T_{1a} - T_{2b}} \right) \quad (\text{A.6.16})$$

where

$$\alpha = a(T_{1a} - T_{2b}) \quad (\text{A.6.17})$$

But

$$2 \frac{\Delta T_m}{T_{1a} - T_{2b}} = \frac{\Delta T_1}{T_{1a} - T_{2b}} + \frac{\Delta T_2}{T_{1a} - T_{2b}} \quad (\text{A.6.18})$$

And

$$(T_{1a} - T_{2b}) C_p W_{nl} = Q \quad (\text{A. 6. 19})$$

or

$$\frac{\Delta T_{1a}}{T_{1a} - T_{2b}} - \frac{\Delta T_{2b}}{T_{1a} - T_{2b}} + \frac{\Delta W_{nl}}{W_{nlo}} = \frac{\Delta Q}{Q_o} \quad (\text{A. 6. 20})$$

Equations A. 6. 11 and A. 6. 16 combine into

$$\left( \frac{\beta \tau D}{1 + \tau_n D} \right) \frac{\Delta Q}{Q_o} = \alpha \left( \frac{\Delta T_c}{T_{1a} - T_{2b}} - \frac{\Delta T_m}{T_{1a} - T_{2b}} \right) \quad (\text{A. 6. 21})$$

Inserting Equations A. 6. 18 and A. 6. 20

$$\frac{\beta \tau D}{1 + \tau_n D} (t_{1a} - t_{2b} + w_{nl}) = \frac{\alpha}{2} (t_{1a} + t_{2b}) + \alpha t_c \quad (\text{A. 6. 22})$$

In which the lower case letters indicate variables which are non-dimensionalized. Of the four variables in Equation A. 6. 22,  $t_{1a}$  reflects the response to the  $t_{2b}$ ,  $w$ , and  $t_c$  inputs.

$$\left[ \frac{\alpha}{2\beta} \left( 1 + \frac{1}{\tau_n D} \right) + 1 \right] t_{1a} = \left[ 1 - \frac{\alpha}{2\beta} \left( 1 + \frac{1}{\tau_n D} \right) \right] t_{2b} - w_n + \frac{\alpha}{\beta} \left( 1 + \frac{1}{\tau_n D} \right) t_c \quad (\text{A. 6. 23})$$

The initial input to the system is a flow change which will develop a corresponding outlet temperature response. However, this response may be eliminated with a rod manipulation. This amounts to a feed forward compensation in which a parallel path signal properly formed may just offset any disturbance commuted along the normal channel. This cancellation manipulation is governed by

$$w_n = \frac{\alpha}{\beta} \left( 1 + \frac{1}{\tau_n D} \right) t_c \quad (\text{A. 6. 24})$$

which comes from Equation A.6.23

The reactor transfer relationship takes the form

$$t_{1a} = \frac{1 - K_R}{1 + K_R} + \frac{\frac{2K_R}{1 + K_R}}{(1 + K_R) \tau_n D + 1} \quad t_{2b} = \frac{1}{1 + K_R} \quad 1 - \frac{1}{(1 + K_R) \tau + 1} \quad w$$

$$+ 2 \frac{1}{K_R + 1} + \frac{\frac{K_R}{K_R + 1}}{(K_R + 1) \tau_n D + 1} \quad t_c \quad (\text{A. 6. 25})$$

$$K_R = \frac{2 \beta}{\alpha} \quad (\text{A. 6. 26})$$

And the control relationship is

$$t_c = \frac{K_R}{2} \left( \frac{\tau_n D}{1 + \tau_n D} \right) \cdot w. \quad (\text{A. 6. 27})$$

Many actuators appear dynamically as first order lags such as valve actuators. This assumes the actuator capacity dominates and the inertia is small. However in the reactor rod motion, opposite is the case. The dominant actuator dynamics are the actuator and rod inertia. This is a second order system. The cascade control principle can, however, treat the actuator and rod in a manner similar to first order systems to provide a fast control action. Figure A.6.2 provides a block diagram of the control scheme.

The inner most controller manipulates the rod actuator. This controller senses the error between rod velocity and a velocity set point. The velocity set point is the output of another controller which senses the error between rod position and the rod position set point. This outer control loop alone is the typical mode of control. With the inner controller properly adjusted, however, the effective outer loop dynamics are reduced. Therefore, a higher gain and

improved speed of response with outer controller results.

A hypothetical reactor used in the computer has a negative temperature coefficient

$$\alpha = 5 \times 10^{-5} \frac{1}{F^{\circ}}$$

This value comes from an example presented on Page 343 in Reference 9.

The computer model and parameter values are presented in Figure A.6.1.

The normalizing values are as follows

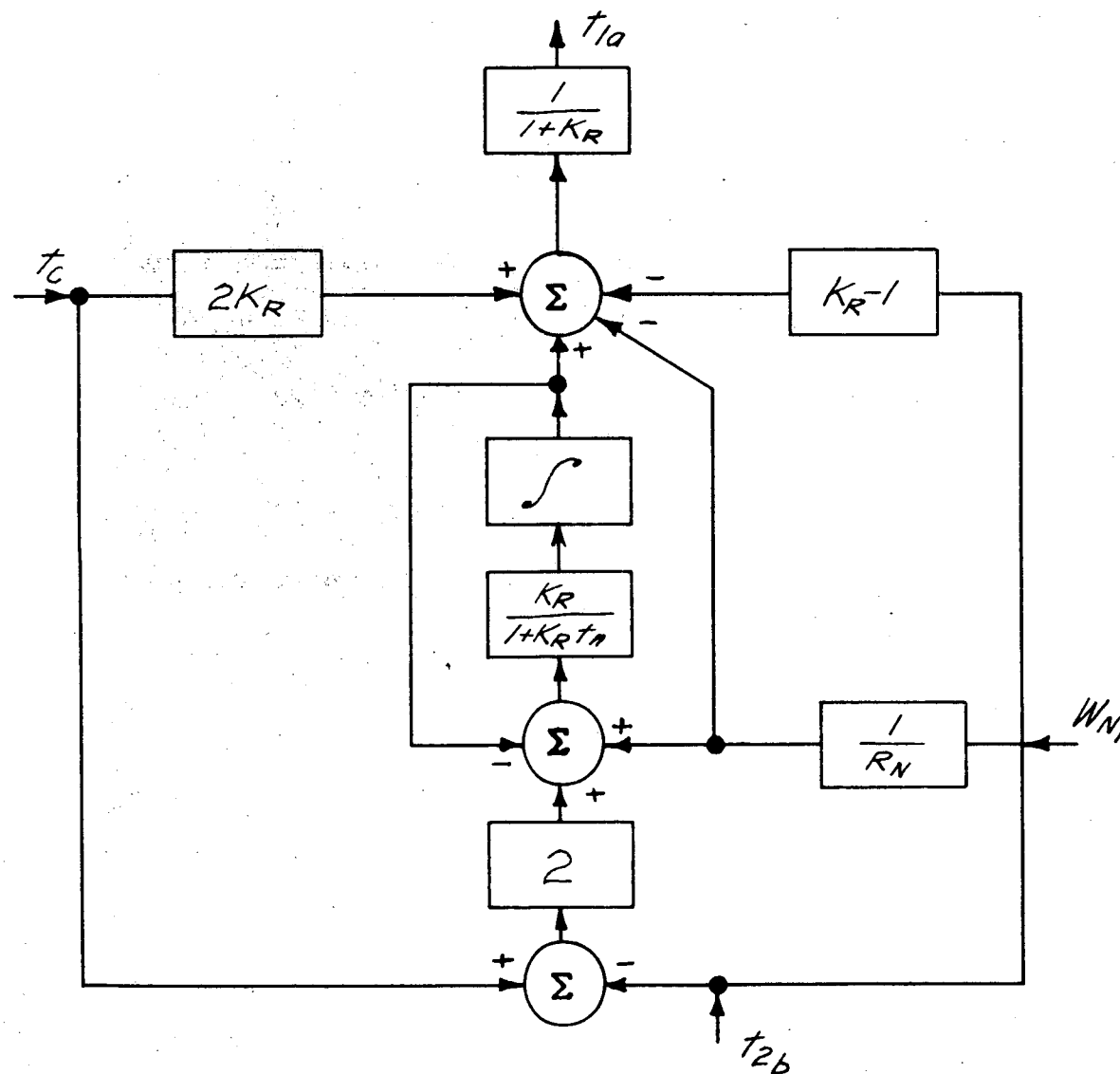
$$T_{1a} - T_{2b} = 1200^{\circ}\text{F} - 723^{\circ}\text{F}$$

$$Q_o = 239,000,000 \text{ BTU/hr}$$

$$W_{no} = 1,665,000 \text{ lbs/hr}$$

From Reference 6,  $\tau_n = 12.3$  secs for the high-low frequency model.

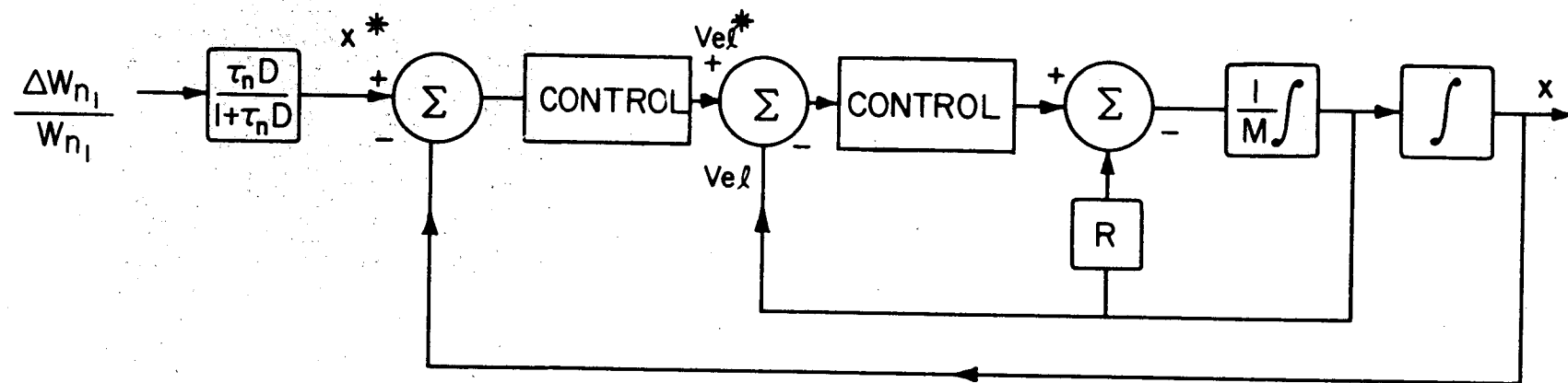
FIGURE A.6.1  
REACTOR CONTROL MODEL



VARIABLE	100%	20%
$K_R$	1.67	1.67
$\tau_n$	12.5	12.5
$R_N$	1	.2

- A.6.7 -

# REACTOR ROD CONTROL LOOP



— A.6.8 —

FIGURE A.6.2

## APPENDIX 7 - THE MONOTONE ANALOGY

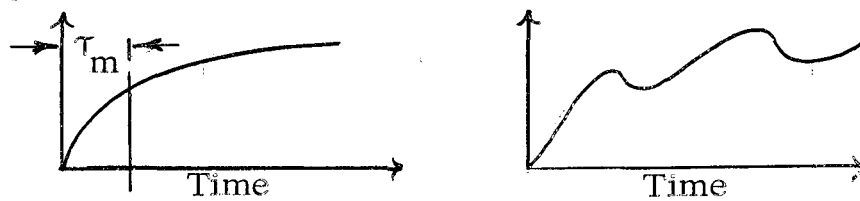
The biggest problem in systems analysis and control is modeling. Modeling necessarily involves many simplifications and approximations to the actual physical system. The nature or detail of the model is subordinate to the problem to be solved. There is no need for a model to correspond to the physical system in any way other than what is necessary to the problem. However, this is rarely a plaguing issue in modeling. More so however the problem rests upon determining the adequacy or inadequacy of a model.

The monotone analogy provides a system of measure by which models may be quantitatively compared. The method is rigorously proven and demonstrated in Reference 5. The impulse response of a linear system may be represented by the function in Equation A.7.1. The exponent is a Taylor series expansion in the dynamic operator  $D$ .

$$e^{(\delta - \frac{T_m D}{1!} + \frac{T_s^2 D^2}{2!} - \frac{T_a^3 D^3}{3!} + \dots)} \quad (\text{A.7.1})$$

The coefficients have the inverse dimension of the  $D$  operator. That is the coefficients have the dimensions of time, time<sup>2</sup>, time<sup>3</sup>, . . . H. Paynter in Reference 5 has defined the coefficients so that each constant has the dimensions of time. The constants possess a geometrical interpretation which is one of the strong points of the analogy.

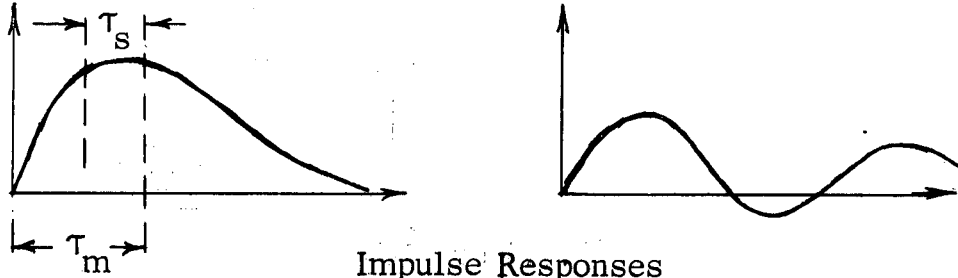
A monotone response is single valued in the dependent variable that is for a given output there is one and only one time corresponding to this response. In Figure A.7.1, the step responses are monotone and non-monotone respectively.



Step Responses

Figure A.7.1

The step response is the time integral of the impulse response. Therefore, the impulse of a monotone function cannot be under-shooting. The impulse-responses of the corresponding step response in Figure A.7.1 are in Figure A.7.2.



Impulse Responses  
Figure A.7.2

The first order coefficient in Equation A.7.1 is the mean delay time,  $T_m$ . This locates the vertical axis of the geometric response. The second order coefficient,  $T_s$  the dispersion time, represents the radius of gyration of the area about its center of gravity; and so on for the remaining time constants. However, these two time constants give sufficient information to model the low frequency behavior of the response.

A graphical method for evaluating the time constants utilizes the 16%, 50%, and 84% response values to a step response.

$T_{16}$ ,  $T_{50}$ , and  $T_{84}$  respectively.

$$T_m = \frac{T_{16} + T_{84}}{2} \quad (\text{A.7.2})$$

$$T_s = T_{84} - T_m + \frac{1}{2} (T_m - T_{50}) \quad (\text{A.7.3})$$

These expressions were used in approximating the terminal responses of the exchangers for the control study. A tabulation of the approximation and block diagrams are presented in the respective appendices.



## APPENDIX 8 - METHOD OF PERTURBATION AND NORMALIZATION

## A. 8. 1. Perturbation

The majority of the analog computers consist of linear elements. The operations of multiplication by a constant, addition and subtraction and integration are readily performed. However, often the physical variables are not linearly related. Consider all variables expressed such as

$$\psi = \psi' + \Delta\psi \quad (\text{A. 8. 1})$$

where subscript ' refers to some arbitrarily selected value of the variable and  $\psi$  refers to some excursion from this point. Substitute these definitions into the physical statements. If only small excursions (small perturbations) are considered from the operating point  $\psi'$  then to a good approximation all second and higher order terms of the incremental variables  $\Delta\psi$  may be omitted when in the presence of linear terms. As an example

$$\Delta\psi_1 \cdot \Delta\psi_1; \Delta\psi_1 \cdot \Delta\psi_2 \quad (\text{A. 8. 2})$$

are second order; however,

$$\psi' \cdot \Delta\psi \quad (\text{A. 8. 3})$$

is a linear term with a static coefficient numerically equal to  $\psi'$ . This approximation reduces the physical relationships to a linearized form. A variable evaluated by the linearized relation is just an incremental value relative to the arbitrarily chosen operating point,  $\psi'$ . To arrive at the total value of the variable, the incremental value must be added algebraically to the operating point; that is, return to Equation A. 8. 1.

## A. 8. 2. Normalization

In many instances dealing in normalized or non-dimensionalized variables reduces a superficial or redundant complexity in a physical statement. A simple example, consider the statement of fluid flow square law friction .

$$\delta P = fW^2 \quad (\text{A. 8. 4})$$

However, by normalizing to some known value such as

$$\delta P_o = fW_o^2 \quad (\text{A. 8. 5})$$

Equation A. 8. 4 becomes

$$\frac{\delta P}{\delta P_o} = \left( \frac{W}{W_o} \right)^2 \quad (\text{A. 8. 6})$$

A convention adopted in this report defines lower case letters for the normalized variable and capital letters for the dimensional variable. Therefore, Equation A. 8. 6 follows as

$$\delta p = w^2 \quad (\text{A. 8. 7})$$

Provided some steady value is known for the relationship, then any other value may be determined by Equation (A. 8. 6) provided the functionality is known which is the case for the example chosen.

## A. 8. 3. Combined Linearization and Non-Dimensionalization

The equations used in the control study have all been linearized and non-dimensionalized. The perturbed or linearized form of Equation A. 8. 4 is

$$\Delta \delta P = 2fw' \Delta w \quad (\text{A. 8. 8})$$

If a normalization is to the local value  $w'$ , then Equation A. 8. 8 reduces to

$$\frac{\delta P}{P'} = 2 \frac{\Delta w}{w'} \quad (\text{A. 8. 9})$$

For this type of normalization.

Any solution reflects a percentage variation in the local value. However, should some fixed value of normalization be chosen, then Equation A. 8. 8 becomes

$$\frac{\delta P}{P_o} = 2 \frac{w'}{w_o} \frac{\Delta w}{w_o} \quad (\text{A. 8. 10})$$

where the coefficient now varies from load point to load point.

The control models over the load range have all been normalized to the 100% load values. Many of the equations have the following form

$$\frac{\psi_1}{\psi_{10}} = -\frac{\psi_2}{\psi_{20}} K_2 + \frac{\psi_3}{\psi_{30}} K_3 \quad (\text{A. 8. 11})$$

The K's are all static coefficients which represent coefficient or potentiometer settings on the analog computer. The solutions received from the computer are the time dependent variations of the  $\frac{\psi' s}{\psi_o}$

The responses presented in this report are expressed in terms of the input excitation. If the input is 10% of value area then unity response amplitude is 10% of that variable. The percentage however reflects a percent change of the normalizing value. As an example, at a particular time some response

$$\frac{\Delta \psi}{\psi_o} = a \quad (\text{A. 8. 12})$$

where a is the amplitude value read from the oscilloscope trace.

Then

$$\Delta \psi = \psi_o a \quad (\text{A. 8. 13})$$

which is the dimensional value of the variation; however, the problem may be linearized at a different value or point than the point chosen for non-dimensionalization. The total dimensional value then is provided by Equation A. 8. 1 which follows as

$$\psi = \psi' + \psi_o a \quad (\text{A. 8. 14})$$

The specific normalizations are presented in the respective appendices.

The illustration in Figure A. 8. 1 is a isometric view demonstrating the significance and interpretation of the spatially reticulated computer studies of the heat exchangers. These are the uncoupled responses to temperature and flow inputs.

All of the linear model solutions presented use an amplitude scale normalized to the size of the input. The number on the vertical scale means the associated variable value is that number times the size of the input variable variation. As an illustration, in Figure 2. 9 (100% load level) the valve disturbance is 10% change in area than the .01 value of pressure is

$$(10\%) (.01) = .1\% \text{ change}$$

in pressure. Since pressure is normalized to 2200 psi, this value equals a 2.2 psi change in pressure.

A Area  
 $A_D, A_R$  Downcomer, Riser Area  
 $A_H$  Boiler Drum Area  
 $A, B, C$  Two-Phase Energy Equation PARAMETERS, Page A.1.20  
 C Sonic Velocity  
 C Reactor Precursor  
 $C_p$  Specific Heat  
 $C_w$  Wall Heat Capacity  
 $D, d$  Diameter  
 $D$   $\partial/\partial t$   
 e Voltage  
 $G_{SH}, G_x$  Superheater, IHX Heat Transfer Parameter Page 53  
 $G_{FN}, G_{FS}$  Superheater Sodium, Steam Linear Model Flowrate Gains  
 $G_w$  Reticulated Counterflow Model Flow Gain  
 $Q_{ab}$  Boiler Heat Transfer Parameter Page 61  
 $g$  Gravitational Constant  
 $H$  Convection Heat Transfer Coefficient  
 $h_s, h_g$  Saturated Liquid, Vapor Enthalpies  
 $h_{sc}, h_{sh}$  Subcool, Superheat Enthalpies.  
 $I_x$  Boiler Circulation Loop Inertia  
 $J$  Joule's Work-Heat Equivalence  
 $K_1, K_2$  Primary, Secondary Controller Proportional Term  
 $K_x$  Slope - Electrical Power Speed Curves Page 16  
 $K_p$  Pressure Regulator Proportional Term  
 $K_p, K_x$  Density Parameters Page A.1.4  
 $K_p, K_{s1}, K_{sd}$  Boiler Tray Steam Pressure Drop Parameters Pages A.5.7 & A.58  
 $K_R$  Reactor Parameter Page A.6.5  
 $k$  Reactor Reactivity  
 $L$  Length  
 $\lambda$  Neutron Lifetime  
 $M_{cd}, M_H$  Central Downcomer, Boiler Drum Mass Storage  
 $M$  Tongue  
 $m_v, m_l$  Vapor, Liquid Mass Storage

N Speed  
 $n$  Neutron Flux Density  
 $P$  Power  
 $P$  Pressure  
 $P_c, P_s$  Sonic, Critical Pressure  
 $sP_F$  Boiler Tray Perforation Steam Pressure Drop p.s.f.  
 $sP_g$  Boiler Tray Liquid Level Above Weir Gravity Steam Pressure Drop p.s.f.  
 $sP_T$  Total Boiler Tray Steam Pressure Drop p.s.f.  
 $sP_{FR}$  Riser Friction Pressure Drop p.s.f.  
 $sP_{FD}$  Downcomer Friction Pressure Drop p.s.f.  
 $sP_g$  Downcomer - Riser Gravity Head p.s.f.  
 $P_s, P_{sg}, P_g$  Nondimensional Density-Pressure Parameters Page A.5.4  
 $Q$  Heat Transfer Rate  
 $q$  Heat Transfer Rate per Unit Area  
 $R$  Motor Secondary Resistance  
 $R_e$  Reflux Ratio  
 $R_N = W_h/W_{hmax}$   
 $R_g = R_N (T_4 - T_5)/(T_4 - T_5)_{max}$   
 $R_s = W_{s1}/W_{s3max}$   
 $v$  Heat Transfer Resistance  
 $s$  Entropy  
 $T$  Temperature of Page 2  
 $T_0$  Sonic Temperature of  
 $T_a, T_m, T_s$  Monstone Analogy Time Constants secs.  
 $U$  Overall Heat Transfer Coefficient.  
 $V$  Velocity  
 $v_l, v_g$  Liquid, Vapor Specific Volumes  
 $W_{s1}, W_{s2}, W_{s3}$  Steam Flowrate To The Tray, To The Superheater, To The Steam Valve.  
 $W_s, W_{td}$  Water Flowrate To And From The Boiler Tray  
 $W_1, W_2$  In-Flow, Out-Flow Page A.1.17  
 $W_e$  Evaporation Rate  
 $W_{h1}, W_{h2}$  Primary, Secondary Sodium Flowrate  
 $x$  Reactor Rod Position  
 $x$  Mass Quality  
 $x$  Spatial Variable

$x_e, x_f$  Exit And Flowing Mass Quality  
 $y$  Volume Quality  
 $Z_H$  Boiler Drum Liquid Level  
 $Z_t$  Boiler Tray Liquid Level  
 $Z_0$  Pipe Acoustic Impedance  
 $z$  Spatial Variable  
 $\gamma_A, \gamma_B$  Boiler Drum Volumes Page A.5.8  
 $\gamma_{cd}$  Boiler Central Downcomer Vapor Volume Page A.5.2  
 $\gamma_H$  Boiler Drum Volume Below Tray Page A.5.2  
 $\gamma_L$  Boiler Drum Liquid Volume Page A.5.2  
 $\gamma_L, \gamma_V$  Liquid, Vapor Volume Page A.1.17  
 $\gamma_L$  Boiler Tray Liquid Volume  
 $\gamma_{cd}$  Boiler Central Downcomer Liquid Volume Page A.5.2  
 $\alpha$  Reactor Negative Temperature Coefficient.  
 $\alpha$  Heat Transfer Parameter Page 53  
 $\alpha, \alpha_2, \beta, \beta_2, \gamma, \gamma_2$  Counterflow Exchangers Control Model Parameters  
 $\alpha_0, \alpha_k, \alpha_p$  Pressure Drop Parameters Page A.1.13  
 $\beta$  Reactor Delayed Neutron Fraction  
 $\beta$  Heat Transfer Parameter Page 53  
 $\Delta$  Small Variation Of The Associated Variable  
 $\Delta$  Unity Dynamic Operator  
 $\lambda$  Energy Equation Coefficient Page A.3.4  
 $\lambda$  Reactor Delay Group Frequency  
 $\delta$  Time Constant Page 59  
 $\epsilon$  Heat Exchanger Effectiveness  
 $\Gamma$  Nondimensional Flowrate Parameter Page 53  
 $\rho_e, \rho_h$  Riser Exit, Hold Up Mass Densities  
 $\rho_l, \rho_g$  Liquid, Vapor Mass Densities  
 $\tau_1, \tau_2$  Primary, Secondary Controller Reset secs.  
 $\tau_e$  Boiler Sodium Stream Transport Time Constant secs.  
 $\tau_e$  Boiler Two-Phase Time Const.

$\tau_c$  Boiler Tray Condensation Time Constant secs.  
 $\tau_p$  Reactor to IHX Pipe Transport Time Constant secs.  
 $\tau_{p2}$  IHX To Reactor Pipe Transport Time Constant secs.  
 $\tau_{p3}$  I.H.X. To S.H. Pipe Transport Time Constant secs.  
 $\tau_{p4}$  S.H. To Boiler Pipe Transport Time Constant secs.  
 $\tau_{p5}$  Boiler To I.H.X. Pipe Transport Time Constant secs.  
 $\tau_p$  Pressure Regulator Reset secs.  
 $\tau_N$  Reactor Delay Group Time Constant secs.  
 $\tau_R$  Reactor Rod Control Reset secs.  
 $\tau_R$  Riser Transport Time Constant.  
 $\tau_{s1}$  Primary Sodium Pipe Inertia Time Constant secs.  
 $\tau_{s2}$  Secondary Sodium Pipe Inertia Time Constant secs.  
 $\tau_{ai}, \tau_{am}$  Sodium Pump-Motor Inertia Time Constant secs.  
 $\tau_{SH1}$  Superheater Sodium Side Control Model Time Constant secs.  
 $\tau_{SH2}$  Superheater Steam Side Control Model Time Constant secs.  
 $\tau_{x1}$  I.H.X. Primary Sodium Side Control Model Time Constant  
 $\tau_{x2}$  I.H.X. Secondary Sodium Side Control Model Time Constant.